Sea level rise adaptation of rubble mound breakwaters

An adaptation pathway approach including sea level rise uncertainty and numerical overtopping modelling

D.Y.Y. Teng

TUDelft

Deltares

Sea level rise adaptation
of rubble mound breakwaters

An adaptation pathway approach including sea level rise uncertainty
and numerical overtopping modelling

MSc Thesis

of

Djimin Yáng Yàn Teng

In partial fulfilment of the requirements for the degree of

Master of Science
in Civil Engineering

at Delft University of Technology,
Faculty of Civil Engineering and Geosciences,
Department Hydraulic Engineering

to be defended publicly on June 28, 2023

An electronic version of this thesis is available at https://repository.tudelft.nl/.

Front cover image:
Photo by Dick van Duijn, retrieved from: https://zoom.nl/foto/landschap/2341896/zuidpier-ijmuiden-2

Preface

This thesis marks the end of my years as a student at Delft University of Technology, and it finalises my master of Hydraulic Engineering at the faculty of Civil Engineering. During this final period of the master, I have enjoyed learning about both the policy side and technical side of a global challenge, namely the adaptation to sea level rise.

The research was conducted in cooperation with the Coastal Structures and Waves (CSW) department at Deltares. I would like to thank all colleagues at CSW for creating a friendly work environment, showing interest in my work, and helping me in any way, shape, or form. Specifically, I want to thank Menno de Ridder and Joost den Bieman for helping me with questions on numerical modelling and wave signal decomposition.

I especially want to thank the members of my graduation committee. First, I want to express my gratitude to Marcel van Gent, who offered me the opportunity to work on my thesis at Deltares and helped me throughout the process with his vast knowledge on coastal structures. I would also like to thank Mark Voorendt for helping me improve not only my writing skills, but also my critical thinking, for which I will be forever grateful. Lastly, I would like to express special appreciation for Marisol Irías Mata. Our weekly meetings were not only helpful to solve all my struggles with numerical modelling, but also enjoyable due to your positive attitude and support.

Finally, I want to thank my friends, my girlfriend, and my family. I am forever indebted to my parents and sister, who have given me every opportunity in life and shaped me to be the person who I am today. I am also extremely grateful to my girlfriend and friends for their continuous support and reminding me that there is a life to enjoy outside of study and work.

Djimin Teng
Delft, June 2023

Summary

If sea level rises faster than anticipated in the initial design of rubble mound breakwaters, a serious threat is posed to their functionality, which is mostly to shelter ports from wave attack. To limit wave overtopping, existing breakwaters must be adapted to the rising sea level and subsequent increase in wave loading due to reduced depth-induced wave breaking. However, the projections of sea level rise are highly uncertain. To deal with this uncertainty and avoid unnecessary costs for the adaptation of breakwaters, the method of adaptation pathways can be applied. Adaptation pathways are designed to adapt to sea level rise in steps with a sequence of measures instead of designing for a single sea level rise value.

The thesis aims to answer the question: *How can an optimal adaptation pathway for rubble mound breakwaters be determined based on cost and uncertainty of sea level rise, aiming to limit wave overtopping when considering changes in depth-induced wave breaking?*

As a first step to answer the research question, methods are proposed to incorporate changes in depth-induced breaking in the creation of adaptation pathways and incorporate uncertainty of sea level rise in the selection of optimal adaptation pathways for rubble mound breakwaters. These methods are based on existing concepts from literature which are modified to be applicable to adaptation pathways for breakwaters:

- To consider changes in depth-induced breaking when determining wave loading on breakwaters, two empirical estimates are proposed. The maximum significant wave height at the toe of the breakwater is assumed equal to half the water depth at the toe. The spectral period at the toe is assumed to be equal to the deep-water spectral period for shallow foreshores (based on water depth and offshore wave height; $h_t/H_{m0,o} > 1$).
- To account for sea level rise uncertainty in the selection of adaptation pathways based on cost, one method for model uncertainty and one method for scenario uncertainty are proposed. The first method uses an approximated probability distribution based on model uncertainty percentile ranges of a scenario, to estimate the probability of a measure being applied. This probability multiplied by the cost of the measure gives the expected value of the cost of the adaptation measure. The second method deals with scenario uncertainty by computing the weighted average of the cost of pathways for all considered scenarios. The suggested method first uses equal weights for all scenarios and then a variation of the weights is performed for a sensitivity analysis.

The applicability of these methods for creation and selection of adaptation pathways is tested on a case study for the location of IJmuiden (the Netherlands). For the case study, five adaptation measures are considered: placing a low-crested structure, adding a berm, raising the foreshore bed with nourishments, adding a protruding crest wall, and raising the armour crest level. The last three mainly form the optimal pathways in the case study. The case study also shows that using the model uncertainty gives insight into the best adaptation measure to start with and how many measures are likely to be applied. Notably, the same pathways are preferred regardless of sea level rise scenario, similar to the previous research by Hogeveen (2021).

Lastly, the empirical estimates and formulae used to create adaptation pathways are validated with numerical models. An XBeach model is used to compute the wave transformation and an OpenFOAM model is used to compute both wave transformation and overtopping at the breakwater. First, the suggested method to consider depth-induced wave breaking when creating adaptation pathways is validated. The estimates of the significant wave height and spectral period

have a maximum deviation of 21% and 15%, respectively, compared to the numerical results. Moreover, the overtopping expressions used in the case study (Van Gent et al., 2022) are validated. The comparison with the numerical model indicates that the overtopping expressions can predict overtopping results with reasonable accuracy, even for conditions with significant wave breaking on the foreshore, which fall outside the range of validity.

To conclude:

- Based on the case study it is concluded that the proposed method to incorporate sea level rise uncertainty in the selection of optimal pathways is useful to gain insight into the preferred measures and the likelihood of measures being applied in the lifetime of the structure. The results of the case study also indicate that the preferred pathways do not vary between different sea level rise scenarios.
- Based on the numerical validation it is concluded that the proposed method to incorporate depth-induced breaking in the creation of adaptation pathways can be used as a first estimate but more detailed calculation methods such as numerical models are necessary to accurately create adaptation pathways.

It is recommended to perform further numerical and/or physical model tests to increase the accuracy of wave loading and wave overtopping predictions for the purpose of determining more accurate adaptation pathways.

Table of Contents

1. Introduction

1.1. Motivation for the present research

Seaports are essential for many economic activities across the world, with over 80% of world trade volume transported by sea (Asariotis, 2021). Breakwaters are coastal structures often used to shelter these ports from wave attack and reduce sedimentation of navigation channels, among many other possible functionalities. However, changing hydraulic boundary conditions due to sea level rise pose a threat to port transport and infrastructure, specifically if the conditions change faster than was originally anticipated during design. These changing hydraulic conditions influence the functionality of existing breakwaters and could result in the structure being unable to meet the design requirements. Furthermore, current sea level rise projections consist of many different scenarios, all with significant uncertainty bandwidths (see Figure 1.1). In addition, the uncertainties within the scenarios of the IPCC have not systematically reduced over time. Due to these large uncertainties, breakwaters are at risk of having unnecessarily high cost if a too conservative sea level rise is assumed, or reaching the end of functional lifetime earlier than required if sea level rise is underestimated.

To deal with uncertainty in context of sea level rise, many different viable approaches have been proposed in literature, such as assumption-based planning, robust decision making, and adaptive planning (Walker et al., 2013). Specifically for coastal structures, Van Gent (2019) suggests using adaptation pathways to deal with the uncertainties of sea level rise. Recently, adaptation pathways have been applied more frequently but mostly on flood risk management (Versteeg, 2023; Trommelen, 2022). So far, only Hogeveen (2021) applied adaptation pathways for rubble mound breakwaters, for a case study on overtopping. Combinations of a crest wall, a berm, a low-crested structure, and a shallow foreshore were compared using empirical wave overtopping formulae and the accuracy of the formulae was tested with numerical modelling. The results by Hogeveen indicated that the available empirical overtopping formulae were not suited for combination of measures. Consequently, Van Gent et al. (2022) proposed new overtopping expressions for rubble mound breakwaters including separate and combined effects of a crest wall and a berm.

This thesis elaborates on the application of adaptation measures for rubble mound breakwaters and the cost estimation of adaptation pathways. The next section analyses current problems and potential research topics regarding the sea level rise adaptation of rubble mound breakwaters.

Figure 1.1: Global mean sea level rise relative to a baseline of 1995-2014 (Fox-Kemper et al., 2021).

1.2. Problem analysis

The general concept of adaptation pathways is portrayed in Figure 1.2. The pathways start when the current policy or structure no longer achieves the desired functionality, and a choice arises between different actions to solve this problem. The tipping point of an action is reached when the action is no longer effective, thus a new action is required to ensure the objective is reached. A sequence of actions is an adaptation pathway, and all pathways together can be depicted in an adaptation pathway map, see Figure 1.2. The main idea of using adaptation pathways for coastal structures is that investments can be avoided if sea level rise is less than expected, while also having limited additional costs if sea level rises more than expected.

For the example of a breakwater, the horizontal axis usually displays sea level rise instead of time. For the overtopping of a breakwater, the pathways start when the current design would exceed the allowable overtopping during design conditions due to sea level rise. A measure can then be chosen to reduce overtopping. After applying a measure, additional sea level rise can again cause the overtopping to exceed the allowable amount. The sea level rise at which the overtopping first exceeds the allowable amount after applying the measure, is called the tipping point of the applied measure. This tipping point of the measure is determined by the characteristics of the measure, which in turn is based on cost efficiency or physical constraints. When the tipping point of a measure is reached, a new measure must be added to reduce overtopping.
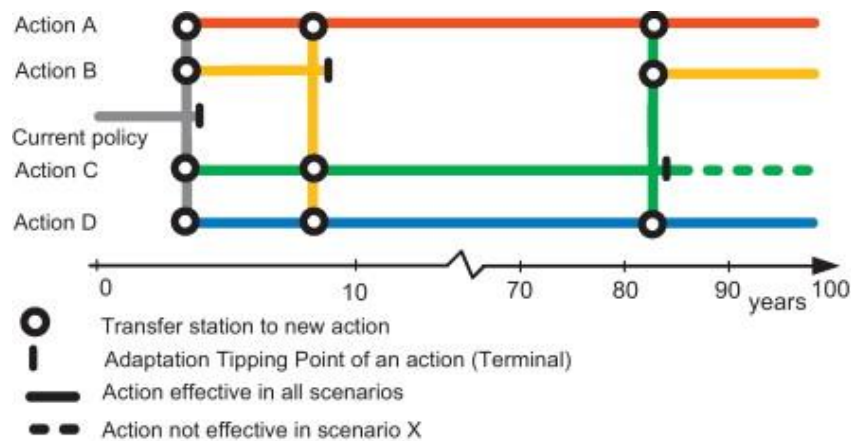
Figure 1.2: Conceptual map of adaptation pathways (Haasnoot et al., 2013).

Adaptation pathways have already been applied in different areas, mostly in flood management (Haasnoot et al., 2019; Trommelen, 2022; Versteeg, 2023). Currently, only Hogeveen (2021) has applied adaptation pathways to breakwaters. There are still several points of interest for research regarding the application of adaptation pathways to breakwaters, which is divided into four main points below.

1. In the thesis by Hogeveen (2021), a cost estimation of the pathways was done with the assumption that the sea level rise would be exactly 1.7 meters, the upper limit of the RCP4.5 scenario by the IPCC. The estimation did not consider the probability of the sea level rise to be less than 1.7 meters and thus the probability of measures at the end of the pathway being unnecessary. In addition, Hogeveen (2021) recommended to consider multiple sea level rise scenarios and to include the likelihood of these scenarios in cost estimation to decide the optimal pathway.

2. As the use of adaptation pathways spreads out investments over time, economic factors such as inflation, discount rate and economic growth are important for estimating costs of the pathways. However, economic factors vary significantly and unpredictably over time which makes it difficult to predict future costs and optimal investment timing. Furthermore, the total costs of measures can consist of many different components such as material, transport, construction, and maintenance costs. While there are examples for flood management in which these costs and economic factors are incorporated for adaptation pathways (De Ruig et al., 2019), the work on rubble mound breakwaters has only incorporated inflation and material costs (Hogeveen, 2021).

3. Adaptation pathways can be created by using empirical formulae to determine tipping points, but the validity of empirical formulae that are derived using physical model tests within a limited range of conditions is not always certain for other conditions. For example, the expressions of Van Gent et al. (2022) are based on conditions in which no significant wave breaking occurs on the foreshore. However, if an adaptation measure such as a raised foreshore bed level or a low-crested structure is applied, significant wave breaking could occur. Therefore, it is not clear whether the overtopping of pathways with a raised foreshore bed or low-crested structure would be accurately calculated using the new guidelines of Van Gent et al. (2022). In addition, rubble mound breakwaters are often in relatively shallow water, thus significant wave breaking might already occur on the foreshore during design conditions, even without any adaptation measures.

4. In addition to the increased water level, the wave loading on rubble mound breakwaters is also very likely to increase due to sea level rise. As stated before, rubble mound breakwaters are often built in relatively shallow water which means that the wave height at the toe of the structure is limited by the water depth, especially for extreme wave conditions. Because the water level rises and the water depth increases, the wave height reaching the breakwater increases due to reduced depth-induced breaking. The previous case study on breakwaters had a simplified approach and assumed there was no change in depth-induced breaking, thus no change in wave conditions due to sea level rise (Hogeveen, 2021).

To summarise, adaptation pathways have been applied frequently for flood risk purposes (Haasnoot et al., 2019; Trommelen, 2022; Versteeg, 2023) but the application for rubble mound breakwaters has been studied only once (Hogeveen, 2021) and is not yet optimal. For the economic assessment, the sea level rise uncertainty has not been taken into consideration and various costs and economic factors have not been incorporated. For the creation of adaptation pathways, the accuracy of overtopping formulae for certain conditions is unknown and changing wave conditions have not been considered so far. The wave conditions and overtopping at the structure determine the effectiveness of the adaptation measures and when (moment in time) the measures need to be applied, both of which influence the selection of optimal adaptation pathways.

1.3. Research outline

1.3.1. Objective of the research

The objective of this thesis is to incorporate changes in depth-induced breaking in the creation of adaptation pathways and incorporate uncertainty of sea level rise in the selection of optimal adaptation pathways for rubble mound breakwaters.

1.3.2. Scope of the research

The scope of the thesis is narrowed down with the following limitations.

- This research analyses adaptation measures that limit wave overtopping, thus other failure mechanisms for a rubble mound breakwater such as toe scour, stability of armour layers and liquefaction of subsoil are not considered.
- For the cost estimation of pathways, the focus in this thesis is on the uncertainty of sea level rise and only limited attention is paid to economic factors and uncertainty of these factors.
- The (potential) change of extreme wave climates due to climate change are not considered, only the change in waves caused by reduced depth-induced breaking due to sea level rise is used. It is also assumed that the design water level increases one-to-one with sea level rise, so if the sea level rises 1 m the design water level also increases 1 m. Morphological changes of the bathymetry due to sea level rise are not considered.
- The adaptation pathways are made for the situation of an existing breakwater. The breakwater is assumed to have none of the considered adaptation measures at the starting point of the pathways.

1.3.3. Research and knowledge questions

The objective leads to the following main research question:

How can an optimal adaptation pathway for rubble mound breakwaters be determined based on cost and uncertainty of sea level rise, aiming to limit wave overtopping when considering changes in depth-induced wave breaking?

The sub-questions of the research are stated below, each emphasising the different parts of the main research question and the different problems stated in Section 1.2. The first sub-question addresses the creation of adaptation pathways and how to consider changes in depth-induced wave breaking due to sea level rise and certain adaptation measures (problem statement 4). The second sub-question focusses on the evaluation of pathways, specifically the determining of optimal pathways based on cost and considering uncertainty of sea level rise in this process (problem statement 1). The third question is related to the validation of pathway creation, and elaborates on the reduction of wave overtopping with adaptation measures and the application of empirical overtopping formulae outside the known validity range (problem statement 3).

1. How can changes in depth-induced breaking be considered when determining tipping points of adaptation pathways for rubble mound breakwaters?

2. How can uncertainty of sea level rise projections be accounted for in the cost assessment of adaptation pathways for rubble mound breakwaters?

3. How do adaptation measures influence wave overtopping discharge in a numerical model compared to empirical formulae for conditions with significant wave breaking on the foreshore?

To help answer the research questions and as guidance for the literature study, knowledge questions are formulated below. Knowledge questions 1 and 2 are related to the creation of adaptation pathways and help answer research sub-question 1 and 3. The purpose of knowledge questions 3 through 5 is to gain an understanding of sea level rise uncertainty, which is necessary to answer research sub-question 3.

1. What are the relevant adaptation measures for wave overtopping at a rubble mound breakwater?
2. What are the relevant empirical formulae to determine tipping points of adaptation pathways for rubble mound breakwaters?
3. What are the different components of uncertainty for sea level rise projections?
4. What sea level rise scenarios should be selected to give a reasonable representation of different future scenarios?
5. What probability distribution can be used to describe model uncertainty of sea level rise?

1.4. Approach and thesis outline

The approach and outline of the thesis is described below.

Step 1

In the first step, a literature study is conducted to answer the knowledge questions; to find the relevant measures and formulae to create pathways for rubble mound breakwaters, and to find the contributions of sea level rise uncertainty and how to include them in the selection of optimal pathways. The answers to the knowledge questions are the contents of Chapter 2:

- The relevant adaptation measures are selected, which are later used to create adaptation pathways for the case study.
- The empirical formulae needed to determine the overtopping at a breakwater and the tipping points of the chosen adaptation measures are selected.
- The different contributions to sea level rise uncertainty are described. It is reviewed which sea level rise scenarios should be considered for the adaptation pathways to cover a reasonable range of different possible futures. In addition, the different descriptions and possible probability distributions of model uncertainty of sea level rise projections are elaborated.

Step 2

This step selects a method to incorporate depth-induced breaking when determining wave loading and subsequently tipping points of adaptation measures, with the purpose of creating adaptation pathways. This method uses existing concepts (i.e., empirical estimates) from literature, with additional assumptions so the method can be applied to adaptation pathways for rubble mound breakwaters. The method is used to answer sub-question 1 and is described in Chapter 3. The accuracy of the suggested method is checked in later steps with numerical models.

Step 3

This step finds methods for the cost evaluation of adaptation pathways, with the purpose of selecting the optimal pathway based on cost. These methods use existing concepts from literature which are modified to be applied to adaptation pathways for rubble mound breakwaters. Methods to include model and scenario uncertainty in the cost estimation of adaptation pathways are described, which answers research sub-question 2. It is also discussed how to include present value in sea level rise adaptation costs and how to assess cost efficiency with the levelised cost of pathways. These methods can be found in Chapter 3.

Step 4

In this step, a case at the location of IJmuiden is described, which is used in later steps to test the applicability of the methods found in steps 2 and 3. This case description makes up chapter 4:

- First, the current situation is elaborated. The main dimensions of a fictitious rubble mound breakwater are determined based on the hydraulic boundary conditions at IJmuiden.

- After describing the current situation (i.e., the actual conditions at IJmuiden but for a fictive breakwater), the focus shifts to the future: adaptation to sea level rise. The dimensions of the adaptation measures for the case study are derived. Together with the dimensions of the main breakwater, this information is used in step 5 to determine the tipping points.
- Lastly, the assumptions necessary for the cost estimation of the adaptation pathways of the case study are made. The cost of material and construction, and the values of inflation and discount rate are elaborated, to be used for the cost estimation in step 6.

Step 5

The adaptation pathways for the case study described in step 4 are created by calculating the tipping points of pathways with the empirical expressions of step 1 and the method to include changing depth-induced wave breaking of step 2. The adaptation pathways can be found in Chapter 5.

Step 6

The optimal pathways for the case study are then determined based on cost estimations for each sea level rise scenario and the combined result, using the methods described earlier in step 3. A sensitivity analysis is also performed to see the impact of the main assumptions on the selection of optimal pathways. This is described in Chapter 5.

Step 7

The accuracy of the empirical overtopping formulae of step 1 and the estimates of step 2, regarding the influence of adaptation measures on overtopping and depth-induced breaking, is checked with the numerical models. The tipping points of adaptation pathways are determined in step 5 with these estimates and empirical expressions for wave loading and overtopping. The exact tipping points are not determined with the numerical models as that would be very time-consuming. Instead, a general validation is performed to check the accuracy of these estimates and empirical expressions, which gives an indication on the accuracy of the tipping points determined in the case study. This step consists of sub-steps 7a and 7b.

a. The set-up of the numerical models is determined, which is described in Chapter 6:

- The choice of models and software is shortly elaborated.
- The model set-up is described. One model is used for wave transformation on the foreshore and the other computes both the wave transformation and overtopping at the breakwater.

b. The validation is performed, which is shown in Chapter 7:

- The wave transformation including depth-induced breaking on the foreshore is compared between the numerical models and the empirical estimates of the suggested method. This finalises the answer to research sub-question 1. The two numerical models are compared with each other as well, to determine which model should be used for the conclusions of the validation.
- The overtopping as obtained with the numerical model is compared to the overtopping as calculated with the empirical overtopping formulae, to see how the effectiveness of the adaptation measures differs. Sub-question 3 is answered with this comparison.

Step 8

In the last step, the limitations, assumptions, results of the case study, and the general applicability of the methods are discussed. Furthermore, the conclusions and recommendations are given for the case studied here and the general application of adaptation pathways on rubble mound breakwaters. This information is included in Chapter 8 and 9.

2. Theoretical background

This chapter describes the answers to the knowledge questions of Section 1.3.3. First, the relevant measures to reduce wave overtopping, which are considered in the case study, are identified in Section 2.1. Hereafter, Section 2.2 presents the formulae used to determine the tipping points in pathways, based on wave overtopping discharge and the influence of the different measures on overtopping. Lastly, it is elaborated which sea level rise scenarios are considered and how the model uncertainty is quantified in Section 2.3.

2.1. Selection of relevant adaptation measures to reduce wave overtopping

Wave overtopping occurs when wave run-up exceeds the crest level of a structure, see Figure 2.1. The freeboard (R_c), which is the difference between the crest level and the still water level (SWL), is one of many parameters which influences wave overtopping.
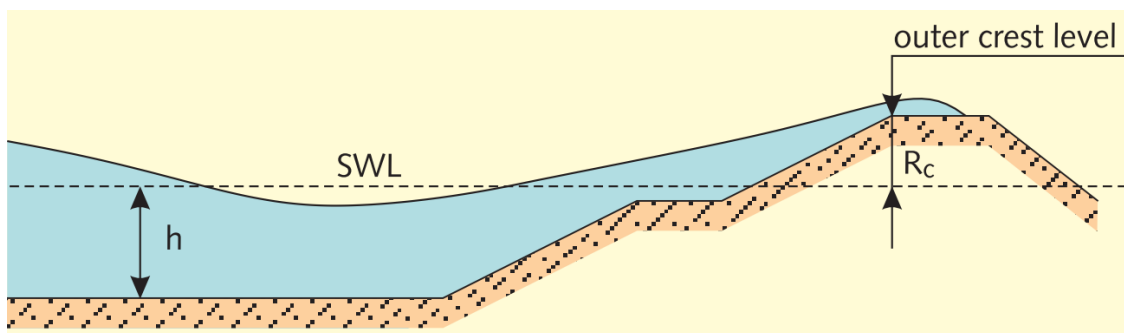
Figure 2.1: Concept of wave overtopping at a structure (TAW, 2002).

The reduction of wave overtopping at rubble mound breakwaters can be achieved in several ways. The wave loading itself can be reduced before it reaches the breakwater. Energy dissipation can also occur on the seaward slope of the breakwater itself. Lastly, the simplest measure is to increase the freeboard of the breakwater. Based on these principles, Hogeveen (2021) used a low-crested structure, a raised foreshore, a berm, and a crest wall as adaptation measures. These same measures will also be used in this thesis for the creation of the adaptation pathways.

Another adaptation measure for existing breakwaters is to increase of the breakwater armour crest level, which increases the freeboard. However, this may be unwanted at certain locations because of the extra space it requires on the lee side of the structure, the extra load on the subsoil or requirements set by clients. Nonetheless, it is a relevant measure to reduce wave overtopping and is therefore used in the creation of the adaptation pathways for this thesis.

To summarise, all measures considered in the adaptation pathways of this thesis are listed below and depicted in Figure 2.2. Hereby, the relevant adaptation measures for wave overtopping at a rubble mound breakwater are determined, answering knowledge question 1.

- Increase of the armour crest level.
- Raise of the foreshore bed level using sediment nourishments.
- Add a low-crested structure, in the form of an offshore breakwater.
- Add a non-reshaping berm on the seaward slope.
- Add a protruding crest wall without recurved parapet.
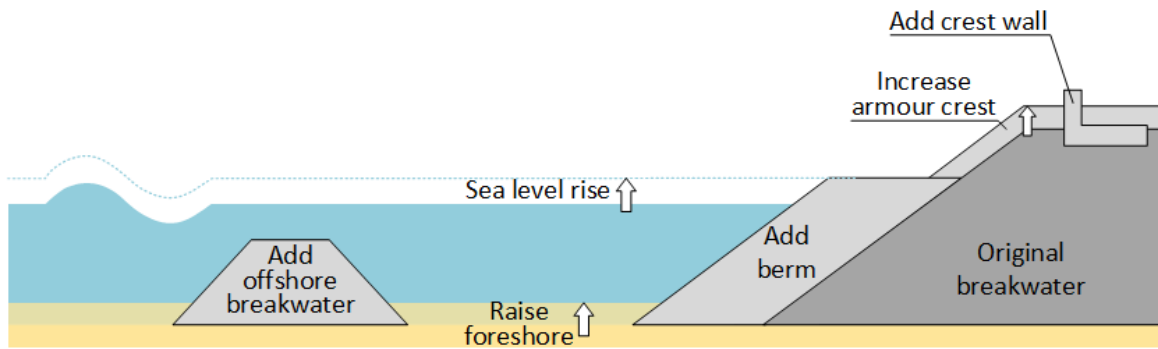
Figure 2.2: Adaptation measures to reduce overtopping at a rubble mound breakwater.

2.2. Empirical formulae to determine tipping points

2.2.1. Determining tipping points

To determine the tipping point of a measure, two parameters have to be known: The maximum allowable overtopping discharge and the overtopping discharge during design conditions. If the overtopping discharge during design conditions (q) exceeds the maximum allowable overtopping discharge (q_{max}), the tipping point of a measure is reached, and a new measure is necessary.

The maximum allowable overtopping is often based on the functional requirements of the breakwater. This requirement must be determined per case and is discussed further in Section 4.2 when describing the case study. The overtopping during design conditions can be calculated using empirical formulae. To determine tipping points, these empirical overtopping expressions can be formed into a limit state function where the breakwater 'fails' when $q > q_{max}$.

The next three sections elaborate on the relevant empirical formulae to calculate overtopping discharge at a breakwater, and thus to determine the tipping points of adaptation pathways.

2.2.2. Overtopping formula to determine tipping points

In the expressions of overtopping guidelines for non-breaking waves, such as TAW (2002) and EurOtop (2018), the effect of a non-reshaping berm is not included, and no guidance is given for a protruding crest wall on rubble mound breakwaters. Non-breaking waves are defined as waves with a breaker parameter higher than a value between 2.0 and 2.5 (TAW, 2002). Rubble mound breakwaters are very often built with a slope of 1:2 or steeper, resulting in the use of formulae of non-breaking or surging waves for its design. Because a berm and a crest wall are both considered adaptation measures in this report, it is necessary for the creation of the adaptation pathways to use formulae that include the influence of these measures.

As stated in Section 1.1, Hogeveen (2021) already concluded that further research had to be done on berm and crest wall influences. At that time, the formula by Krom (2012) was the only one which included a non-reshaping berm for non-breaking waves, but it was based on relatively little data. Subsequently, Van Gent et al. (2022) made new expressions for overtopping at rubble mound breakwaters, including the influence of a berm, a crest wall and roughness. These expressions were also made for the combination of a berm and a crest wall, with climate adaptation of rubble mound breakwaters in mind. Therefore, these expressions are deemed best suited for creation of the adaptation pathways and are thus used in this thesis. There are also newer modified expressions proposed by Irías Mata and Van Gent (2023), but these are not used here, as those expressions were published after most of the current research was performed.

The proposed overtopping formula by Van Gent et al. (2022) is depicted in Equation 2.1. The formulae for the wave steepness and influence factors are given in Equation 2.2 through Equation 2.5. The influence factor formulae for oblique waves and recurved parapets are omitted as both influences are not considered in this report. These equations are derived using a 1:2 slope in the model tests.

$$\frac{q}{\sqrt{g \cdot H_{m0}^3}} = 0.016 \cdot s_{m-1,0}^{-1} \cdot \exp\left(-\frac{2.4 \cdot R_c}{\gamma_f \cdot \gamma_b \cdot \gamma_\beta \cdot \gamma_v \cdot \gamma_p \cdot H_{m0}}\right) \tag{2.1}$$

In which:

$$s_{m-1,0} = \frac{2\pi \cdot H_{m0}}{g \cdot T_{m-1,0}^2} \tag{2.2}$$

$$\gamma_f = 1 - 0.7 \cdot \left(\frac{D_{n50}}{H_{m0}}\right)^{0.1} \tag{2.3}$$

$$\gamma_v = 1 + 0.45 \cdot \left(\frac{R_c - A_c}{R_c}\right) \tag{2.4}$$

$$\gamma_b = 1 - 18 \cdot \left(\frac{s_{m-1,0} \cdot B}{H_{m0}}\right)^{1.3} \cdot \left(1 - 0.34 \cdot \left(\frac{B_L}{s_{m-1,0} \cdot A_c}\right)^{0.2}\right) \tag{2.5}$$

With:

q	= Overtopping discharge	[m³/s/m]
g	= Gravitational acceleration	[m/s²]
H_{m0}	= Spectral significant wave height at toe of structure	[m]
$s_{m-1,0}$	= Wave steepness	[-]
R_c	= Freeboard relative to still water level	[m]
γ_f	= Influence factor roughness	[-]
γ_b	= Influence factor berm	[-]
γ_β	= Influence factor oblique waves	[-]
γ_v	= Influence factor crest wall	[-]
γ_p	= Influence factor recurved parapet	[-]
$T_{m-1,0}$	= Spectral wave period at toe of structure	[s]
D_{n50}	= Nominal armour stone diameter	[m]
A_c	= Crest level of the armour at the crest	[m]
B	= Berm width	[m]
B_L	= Berm level measured from the level of armour at the crest	[m]

To determine the tipping points of measures, the overtopping formula in Equation 2.1 can be rewritten and used in the limit state function for tipping points, see Equation 2.6. The first value of sea level rise at which Equation 2.6 no longer holds, therefore when q>q_max, is when the tipping point is reached.

$$q = 0.016 \cdot \frac{\sqrt{g \cdot H_{m0}^3}}{s_{m-1,0}} \cdot \exp\left(-\frac{2.4 \cdot R_c}{\gamma_f \cdot \gamma_b \cdot \gamma_\beta \cdot \gamma_v \cdot \gamma_p \cdot H_{m0}}\right) < q_{max} \tag{2.6}$$

The formulae of Van Gent et al. (2022) can directly account for an increase of the armour crest height, addition of a berm and addition of a crest wall. The other considered measures, the addition of an offshore low-crested structure and the raised foreshore level influence the wave input of the overtopping formula. Therefore, separate formulae are necessary to calculate the new wave input based on these measures, which are treated in the next two subsections. All these formulae combined are the relevant empirical formulae for the chosen adaptation measures of Section 2.1, answering knowledge question 2.

2.2.3. Influence of foreshores on overtopping discharge

The foreshore has a large influence on wave conditions, because of processes like wave shoaling and depth-induced breaking, waves at the toe of a structure differ from deep-water waves. This wave transformation on foreshores is often computed with wave models like SWAN or SWASH. As sea level rise and certain adaptation measures influence the water depth, using wave models for all adaptation pathways can be very time-consuming. For a simpler approach, empirical formulations of the influence of foreshores can be used.

For the wave overtopping calculations, the influence of a foreshore on the significant wave height and spectral wave period at the toe are most important. Thus, empirical relations that describe the influence of the foreshore on these parameters are relevant.

Extending the classification by Van Gent (1999), Hofland et al. (2017) defined classes of foreshore with the relation of water depth (h_t) and offshore wave height ($H_{m0,o}$):

- Offshore is defined as $h_t/H_{m0,o} > 4$, where no depth-induced breaking occurs.
- Shallow is defined as $1 < h_t/H_{m0,o} < 4$. Depth-induced breaking starts in this range, while the wave spectrum is still similar to the offshore spectrum.
- Very shallow is defined as $0.3 < h_t/H_{m0,o} < 1$. The wave height is reduced to 50% to 60% of the offshore wave height $H_{m0,o}$. The wave spectrum is flattened, and low-frequency energy is increased (infra-gravity waves).
- Extremely shallow is $h_t/H_{m0,o} < 0.3$, which is when most high frequency wave energy is dissipated, and low-frequency energy has taken over.

For the influence of foreshores on the significant wave height, a common rule of thumb for depth-induced breaking is given in Equation 2.7.

$$H_{m0,t,max} = \frac{h_t}{2}$$

(2.7)

If the incoming wave height is higher than the maximum wave height at the toe of the structure ($H_{m0,t,max}$) calculated in Equation 2.7, the wave height is reduced to half the water depth (h_t) due to depth-induced breaking. This wave height should then be used as input for the overtopping calculations (Equation 2.1).

The influence of the foreshore on the spectral period can be included by using the method of Hofland et al. (2017), but the proposed formula is not used in this thesis thus also not shown here. The approach for the spectral period is elaborated in Section 3.1.

To conclude, the foreshore can influence the wave height and in turn influences the overtopping discharge. Therefore, raising the bed level of the foreshore can be used as an adaptation measure to reduce the incoming wave height and overtopping. The tipping point can then be calculated using Equation 2.6.

2.2.4. Influence of low-crested structures on overtopping discharge

Low-crested structures, like a foreshore, influence the incoming waves by dissipating wave energy. The wave transmission over low-crested structures is often expressed in a transmission coefficient, which is a relation between the transmitted and incoming significant wave height, see Equation 2.8. Empirical formulae for the influence of low-crested rubble mound structures were proposed by Briganti et al. (2003) based on earlier research of d'Angremond et al. (1996). These expressions can be applied to both emerged and submerged structures.

Recently, a new expression was made by Buis (2022) using physical model tests, specifically for the influence of submerged structures. This new formula was found to perform better than the formulae by Briganti et al. (2003) and d'Angremond et al. (1996) for submerged rubble mound structures within the tested range of parameters. Equation 2.9 gives the transmission coefficient as proposed by Buis (2022).

$$K_t = \frac{H_{m0,t}}{H_{m0,i}} \tag{2.8}$$

$$K_t = -0.59 \cdot \exp\left(\frac{R_c}{H_{m0}}\right) - 0.042 \cdot \frac{h}{H_{m0}} + 1.12 \tag{2.9}$$

With:

K_t	= Wave transmission coefficient	[-]
$H_{m0,i}$	= Incoming significant wave height	[m]
$H_{m0,t}$	= Transmitted significant wave height	[m]
R_c	= Freeboard, negative for submerged crest	[m]
h	= Height of the structure	[m]

For submerged rubble mound structures, the spectral wave period also changes depending on the transmission coefficient. In general, the spectral wave period decreased (Buis, 2022). However, no clear relation was given for the change in spectral wave period. Therefore, the change in spectral wave period due to a low-crested structure is neglected in this thesis.

By placing a low-crested structure, wave height can be influenced according to Equation 2.9. If the wave height at the toe of the original breakwater is reduced by placing the low-crested structure, this reduced wave height is used to calculate overtopping with Equation 2.1. Therefore, placing a low-crested structure can be used as an adaptation measure to reduce wave height and consequently overtopping. The tipping point of this measure can be calculated using Equation 2.6.

2.3. Uncertainty of sea level rise projections

2.3.1. Contributions to sea level rise uncertainty

The variance of sea level rise projections can be split into three different components (De Vries et al., 2014), which answers knowledge question 3:

- <u>Natural variability</u> is the deviation from the mean sea level varying over time.
- <u>Scenario uncertainty</u> is based on human activity, mostly greenhouse gas (GHG) emissions, and is often considered by using different scenarios. For example, the IPCC uses Shared Socio-economic Pathway (SSP) scenarios with different trajectories for GHG emissions.
- <u>Model uncertainty</u> is the uncertainty within the models used to predict sea level rise, which is dependent on uncertainty of many physical, chemical, and biological processes, but also model inaccuracies and methodological uncertainties (De Vries et al., 2014).

The contribution of natural variability for the total variance of projections is insignificant for the time horizon considered in adaptation pathways and is therefore not considered in this thesis.

2.3.2. Sea level rise scenarios

The different sea level rise scenarios used in the creation of adaptation pathways should be a good representation of possible future scenarios. Because the SSP scenarios by the IPCC are publicly available and detailed information on these scenarios is published in IPCC reports, these scenarios are considered in this thesis. However, the likelihood of occurrence of the SSP scenarios is not assessed (IPCC, 2021) and cannot be used to select scenarios. Therefore, another way of selecting the scenarios has to be used, which is elaborated below.

In Hogeveen (2021) single adaptation measures adapted to steps of 0.3 m to 0.6 m of sea level rise. Thus, if two scenarios for example only differ 0.05 m in sea level rise in 2100, it is not necessary to consider both scenarios as they likely result in the same preferred adaptation pathways. Therefore, the selection of scenarios is made such that the scenarios have significantly different sea level rise values at 2100. According to KNMI (2021), it is also important to take into account extreme scenarios that have low likelihood of occurrence. This is also considered in the selection of scenarios.

The selected scenarios are stated below and the projected sea level rise values for 2100 are presented in Table 2.1 (Fox-Kemper et al., 2021). These projections are used to represent the possible future scenarios, thus answering knowledge question 4.

- SSP1-1.9, a scenario with very low GHG emissions and CO_2 emissions declining to net zero around 2050.
- SSP2-4.5, a scenario with intermediate GHG emissions and CO_2 emissions remaining similar to current levels until 2050.
- SSP5-8.5, a scenario with very high GHG emissions and CO_2 emissions doubled by 2050.
- SSP5-8.5 Low Confidence (LC), a scenario with the same emissions as SSP5-8.5 but with larger uncertainty ranges. This scenario includes high uncertainty of the ice sheet (melting) processes. Currently there is relatively limited quantitative information about these processes, hence the low confidence intervals.

Table 2.1: Sea level rise values for Maassluis in 2100, relative to baseline 1995-2014, for selected scenarios (Garner et al., 2021).

SSP scenario	17th percentile (m)	Median (m)	83rd percentile (m)
SSP1-1.9	0.22	0.42	0.66
SSP2-4.5	0.41	0.60	0.84
SSP5-8.5	0.57	0.81	1.12
SSP5-8.5 LC	0.57	0.90	1.36

2.3.3. Sea level rise model uncertainty

Model uncertainty of sea level rise can be described in two different ways. Typically, model uncertainty is given in graphs such as Figure 1.1 and 2.3, where at a certain moment in time a range of sea level rise is given. This uncertainty is often expressed in terms of percentiles. The shaded area in Figure 2.3 could for example portray the 17th and 83rd or 5th and 95th percentile range. The uncertainty of sea level rise at a certain moment in time can be described relatively accurate with a normal distribution (De Vries et al., 2014). The standard deviation of this normal distribution can then easily be determined using the percentile ranges given in data of sea level rise projections.
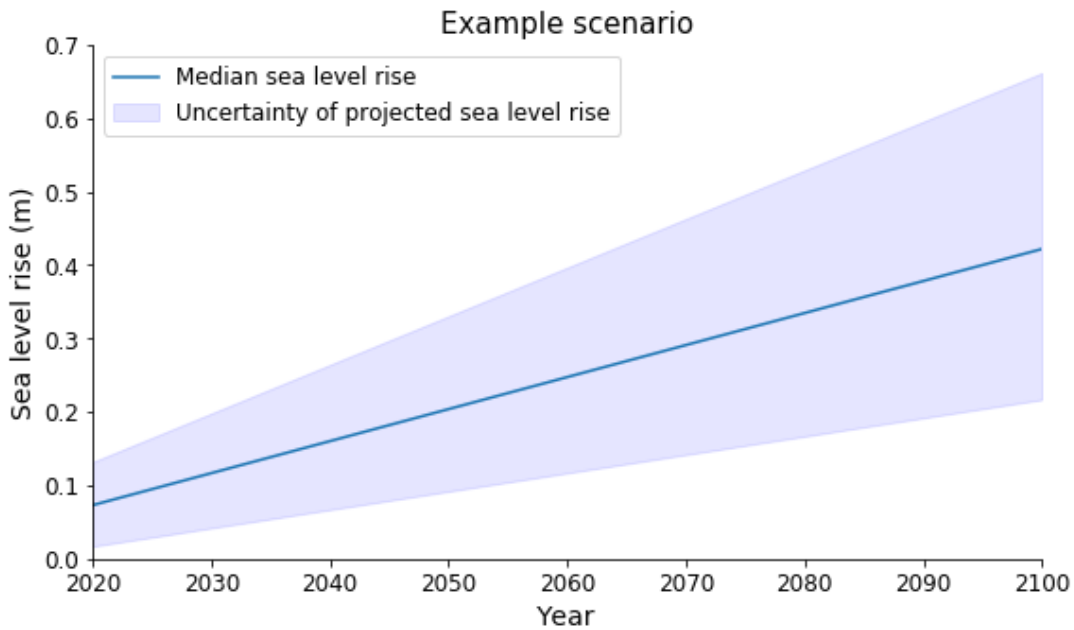
Figure 2.3: Example of a sea level rise projection with model uncertainty.

An alternative perspective is to look at the range of time in which specific values of sea level rise are reached. An example is given in Figure 2.4 obtained from a tool made by the NASA Sea Level Change Team. Because the use of this alternative perspective is relatively new, limited data is currently available for this projected timing uncertainty.
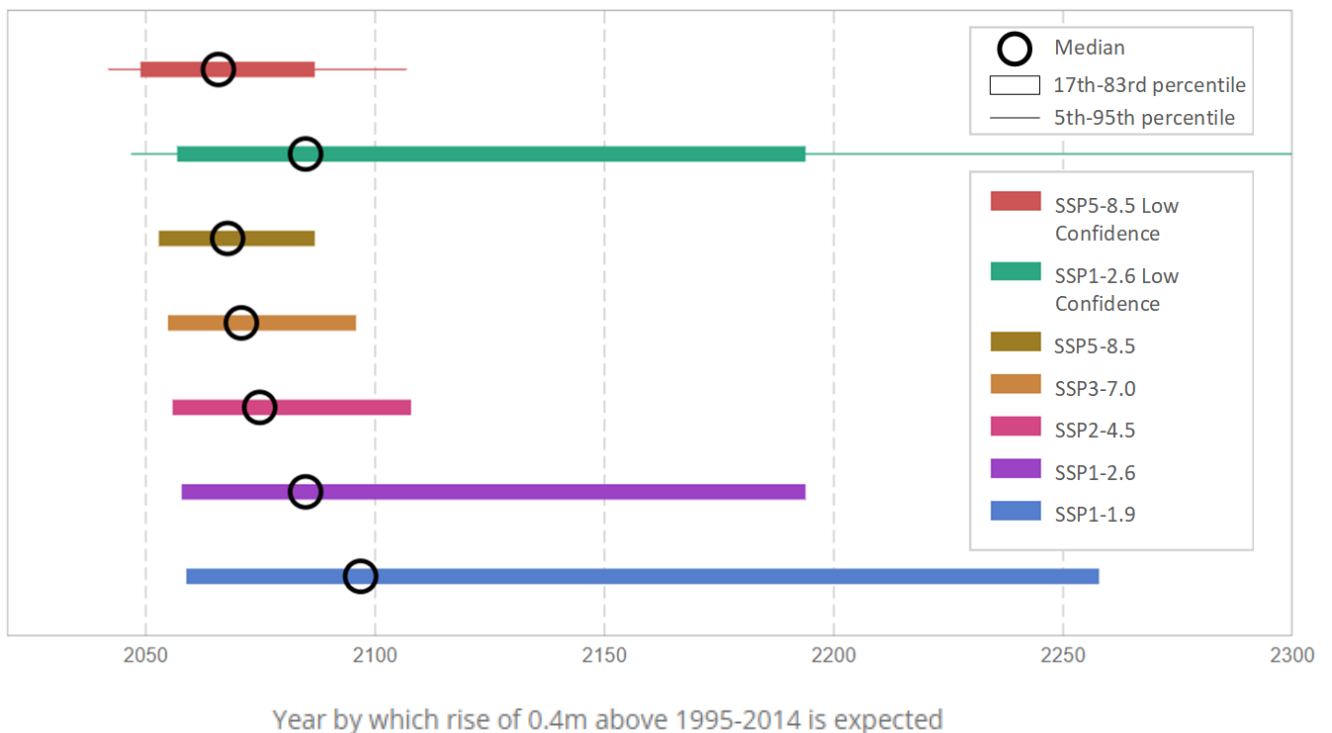
Figure 2.4: Projected timing of 0.4 m sea level rise in Maassluis for different scenarios (Adapted from Garner et al., 2021).

To the author's knowledge, there is no literature that suggests an accurate probability density function for the uncertainty of projected timing of sea level rise. It can be seen in Figure 2.4 that the uncertainty of projected timing is very asymmetrically distributed around the median, unlike the

uncertainty of projected sea level rise values in Figure 2.3. The skewness of the timing uncertainty changes for the chosen sea level rise value. This means that the normal distribution cannot be used to accurately describe the model uncertainty of projected timing.

To summarise, there are two ways to describe model uncertainty of projections: uncertainty of sea level rise values or uncertainty in timing of sea level rise. The uncertainty of sea level rise values for specific moment in time can be described with reasonable accuracy using a normal distribution (De Vries et al., 2014), but a probability distribution for the uncertainty in timing has not yet been suggested in literature. This answers knowledge question 5. Based on this answer, the uncertainty of sea level rise values is used in this thesis to describe the model uncertainty of sea level rise.

2.4. Concluding remarks

This chapter describes the theoretical background which is necessary to answer the research sub-questions. For this purpose, knowledge questions are answered related to the creation of pathways (questions 1 and 2) and the uncertainty of sea level rise (questions 3, 4 and 5).

1. What are the relevant adaptation measures for wave overtopping at a rubble mound breakwater?
   - Increase the armour crest level.
   - Raise the foreshore bed level.
   - Add a low-crested structure.
   - Add a berm on the seaward slope.
   - Add a protruding crest wall.
2. What are the relevant empirical formulae to determine tipping points of adaptation pathways for rubble mound breakwaters?
   - The overtopping expressions by Van Gent et al. (2022), which can account for the influence of a crest wall, a berm, and the armour crest level.
   - A common rule of thumb (i.e., the maximum significant wave height is equal to half the water depth) to account for the influence of the foreshore.
   - The expression by Buis (2022) to account for the influence of low-crested structures.
3. What are the different components of uncertainty for sea level rise projections?
   - Natural variability
   - Scenario uncertainty
   - Model uncertainty
4. What sea level rise scenarios should be selected to give a reasonable representation of different future scenarios?
   - SSP1-1.9
   - SSP2-4.5
   - SSP5-8.5
   - SSP5-8.5 LC
5. What probability distribution can be used to describe model uncertainty of sea level rise?
   - A normal distribution can be used as an approximation for the model uncertainty of sea level rise values at a certain moment in time.

3. Methods for creation and evaluation of adaptation pathways

This chapter describes methods that can be used in the creation and evaluation of pathways for sea level rise adaptation of breakwaters. The method for creation of pathways is specifically to consider the depth-induced breaking and its changes due to sea level rise when determining tipping points. The evaluation methods have the purpose of determining the optimal pathway based on cost. These methods use existing concepts from literature with additional assumptions so they can be applied to adaptation pathways for rubble mound breakwaters. Only the method of Section 3.1 is used for creation of pathways, all other sections focus on cost estimation of adaptation pathways and the selection of the optimal pathway.

Section 3.1 gives an answer to research sub-question 1 with a method that uses empirical estimates to include depth-induced wave breaking when determining tipping points. Section 3.2 addresses how to use sea level rise uncertainty in cost estimation, thus giving an answer to the second research sub-question. The use of present value in sea level rise adaptation is discussed in Section 3.3, and in Section 3.4 a method is given to assess cost efficiency of pathways. Lastly, concluding remarks are given in Section 3.5.

3.1. Method to include changes in depth-induced breaking in tipping points

Changing depth-induced wave breaking due to sea level rise influences the wave loading at a structure and thus the overtopping. Therefore, this is important to consider when determining tipping points of adaptation measures for breakwaters. Before the chosen method is discussed to account for the effect of sea level rise and certain adaptation measures on wave loading, the assumed effect of sea level rise on design water levels and wave climates is elaborated below.

The actual effect of sea level rise on extreme sea level events at coastal locations is a current research topic (Fox-Kemper et al., 2021). Therefore, a simplified relation between sea level rise and design water level is assumed to determine the toe wave conditions. In this thesis, the design water level is assumed to increase one-to-one with sea level rise. This relation of the design water level with sea level rise is described in Equation 3.1 below. For example, if the original design water level is NAP +0 m and sea level rises with 1 m, the new design water level is NAP +1 m.

$$DWL(SLR) = DWL_0 + SLR \qquad (3.1)$$

With:

$DWL(SLR)$	= Design water level as function of sea level rise	[m NAP]
DWL_0	= Original design water level	[m NAP]
SLR	= Sea level rise	[m]

Another important simplification is the assumption that the offshore wave climate does not change due to climate change and sea level rise. Thus, it is assumed that the offshore design wave height and wave periods for the chosen return periods do not change over time or due to sea level rise.

With the assumptions stated above, the effect of sea level rise on the wave conditions at the structure is only present in the wave transformation and depth-induced breaking on the foreshore. Physical models or numerical wave models could give relatively accurate results for this purpose, but the number of tests needed to create adaptation pathways is very high. A less time-consuming approach is selected, where simple (empirical) relations are used. Because these empirical relations are simple approximations, the accuracy of the results should be checked. For example, for this method a check is performed with numerical models in chapter 7.

Significant wave height

The rule of thumb presented in Section 2.2.3 is a simple way to account for changes in significant wave height due to depth-induced breaking. Therefore, this method uses the rule of thumb to determine the wave loading at the toe of a structure. The rule of thumb is repeated below in Equation 3.2, and Equation 3.3 shows how to compute the water depth at the toe. The rule gives an estimate for the wave height at the toe. This wave height can be used as input for overtopping calculations and hence the determination of tipping points of measures, see Section 2.2.

$$H_{m0,t,max} = \frac{h_t}{2} \tag{3.2}$$

In which:

$$h_t = DWL(SLR) - BL \tag{3.3}$$

With:

$H_{m0,t}$	= Significant wave height at the toe	[m]
h_t	= Water depth at the toe	[m]
$DWL(SLR)$	= Design water level as function of sea level rise	[m NAP]
BL	= Bed level at the toe	[m NAP]

Spectral period

The rule of thumb only accounts for the significant wave height, but overtopping expressions like those of Van Gent et al. (2022) also use the spectral period to compute the overtopping discharge. To estimate the spectral period, the results of Hofland et al. (2017) can be used. However, the formula Hofland et al. (2017) proposes is dependent on the foreshore slope, which might not be known yet when making a preliminary version of adaptation pathways. If the slope is unknown and the foreshore is shallow ($h_t/H_{m0,o} > 1$), it is suggested to simply use the deep-water value of the spectral period in the overtopping expressions as a first estimate. The latter approach is used in this thesis.

Determining tipping points

With the estimates of the wave height and period stated above, and with the expression of Buis (2022) if a low-crested structure is applied (see Section 2.2.4), the wave loading at the toe of the breakwater can be determined. Subsequently, the overtopping discharge can be computed with e.g., the expressions of Van Gent et al. (2022), and the tipping points of adaptation measures can be determined as described in Section 2.2.1 and Section 2.2.2.

3.2. Method to implement sea level rise uncertainty in cost estimation

This section answers the second research sub-question on how uncertainty of sea level rise can be included in the cost assessment of adaptation pathways. Naturally, there are many ways to do so. One recent example is a framework for flood risk strategies made by Trommelen (2022), which uses deterministic calculations to select promising pathways and a probabilistic assessment to compare their robustness. Here, a similar approach is taken. The cost estimation and the implementation of sea level rise uncertainty is done by using probabilities in a deterministic manner. A sensitivity analysis is then performed to see how robust the results are.

3.2.1. Sea level rise model uncertainty in cost estimation

As stated in Section 1.2, the reason to use adaptation pathways for breakwaters is to potentially avoid unnecessary investments for sea level rise adaptation measures, while also having limited additional costs if the sea level rises more than expected. Thus, there is probability of a measure in

the pathway not being implemented and this can be included in cost estimation of pathways by using sea level rise model uncertainty. This probability is used for cost estimation of pathways in the method described below.

The method to include sea level rise model uncertainty in cost estimation of pathways is described by Equation 3.4.

$$C_{p,s} = \sum_{m=1}^{n} C_m \cdot (1 - p_{m,s}) \tag{3.4}$$

With:

$C_{p,s}$	= Expected cost of a pathway for scenario s	[€]
C_m	= Cost of measure m	[€]
$p_{m,s}$	= Probability that measure m is not applied in scenario s	[-]
n	= Number of measures in a pathway	[-]
p	= Subscript indicating a specific pathway	[-]
m	= Subscript indicating a specific measure	[-]
s	= Subscript indicating a specific scenario	[-]

The method gives the expected value of the cost of pathways. This expected cost of pathways should not be used without the context of the total cost of pathways. As Kwakkel (2020) warns, expected cost can give a wrong impression of the possible future costs. In reality, the cost of an adaptation measure is invested or not, but expected values can be anywhere in between. Thus, expected cost of pathways should be additional information on what can reasonably be expected for the chosen scenario and the different expectations between scenarios. It considers the model uncertainty of sea level rise projections, without the need for e.g., a time-consuming Monte Carlo simulation.

The probability of a measure not being implemented depends on multiple factors:

- The sea level scenario that is assumed for cost estimation.
- The trigger value of a new measure. This is the sea level rise value at which it is decided that a new measure is needed. The trigger value is necessary to ensure a new measure is applied before the tipping point of the current measure has been passed. It depends on the implementation time needed for the new measure, the rate of sea level rise and the tipping point of the current measure. If there is (practically) no implementation time, the trigger value of a new measure and tipping point of the current measure are the same value of sea level rise.
- The end of adaptation lifetime of the breakwater. In this thesis, the end of adaptation lifetime is defined as the first year or moment in time in which decision-makers decide to not apply new measures even if the trigger value is reached. The end of adaptation lifetime is thus related to the desired design lifetime.

Based on the chosen sea level rise scenario, the trigger value of a new measure and the end of adaptation lifetime of the breakwater, the probability of a new measure not being implemented can be found using the following steps:

1. Define the probability distribution of sea level rise model uncertainty for the chosen scenario in one of two ways:

a. Use the distribution for projected timing uncertainty of the trigger value.
   b. Use the distribution for projected sea level rise value uncertainty at the end of adaptation lifetime.

2. Determine the probability of a measure not being implemented:
   a. Determine the probability that the trigger value happens after the end of adaptation lifetime.
   b. Determine the probability of the projected sea level rise value at the end of adaptation lifetime being lower than the trigger value.

In step 1 above, a choice is given between two ways of expressing model uncertainty for sea level rise projections. As stated in Section 2.3.2, there is currently limited data available for projected timing uncertainty (option a) and it is difficult to find an accurate probability distribution as the skewness changes for chosen sea level rise values. Therefore, using the uncertainty of sea level rise values at a certain moment in time (option b), specifically the end of adaptation lifetime, is the chosen method. An example of how this probability is determined is given in Figure 3.1.

In the example of Figure 3.1, the end of adaptation lifetime of the breakwater is 2100. On the right side, the probability distribution of model uncertainty at 2100 is partially pictured, which is step 1b. Based on the trigger value of the measure at 0.3 m of sea level rise and the probability distribution, the probability of the new measure not being applied is determined (step 2b).
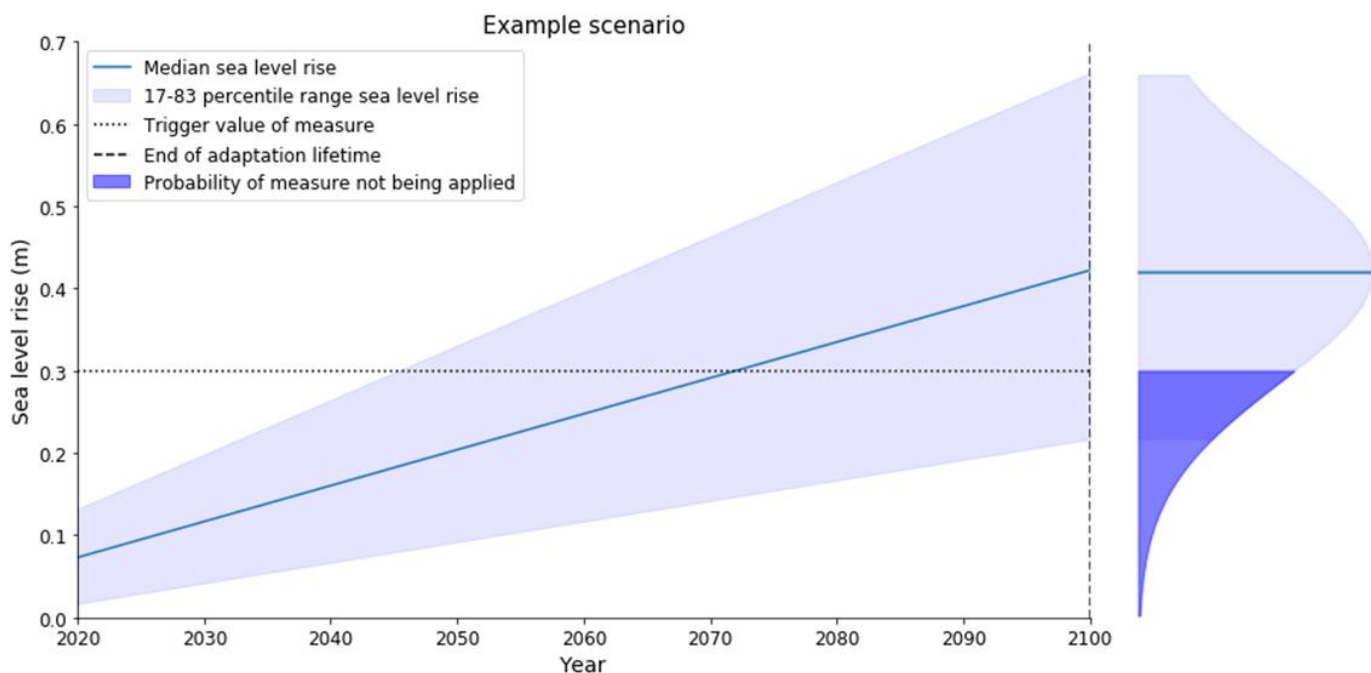
Figure 3.1: Example of how to determine probability of measure being applied, steps 1b-2b.

When using this method for breakwaters, it can be assumed that the trigger value for a new measure is equal to the tipping point of the previous measure. Trigger values are important for flood risk measures because of the relatively long implementation time, which can be up to 20 years (Trommelen, 2022). This can have a large effect on the costs of measures when using net present value calculations. The implementation time needed for adaptation measures of breakwaters is likely much shorter, as the construction of complete breakwaters can be done in 1-2 years. Therefore, it is assumed the implementation time is negligible and the trigger value for a new measure equals the tipping point of the previous measure.

3.2.2. Sea level rise scenario uncertainty in cost estimation

To deal with the plethora of different possible futures, some cases in literature assign weights or probabilities to considered scenarios (Woodward et al., 2011; Kind et al., 2018; Pachos et al., 2022). It is also argued that assigning probabilities to future scenarios should not be used to deal with uncertainty in climate adaptation. Kwakkel (2020) states that these probabilities are meaningless for the long-time horizon involved in climate adaptation and it is possible that the expected value over a set of scenarios is not obtained in any single scenario, causing a misrepresentation of the results. However, in this case the adaptation pathways approach is used to deal with this uncertainty and the probabilities for scenarios would only be used to compare different options within the approach of adaptation pathways. Therefore, assigning probabilities can be used to give a general overview of pathway costs for all considered scenarios.

The difficulty with assigning probabilities or weights to scenarios is that no guidelines are currently provided on how to distribute these. For example, the IPCC does not assess the likelihood of their SSP scenarios. Therefore, the probabilities or weights of the considered scenarios must be assumed. One possibility to deal with this deep uncertainty is to assign the same probability or weight to each outcome, which is done by Buurman and Babovic (2016) and Woodward et al. (2011). Kind et al. (2018) and Pachos et al. (2022) use different methods based on scenario trees and expert judgement.

Because the probabilities of the IPCC scenarios are unknown, weights are assumed for each considered scenario to include scenario uncertainty in cost estimation, see Equation 3.5. The least subjective method is to assign the same weight to all scenarios considered, which is the method of choice. The cost estimation is then simply an average of all considered scenarios. The influence of the assumed probabilities must be checked with a sensitivity analysis, as for example done in Chapter 5.

$$C_p = \sum_{s=1}^{n} w_s \cdot C_{p,s} \tag{3.5}$$

With:

C_p	= Cost estimation of pathway p	[€]
$C_{p,s}$	= (Expected) cost of pathway p for scenario s	[€]
n	= Number of considered scenarios	[-]
w_s	= Weight assigned to scenario s	[-]
p	= Subscript indicating a specific pathway	[-]
s	= Subscript indicating a specific scenario	[-]

3.3. Method to use present value for cost estimation of adaptation pathways

Adaptation pathways are based on postponing investments, which means the changing value of money over time is important for the cost assessment. A commonly used tool to translate future costs and benefits into present value is Net Present Value (NPV). Unlike in flood risk examples, for adaptation measures to reduce overtopping, benefits are not defined in terms of monetary value. Therefore, it is only the present value of the costs that need to be considered.

The two factors that influence the value of money over time are the inflation and the discount rate. Inflation represents the decreasing value of money over time due to increasing prices. The discount

rate reflects the preference to have money now over having the same money later, because of the potential profits or interest to be gained (Gallo, 2014).

In certain cases, the used discount rate already accounts for inflation, for example when the interest rate of loans is used as or included in the discount rate (Trommelen, 2022). If the discount rate does not yet include inflation, Equation 3.6 and 3.7 can be used to calculate present value of costs.

$$C_{PV} = \frac{C_t}{(1+r)^{t-t_c}}$$ (3.6)

In which:

$$C_t = C_0 \cdot (1+i)^{t-T}$$ (3.7)

With:

C_{PV}	= Present value of the cost	[€]
C_t	= Cost in year t	[€]
C_0	= Cost based on data from year T	[€]
r	= Discount rate per year	[-]
i	= Inflation rate per year	[-]
t	= Year in which the cost is made	[-]
T	= Year in which the cost data is determined	[-]
t_c	= Current year	[-]

A difficulty with using Equation 3.6 and 3.7, is that the present value depends on time, but tipping points and trigger values are expressed in meters of sea level rise. However, it is uncertain in what year this sea level rise occurs and thus when the cost for the measure is made. In this thesis, the median of a sea level rise projection is used to determine in which year a certain value of sea level rise occurs. The timing of implementation could change the optimal pathway in cost. Depending on the ratio of discount rate and inflation, it can be more or less attractive to postpone costs. The effect of different timings on the cost of measures can be seen in the results of different scenarios, because more extreme scenarios have accelerated sea level rise rates compared to milder scenarios.

To determine the timing of sea level rise values, available data on the chosen sea level rise scenarios can be used for interpolation. Care must be taken if the sea level rise values fall outside of the data bounds for the scenarios, which can happen quite easily for mild scenarios. At the upper bound of the data, the uncertainty of timing is already very significant, see for example the data by Garner et al. (2021). Extrapolation of data with high uncertainty ranges naturally gives very uncertain results.

3.4. Method to determine cost efficiency of adaptation pathways

Hogeveen (2021) made pathways for breakwaters to adapt to exactly 1.7 m of sea level rise. However, if pathways with different sea level rise adaptation are made, the pathways cannot be compared based on only costs, as the 'benefit' (the amount of sea level rise it can adapt to) of the pathways are not equal. A simple solution is to use cost efficiency for this comparison instead. Cost efficiency is often calculated by dividing the cost by the benefit. An example is levelised cost of energy, which is cost per energy unit generated, for instance expressed in €/MWh. Below, it is shortly elaborated why pathways can have different sea level rise adaptation values and the method to assess cost efficiency is presented.

The characteristics of an adaptation measure determine how much sea level rise can be adapted to. These dimensions are determined by a number of factors e.g., economical optimisation of material use, construction process considerations and potential client requirements. For example, the increase of a foreshore bed level by means of sand nourishment has a minimum height of the added sand layer based on the accuracy of dredging equipment. It is likely that the optimal dimensions of the measures result in significantly different adaptation values. This results in pathways being uneven in terms of sea level rise adaptation.

One way to compare the pathways is to use levelised costs i.e., cost per meter of sea level rise adaptation, as a measurement of cost efficiency. A lower levelised cost means higher cost efficiency. Equation 3.8 depicts how to calculate levelised cost for a measure.

$$LC_m = \frac{C_m}{S_m} \tag{3.8}$$

With:

LC_m	= Levelised cost of measure m	[€/m]
C_m	= Cost of measure m	[€]
S_m	= Sea level rise adaptation of measure m	[m]
m	= Subscript indicating a specific measure	[-]

If levelised cost is used together with the method described in Section 3.2.1, it is important to calculate the levelised cost per measure first, before adding them up to obtain the total pathway levelised cost. Otherwise, measures that have an insignificant contribution to the pathway cost due to their low probability of being applied, would have disproportional impact on the levelised cost with their sea level rise adaptation.

When using levelised cost, it is important to give context in terms of the regular non-levelised total cost and the total amount of sea level rise adaptation of pathways. If the difference in total sea level rise adaptation is significant, the comparison of levelised cost is not useful to select preferred pathways. However, which difference in adaptation is considered significant, is a subjective decision. If it is assumed the difference in sea level rise adaptation of pathways is insignificant, a sensitivity analysis should be performed to check this assumption. The sensitivity analysis should check which pathways are preferred for example within groups of pathways with similar adaptation or for various minimum sea level rise adaptation requirements. An example of this sensitivity analysis for the case study is shown in Section 5.3.2.

3.5. Concluding remarks

In this chapter, two main steps are taken to reach the objective "*to incorporate changes in depth-induced breaking in the creation of adaptation pathways and incorporate uncertainty of sea level rise in the selection of optimal adaptation pathways*":

1. The method of Section 3.1 describes how to consider changes in depth-induced breaking due to sea level rise when determining the tipping points of adaptation measures and consequently the creation of adaptation pathways.
2. The methods of Section 3.2 through 3.4 facilitate the selection of the optimal pathway based on cost. Specifically, Section 3.2 describes how to incorporate sea level rise uncertainty in this selection of the optimal adaptation pathways based on cost.

In the following chapters, the methods are tested to gain insight into their application by applying the methods in a case study. The method of Section 3.1 is also validated with numerical models.

4. Description of the case study

This chapter describes the case study used to test and apply the methods for the creation and selection of the optimal pathways of Chapter 3. First, the location of choice and the assumed design starting points are elaborated in Section 4.1 and 4.2. Hereafter, the hydraulic boundary conditions for the case study are given in Section 4.3. Then Sections 4.4 and 4.5 present the assumed dimensions of the breakwater and adaptation measures. Lastly, Section 4.6 shows the assumptions for the case study regarding the cost estimation of the adaptation measures, and Section 4.7 gives the concluding remarks.

4.1. Location of the case study

A breakwater located in the Netherlands is chosen, because data for hydraulic boundary conditions along the Dutch coast can easily be obtained. None of the breakwaters along the Dutch coast are typical modern rubble mound breakwaters and there are no specific reasons to choose one over the other. Therefore, it is simply chosen to study the IJmuiden breakwater location (Figure 4.1).

The breakwater at the chosen location of IJmuiden is a special case with a design very different from modern rubble mound breakwaters (Van Hoven et al., 2004). Therefore, a fictive breakwater is used to obtain results more representative for modern rubble mound breakwaters. The added benefit is that a fictive breakwater can be designed without any of the considered adaptation measures, so all measures can be applied in the pathways.

Figure 4.1: Chosen location of the case study, IJmuiden, the Netherlands.

4.2. Design starting points

Before the fictive breakwater can be designed, the design requirements of the breakwater must be determined. For actual design of breakwaters, these design requirements are based on functional criteria and intended operational use. The following starting points are assumed for the fictive design:

- Maximum allowable wave overtopping discharge: 50 l/s/m. For the design of a breakwater, this parameter is based on functional criteria and structural requirements, as stated in for example the EurOtop (2018) or Rock Manual (CIRIA et al., 2007). For the chosen allowable discharge, the rear side of the breakwater should be properly designed for overtopping.

- Design lifetime of 50 years. This is a typical design lifetime for breakwaters according to Van den Bos & Verhagen (2018).
- 2080 is the assumed end of adaptation lifetime of the breakwater, based on the assumed design lifetime. It is conservatively rounded up to 2080, instead of rounding down to 2070.
- Target failure probability of 15% during its design lifetime. This parameter is normally based on the consequences of failure of the breakwater. The typical range for breakwaters is 5-20% or more according to Van den Bos and Verhagen (2018).
- A return period of 308 years is obtained using the rewritten Poisson distribution in Equation 4.1, the assumed design lifetime and target failure probability.

$$R = \frac{T_L}{-\ln\left(1 - p_{f,T_L}\right)} \tag{4.1}$$

With:

R	= Return period	[year]
T_L	= Design lifetime	[year]
p_{f,T_L}	= Target failure probability during design lifetime	[-]

4.3. Hydraulic boundary conditions

4.3.1. Deep-water wave conditions

HydraNL (v2.8.2) is used to obtain the deep-water wave conditions at the location of IJmuiden. This probabilistic model gives hydraulic loads for specific return periods and is applied by Dutch water boards to assess or design flood defences. The significant wave height and spectral wave period can be determined for any return period with HydraNL. Based on the significant wave height and spectral wave period, the wave steepness is determined using Equation 2.2 from Section 2.2.2. For simplicity, especially for the numerical modelling in Chapter 6 and 7, the waves are assumed to be perpendicular to the structure, so obliqueness is not considered.

For the return period of 308 years, the following deep-water wave conditions are computed using HydraNL and Equation 2.2.

- Significant wave height of 7.35 m
- Spectral wave period of 10.59 s
- Wave steepness of 0.042

4.3.2. Toe wave conditions

To determine the overtopping with the expressions from Section 2.2.2, the wave conditions at the toe of the structure are needed. Using the method of Section 3.1 to obtain the toe wave conditions, the water depth at the toe is needed, so the bathymetry and design water level must be determined. The design water level changes due to sea level rise and the bathymetry is dependent on the applied adaptation measures, which means the wave conditions at the toe of the structure also change. Therefore, only the initial toe wave conditions without sea level rise or adaptation measures are given in this section.

In this case study, the method as described in Section 3.1 is used to include the changing wave loading. An important assumption of this method is that the design water level increases one-to-one with sea level rise. For example, if the original design water level is NAP +0 m and sea level rises with 1 m, the new design water level is NAP +1 m. For the sea level rise data, the IPCC sea level rise projections data of Garner et al. (2021) is used in this case study. In the data of Garner et al. (2021),

there is no data for the location of IJmuiden. Therefore, the sea level rise projection data for Maassluis is used for this case study, which is the data point closest to the location of IJmuiden. Note that this is only for the sea level rise projections, and no other hydraulic boundary conditions.

The bathymetry of the foreshore at the breakwaters of IJmuiden is relatively complex and has high spatial variance, which means it is difficult to determine the toe level. This is especially the case for the southern breakwater because of the trench in front of it. Kuiper and Van Gent (2006) assumed a toe level of NAP −12 m to be representative for the southern breakwater using a bathymetry map created by Rijkswaterstaat. Based on the same map, the northern breakwater toe level is estimated to be NAP −8 m. The northern breakwater has a simpler bathymetry of the foreshore, making it easier to define the toe level, and will therefore be used in the case study.

For a return period of 308 years, the water level is NAP +3.95 m according to the HydraNL model. Combining a wave height and water level with both a return period of 308 years is a conservative estimate. However, the joint distribution wave height and water level is not given by HydraNL, thus this water level will be used as an approximation.

The initial water depth at the toe is 11.95 m, based on the toe level of NAP −8 m and the water level of NAP +3.95 m for a return period of 308 years. This water depth can be used to compute the significant wave height at the toe of the structure with Equation 3.2 from Section 3.1. The significant wave height at the toe is then approximately 5.98 m.

With the publicly available data, it is difficult to determine the slope of the foreshore at Ijmuiden, so the formula of Hofland et al. (2017) is not used here to determine the spectral period at the toe. In the method of Section 3.1 it is stated that the spectral period at the toe can be assumed to be equal to the offshore value if the ratio of the water depth at the toe and offshore significant wave height is larger than 1. For the initial conditions without sea level rise or adaptation measures, the ratio of the water depth at the toe and offshore significant wave height is approximately 1.6, thus the foreshore is defined as shallow. Therefore, based on the results of Hofland et al. (2017) it is assumed that the change in spectral wave period is likely insignificant at this ratio, and the spectral wave period at the toe is assumed to be equal to the deep-water spectral wave period.

To conclude, the following initial toe conditions are used for this case study:

- Design water level of NAP +3.95 m
- Bed level at the toe of NAP −8 m
- Water depth of 11.95 m
- Significant wave height of 5.98 m
- Spectral wave period of 10.59 s

4.4. Dimensions of the initial breakwater

A fictive breakwater is used in the case study to obtain results that are more representative of modern breakwaters. The breakwater design is simplified, and no optimisation is done as normally would be the case, because the focus of the thesis is on adaptation pathways and not the initial breakwater design. The use of this breakwater is solely to compute the overtopping for the adaptation pathways. For the overtopping calculations, the following parameters need to be known:

- Slope of the structure
- The D_{n50} of the armour layer
- The initial crest height

All other parts of a breakwater design that are not necessary for overtopping calculations, such as the toe, bed protection, core and filter layers, are not determined.

The slope is chosen to be 1:2, which is a typical slope for rubble mound breakwater, and the slope Van Gent et al. (2022) used in the tests to create their overtopping expressions. Section 4.4.1 elaborates on the calculation of the armour stone size and in Section 4.4.2 the crest height is determined.

4.4.1. Armour layer

The nominal diameter of the armour layer is a design parameter based on the stability of the armour on a slope under wave attack. Even though this thesis does not consider stability of the breakwater, the nominal diameter is still needed to calculate the roughness influence factor of the overtopping expressions (see Section 2.2.2).

To determine the armour stone size for rubble mound breakwaters, commonly used formulae are the Van der Meer (1988) equations or the shallow water variations by Van Gent et al. (2003). The Rock Manual (CIRIA et al., 2007) advises to use the shallow water equations if the water depth is less than three times the significant wave height, which is true in this case study. Therefore, one of the formulae proposed by Van Gent et al. (2003) will be used to compute the armour stone size.

The first option is to use the Van der Meer (1988) equations that have been adapted for shallow water. However, these equations require the wave height exceeded by highest 2% of waves at the toe of the structure as input, which is unknown for the chosen location. The second option is a formula created by Van Gent et al. (2003), as an alternative to the shallow water Van der Meer equations. This formula is used to calculate the armour stone size (see Equation 4.2 and 4.3).

$$\frac{S}{\sqrt{N}} = \left(0.57 \cdot \frac{H_s}{\Delta \cdot D_{n50}} \cdot \sqrt{\tan(\alpha)} \cdot \frac{1}{1 + D_{n50c}/D_{n50}} \right)^5 \tag{4.2}$$

In which:

$$\Delta = \frac{\rho_s - \rho_w}{\rho_w} \tag{4.3}$$

With:

S	= Damage level	[-]
N	= Number of waves	[-]
H_s	= Significant wave height at the toe	[m]
Δ	= Relative mass density	[-]
ρ_s	= Mass density of stone	[kg/m³]
ρ_w	= Mass density of water	[kg/m³]
D_{n50}	= Nominal diameter of the armour	[m]
α	= Angle of the seaward slope	[°]
D_{n50c}	= Nominal diameter of the core	[m]

Before the nominal diameter of the armour can be calculated, assumptions must be made for other design aspects of the breakwater:

- The chosen damage level corresponds to intermediate damage (Van den Bos & Verhagen, 2018).
- Based on the wave period, the assumed number of waves represents a storm of approximately 3-4 hours.

- The mass densities of the armour stone and water are assumed to be typical values.
- The slope of the breakwater was already defined as 1:2.
- It is assumed that there is one filter layer between the core and the armour layer. Typical ratio between the nominal diameters of layers is 2 to 3 (Van den Bos & Verhagen, 2018). Here a ratio of 2 is assumed, thus the armour is 4 times larger than the core diameter. This falls within the tested ranges of Van Gent et al. (2003).

Table 4.1 gives an overview of all used values for the calculation and the resulting nominal diameter of the armour. The only standard grading sufficient for this design is the largest grading of HM$_A$ 10-15 ton with a nominal diameter of 1.68 m (CIRIA et al., 2007). It is very likely that using concrete armour units is more economical in this situation, because the chosen standard grading is very expensive. However, this is not very significant to the research conducted in this thesis, so no further design iterations are performed.

Table 4.1: Input to calculate the necessary nominal diameter of the armour layer.

Parameter	Symbol	Value	Unit
Damage level	S	6	-
Number of waves	N	1200	-
Mass density stone	ρ_s	2700	kg/m³
Mass density water	ρ_w	1025	kg/m³
Nominal diameter ratio	D_{n50c}/D_{n50}	0.25	-
Angle of seaward slope	α	26.57	°
Nominal diameter of armour	$\boldsymbol{D_{n50}}$	**1.68**	**m**

4.4.2. Crest height

It is important for the creation of adaptation pathways to know the initial crest height of the breakwater before adaptation measures are applied. This initial crest height consists of two parts, the minimally required crest height and any extra crest height already added in the design phase to deal with e.g., sea level rise and soil subsidence. The minimum crest height is computed using the boundary conditions, allowable overtopping, and design assumptions. The extra crest height is a design choice and the assumed value for this case study is elaborated. For simplicity extra crest height for soil subsidence is not considered here, but for a more complete design this should be investigated.

To calculate the minimally required freeboard for the breakwater without any adaptation measures, the overtopping expression of Van Gent et al. (2018) can be rewritten, as shown in Equation 4.4. The minimum crest height is then the summation of the freeboard and the design water level.

Without any adaptation measures, the only influence factor that is not equal to one is the roughness factor. This roughness factor is computed with Equation 2.3 (Section 2.2.2) using the diameter of the armour stated in Table 4.1 and the wave height of 5.98 m determined in Section 4.3.2. Equation 2.2 stated in Section 2.2.2 is used to calculate the wave steepness based on the wave conditions at the toe (Section 4.3.2). Table 4.2 displays the inputs of Equation 4.4 and the resulting minimum freeboard of 5.79 m. As the initial design water level is NAP +3.95 m, the minimum crest level is NAP +9.74 m.

$$R_{c,min} = -\ln\left(\frac{q_{max}}{1000} \cdot \frac{s_{m-1,0}}{0.016 \cdot \sqrt{g \cdot H_{m0}^3}}\right) \cdot H_{m0} \cdot \frac{\gamma_f \cdot \gamma_b \cdot \gamma_\beta \cdot \gamma_v \cdot \gamma_p}{2.4} \qquad (4.4)$$

Table 4.2: Input to calculate minimum freeboard.

Parameter	Symbol	Value	Unit
Maximum allowable overtopping discharge	q_{max}	50	l/m/s
Wave steepness	$s_{m-1,0}$	0.034	-
Gravitational acceleration	g	9.81	m/s^2
Significant wave height at toe	H_{m0}	5.98	m
Influence factor roughness	γ_f	0.38	-
Influence factor berm	γ_b	1	-
Influence factor oblique waves	γ_β	1	-
Influence factor crest wall	γ_v	1	-
Influence factor parapet	γ_p	1	-
Minimum freeboard	$\boldsymbol{R_{c,min}}$	**5.79**	**m**

For existing breakwaters, it is very likely that sea level rise has already been considered in the initial design by for example constructing the crest height above the minimally required value. This determines the starting point of the adaptation pathways and must therefore be assumed for the case study. The value of sea level rise that is considered in the initial design is likely very different for existing breakwaters, depending on when it was built, the design lifetime and the choices made by the designers.

For this case study, it is assumed the crest height is increased by 0.26 m compared to the minimum, thus the initial crest level is NAP +10.0 m (see Table 4.3). The extra crest height of 0.26 m allows for approximately 0.17 m of sea level rise before the tipping point of the initial breakwater is reached. This difference is caused by the reduced depth-induced wave breaking due to sea level rise and the consequent increase in wave height, and calculated with the method of Section 3.1. This sea level rise value of 0.17 m is the starting point for the adaptation pathways of Chapter 5.

Table 4.3: Assumed crest level of the original breakwater.

Parameter	Value	Unit
Minimum crest level	+9.74	m NAP
Initial design adaptation	0.26	m
Crest level	+10.0	m NAP

Once again, the design of the breakwater could be optimised with more design iterations. Because the breakwater height is very significant, it would likely be more cost-efficient to make the slope of the breakwater steeper to reduce material use. However, this is not very significant to the research conducted in this thesis, so no further design iterations are performed.

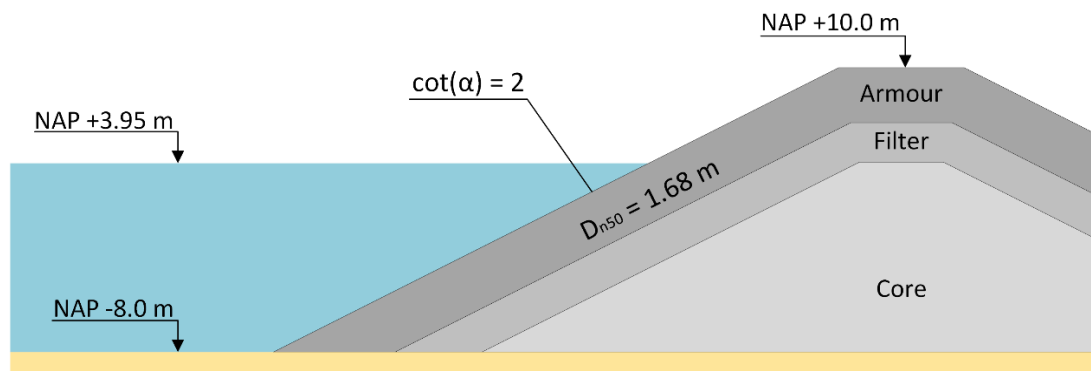The most important characteristics of the breakwater are displayed in Figure 4.2.

Figure 4.2: Characteristics of the breakwater with the original design water level and toe bed level.

4.5. Adaptation measure dimensions

For each adaptation measure, the dimensions necessary for pathway creation and cost estimation are assumed and elaborated in this section. The dimensions of a measure determine how much sea level rise it can adapt to and thus the tipping point of a measure. Outside of economic optimisation, certain restraints also influence the desired dimensions of measures. The dimensions of measures are mostly based on examples and physical restraints and no economic optimisation is done. A general consideration is also that the measures should not adapt to too large values of sea level rise, such that likely only one measure is necessary, because this would defeat the purpose of using adaptation pathways to avoid potentially unnecessary costs.

4.5.1. Additional crest wall

For a protruding crest wall, the dimensions are mostly restricted by wave forces acting on the wall. EurOtop (2018) warns that the wave forces on the crest wall increase drastically if the wall is significantly higher than the armour crest in front of it. These wave forces on crest walls determine the necessary dimensions, but they are still an active research topic (Sigalas, 2019; Irías Mata, 2021). Therefore, it is currently difficult to determine the dimensions of a protruding crest wall in a simple manner. For this reason, dimensions of the crest wall are assumed based on real life examples.

Two structures with protruding crest walls are taken as example:
- Colombo, Sri Lanka (Dassanayake et al., 2008).
  The crest of the wall protrudes 2.7 m above the crest of the armour. However, this is a special case because the acceptable overtopping is very low. This is apparent from the breakwater design, as the freeboard during design conditions is 12.8 m for a significant wave height of 6.4 m. The wave height is comparable to the case study of this thesis, but the freeboard is much larger.
- Palm Deira, Dubai, United Arab Emirates (Van den Bos & Verhagen, 2018).
  The crest of the wall protrudes 0.75 m above the crest of the armour. The design freeboard is unknown, but likely in the order of 5 m, and the significant wave height is 5.5 m. Both are comparable to this case study. An important difference is that this example is a land reclamation, thus the cross-section of the structure is quite different.

The considered examples both have significant differences with the considered case study. Nonetheless, it does give an indication for the dimensions of protruding crest walls. Based on these examples, it is assumed that the crest wall protrudes 1 m above the crest of the armour when it is constructed. Other dimensions of the crest wall necessary for the cost estimation are chosen to be similar to an example by Vos-Rovers et al. (2008). The wall is assumed to be 1 m thick (t) and the base slab is 5 m wide (W_b). The assumed dimensions are displayed in Figure 4.3.
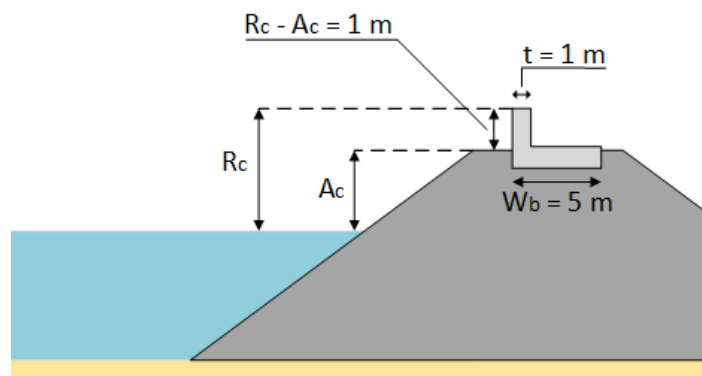
Figure 4.3: Crest wall dimensions.

4.5.2. Increased armour crest level

There are multiple ways to increase the armour crest height. One example is adding an extra layer of armour units on top of the existing structure. Another way is to remove the present armour layer, raise the breakwater with cheaper, first underlayer material, and then place back the armour units. The first example is more expensive in terms of material cost but likely requires less time and construction costs. Both ways of increasing the armour crest height are elaborated in this section.

First, an assumption must be made. If the current armour layer is insufficient for stability due to increase of wave height caused by sea level rise, applying this measure can be used as an opportunity to place larger armour units to ensure stability as well. However, the focus is on overtopping, thus it is assumed the armour stone determined in Section 4.4.1 is sufficient and is not replaced by larger armour units during the lifetime of the structure.

The dimensions of this measure can be limited by the extra space it requires on the lee side of the structure, the extra load on the subsoil or requirements set by clients, as stated earlier in Section 2.1. These are the main restrictions that would determine the dimensions of this measure. For this case study, it is assumed that the armour crest can be raised with a maximum height equal to one layer of armour units.

Adding armour units on top of the existing structure can only be done in layers. As already stated above, it is assumed only one extra layer of stones is added to increase the armour crest height. The increase of the armour crest height can be calculated with Equation 4.5 from the Rock Manual (CIRIA et al., 2007).

$$t = n \cdot k_t \cdot D_{n50} \tag{4.5}$$

With:

t	= Layer thickness	[m]
n	= Number of stones across the layer	[-]
k_t	= Layer coefficient	[-]
D_{n50}	= Nominal diameter	[m]

The layer coefficient is approximately 0.8 for a single layer of armour stones (CIRIA et al., 2007) and the nominal diameter of the armour is 1.68 m. The layer thickness and increase of armour crest height is then 1.34 m if one layer of stones is added.

If the armour layer is first removed, first underlayer material can be used to increase the crest height. This material is smaller in diameter, so the increase of the crest height can also be lower than 1.34 m. The additional flexibility could be valuable for the purpose of sea level rise adaptation.

The method of removing the armour layer and placing first underlayer material to increase the crest height is used for this adaptation measure. Furthermore, the slope is assumed to be 1:2, the same as the original slope of the breakwater. The increase of the armour crest height (t) is assumed to be 1.34 m. The assumptions can also be seen in Figure 4.4.
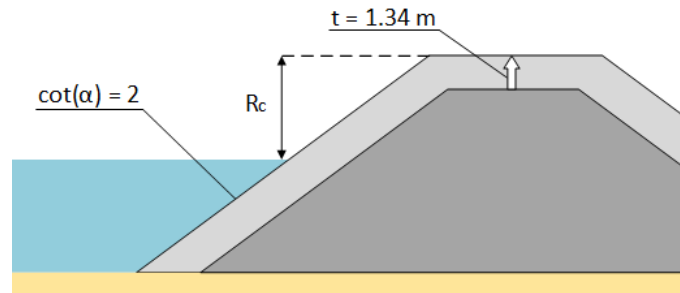
Figure 4.4: Dimensions of the armour crest level increase.

For the cost estimations in Chapter 5, two assumptions have been made for this adaption measure. If the armour crest is raised after a crest wall has already been placed, the combination of both measures is constructed as presented in Figure 4.5. The crest wall then no longer determines the crest height, but it is assumed that reduces material use by half for this measure. Another assumption for the cost estimation is that the crest width of the original breakwater is 8 m.
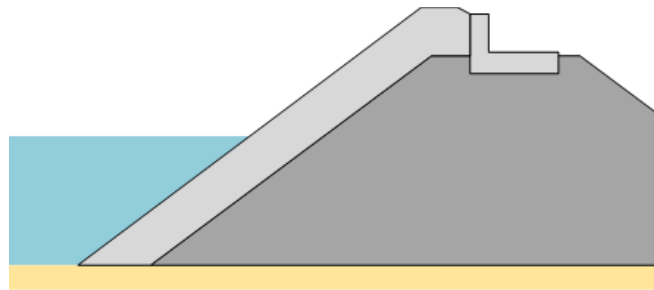
Figure 4.5: Configuration of adding a crest wall before increasing the armour crest level.

4.5.3. Raised foreshore bed level

The foreshore bed level could have various factors that limit its raise. An example could be that the difference in bed levels between the foreshore in front of the breakwater and the fairway of the port should not be too large, because the transition slope between the bed levels cannot be too steep and available space is limited. The limit set in this case study is that the foreshore must be well below low tide.

According to data from Waterinfo (Rijkswaterstaat, n.d.), NAP −1 m is considered low tide for the location of IJmuiden. The original bed level at the breakwater is NAP −8 m, see Section 4.3.2. Based on this information, the increase of the foreshore (F) is chosen to be 2 m. This corresponds to a new bed level of NAP −6 m.

Another important dimension is the length of the raised foreshore. EurOtop (2018) defines the minimum length of a foreshore as one wavelength. For the case study, the length of the raised foreshore is assumed to be one deep-water wavelength. Using the deep-water spectral wave period of 10.59 s in Section 4.3.1, the deep-water wave length and thus the foreshore length (L_F) is calculated to be 175 m. The dimensions of the raised foreshore are summarised in Figure 4.6.
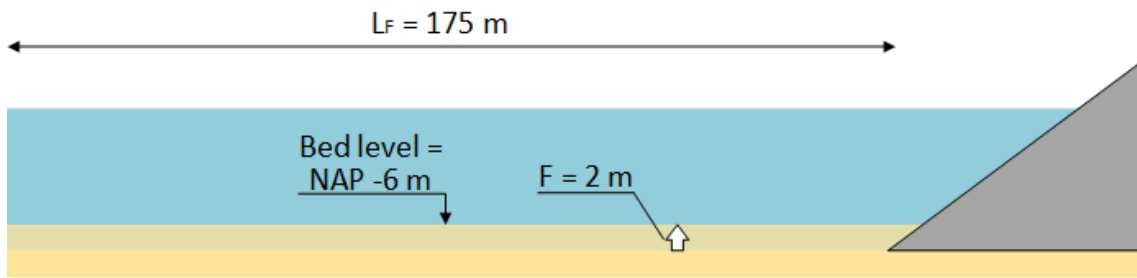
Figure 4.6: Dimensions of the raised foreshore bed level.

4.5.4. Additional low crested structure

Like the foreshore, the height of a low crested structure should for example be limited so it cannot be seen during low tide. So, the crest of the structure should remain below water during low tide, which was determined to be NAP −1 m in the previous section. However, if the crest height is NAP −1 m or lower, the used conditions fall just outside of certain validity ranges for the formula by Buis (2022). The parameters of structure height over water depth (h/d), wave steepness (H_s/L) and structure height over wave height (h/H_s) fall further outside of tested ranges for lower crest heights. The most important condition, namely freeboard over wave height (R_c/H_s), does fall within the tested ranges. Because the conditions outside of validity range are still very close to the limits, the formula by Buis (2022) will still be used for the creation of adaptation pathways.

For the case study, an offshore rubble mound breakwater is used as a low crested structure to reduce incoming wave heights. When constructed, the crest of the offshore breakwater is 6.95 m below the design water level (DWL). This design water level is the initial design water level of NAP +3.95 m plus the sea level rise value at the time of construction. The structural height of the offshore breakwater is thus higher if it is constructed at a higher sea level rise value.

The ideal placement of the low-crested structure is not determined. However, it is assumed that it is close enough to the breakwater, so the waves have experienced depth-induced breaking due to the foreshore before the waves arrive at the low-crested structure. This assumption is important for the overtopping calculation. For the cost estimation of the low-crested structure, the slope and crest width (B_c) are chosen to be 1:1.5 and 4 m respectively, see Figure 4.7.
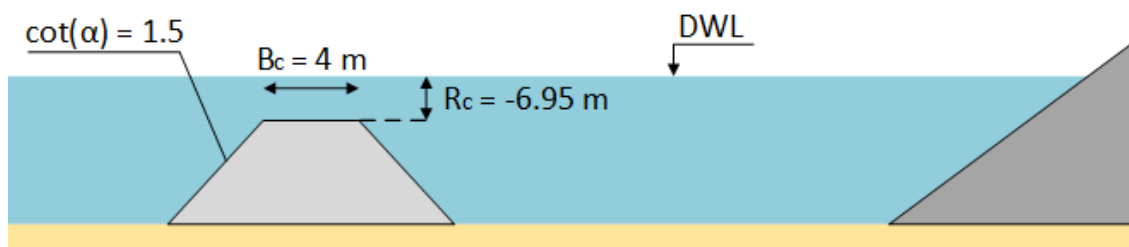
Figure 4.7: Dimensions of the low-crested offshore breakwater.

4.5.5. Additional berm

The dimensions of a berm do not have easily identifiable limitations. Examples are the logical restriction that the height of the berm should be equal or less than the armour crest, and that the width should not be too large for the load on the subsoil. Here, the berm dimensions are assumed such that the tipping points of adding the berm are comparable to the other adaptation measures.

The assumed width of the berm (B) is 10 m and the berm depth (h_b) relative to the design water level (DWL) is −1 m at the time of construction. The berm depth is negative because the berm is emerged when constructed. The slope of the berm embankment is important for the cost calculations in Chapter 5 and is assumed to be 1:1.5. The berm dimensions are summarised in Figure 4.8.
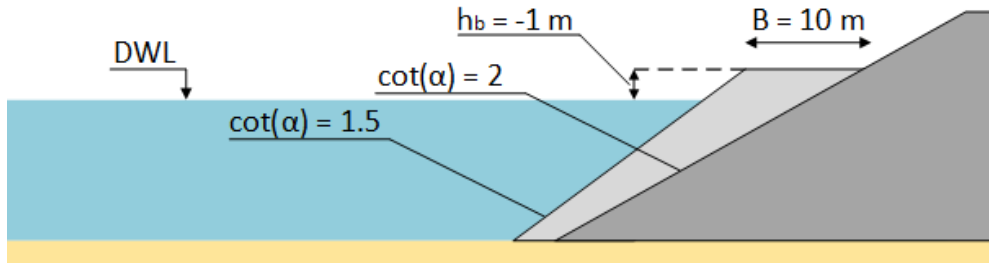
Figure 4.8: Dimensions of the additional berm.

The overtopping formula of Section 2.2.2 is made for slopes of 1:2, but the assumed berm embankment slope is 1:1.5. According to TAW (2002) and EurOtop (2018), the slope of a structure does not influence overtopping discharges for non-breaking waves. However, the results of Irías Mata and Van Gent (2023) indicate that the slope does affect overtopping, although these findings still need to be verified with physical model tests. Furthermore, Chen et al. (2020) showed that the upper slope above the berm has the most influence on overtopping, in terms of roughness. The same conclusion cannot immediately be made for the slope, but it does give an indication on the importance of the upper slope above the berm for overtopping.

Based on the reasons stated above, no influence of the slope has been accounted for the range of slopes in between 1:1.5 and 1:2. It is thus assumed the overtopping formula of Van Gent et al. (2022) can reasonably be used for the overtopping calculations with the berm.

4.6. Assumptions for cost estimation of adaptation measures
4.6.1. Material and construction cost
Generally, the cost of structures can be divided into investment costs and operation and maintenance costs. However, operation and maintenance costs are often difficult to estimate. For example, the morphological study needed to determine how often the foreshore should be nourished to maintain the foreshore at IJmuiden, is a research topic on its own. Therefore, only investment costs of the measures are included in the assessment.

Hogeveen (2021) already concluded that relatively little information on costs of the relevant materials and construction processes is publicly available. Appelquist & Halsnæs (2015) gave cost examples for rock armour structures and beach nourishments based on personal communication with Van Oord and Boskalis, which are two global dredging and offshore contractor companies. These cost examples are used for the material and construction costs in the case study. The assumptions are discussed below, and the results are summarised in Table 4.4.

For the rock armour structures, Appelquist & Halsnæs (2015) make a distinction between rock larger than 1 ton and 'mixed size' rocks. It is assumed that only the armour stones fall into the first category with a price of 30 €/ton and all other rock sizes are mixed size rock of 20 €/ton. A simple approximation for the cost of placement is used as the construction cost, which is 10 €/ton. There are also some indications for long-distance transport, but that is not considered here, because this would require more detailed information on the source location of the material.

For beach nourishments, most projects stay within the range of 1-10 €/m³ sand (Appelquist & Halsnæs, 2015). The prices can vary significantly based on location and can even increase up to 30 €/m³ sand for small projects in remote locations. For the case study, a price of 5 €/m³ sand is assumed, which is the average cost in Europe according to Appelquist & Halsnæs (2015).

The price of concrete depends on the required strength and steel reinforcement. However, because the crest wall has not been designed to this detail, the same cost for concrete as assumed by Hogeveen (2021) is used: 300 €/m³ concrete.

Table 4.4: Assumed material and construction costs (Appelquist & Halsnæs, 2015; Hogeveen, 2021).

Cost category	Value	Unit
Armour rock	30	€/ton
Non-armour, mixed size rock	20	€/ton
Rock placement	10	€/ton
Sand nourishment	5	€/m³
Concrete	300	€/m³

Based on the dimensions of Section 4.5, the volume of material per meter length of the breakwater can be calculated for all adaptation measures. For sand and concrete, the cost of adaptation measures can be calculated directly. Because the cost of rock is in ton, Equation 4.6 has to be used to convert the volume per meter to ton, so the cost of the adaptation measure can be determined. The assumed porosity is 0.4 based on data from the Rock Manual (CIRIA, 2007) and the density of rock is 0.27 ton/m³, as was already assumed in Section 4.4.1.

$$W = A \cdot \rho_s \cdot (1 - n_v) \tag{4.6}$$

With:

W	= Weight of the rock	[ton]
A	= Volume of rock per meter of breakwater	[m²]
ρ_s	= Density of rock	[ton/m³]
n_v	= Volumetric porosity of rock layer	[-]

There are several aspects stated below that are not considered here but could have a significant impact on the cost. This is important context for interpreting the results of the cost estimation in Chapter 5.

- The long-distance transport of armour rock. If the source location of the armour rock is relatively far from the construction site, this could increase the price significantly.
- The potential extra nourishments for maintenance of the foreshore. Maintenance costs are not considered, as stated in the beginning of the chapter. However, specifically for the nourishment of the foreshore, these costs could have a large impact on how economically attractive the adaptation measure is.
- The construction of the crest wall. The horizontal stability of a crest wall should be ensured by either using a shear-key (CIRIA, 2007) or an extended base slab (Vos-Rovers et al., 2008). In both cases, the placement of a crest wall after initial construction of the breakwater will require moving and repositioning of rock. This increases the construction cost of the crest wall.

4.6.2. Inflation and discount rate

To calculate the present value of the costs in the case study, the method described in Section 3.3 is used. For the use of inflation and discount rate, the timing of the tipping points must be known. As stated in Section 3.3, the timing of sea level rise values is determined here with interpolation, by using the median of the chosen sea level rise scenarios. If the sea level rise values fall outside of the used data, then no extrapolation is done for the calculation of present value. In that case, the year 2150 is used for the calculation, which is the last year in the used dataset of Garner et al. (2021). Furthermore, it is assumed that the cost data is accurate for the current year.

For the chosen method of Section 3.3, the inflation and discount rate have to be assumed. The influence of these assumptions is also checked in Chapter 5, in form of a sensitivity analysis.

In literature examples, the used discount rate for the economic evaluation of adaptation pathways varies from 3-4% (De Ruig et al., 2019; Haasnoot et al., 2020; Trommelen, 2022). All these evaluations also use some form of sensitivity analysis on the assumed discount rate. Another possible value for the discount rate is the social discount rate recommended by the Dutch government, which is 2.25% for standard situations (Rijksoverheid, 2020). For this social discount rate, a variation of +/- 0.4% is suggested for sensitivity analysis purposes. There is no significant reason to choose one of the suggested values over the other. Therefore, an initial discount rate of 3% is simply assumed for the case study, and a sensitivity analysis on the value of the discount rate is performed in Chapter 5.

The recent inflation trends highlight the volatile nature of inflation, which is not accurately considered when using average inflation rates. However, due to this same volatile behaviour, the average is the only realistic assumption that can be made. The average inflation rate of 2.1% for the Netherlands between 1990-2020 was determined by Hogeveen (2021) based on data of CBS. A similar value of 2% is used for this case study.

4.7. Concluding remarks

The case study is described in 3 steps:

1. The initial boundary conditions at IJmuiden (without sea level rise and adaptation measures) are determined to be the offshore significant wave height of 7.35 m, offshore spectral wave period of 10.59 s, the design water level of NAP +3.95 m and bed level at the toe of NAP −8 m. The main dimensions of the fictitious rubble mound breakwater are the slope of 1:2, the nominal diameter of the armour layer of 1.68 m, and the crest level of NAP +10.0 m.
2. The main characteristics of the five adaptation measures are assumed: The crest wall protrudes 1 above the armour crest level, the armour crest level is raised with 1.34 m, the bed level of the foreshore is raised with 2 m, the low-crested structure has a freeboard of −6.95 m and a slope of 1:1.5, and the berm is 10 m wide with a crest level at 1 m above design water level.
3. Assumptions necessary for the cost estimation of the pathways are made. The material and construction costs of armour rock, non-armour rock, sand, and concrete are 40 €/ton, 30 €/ton, 5 €/m^3, and 300 €/m^3, respectively. The assumed values of inflation and discount rate are 2% and 3%, respectively.

Now that the case study has been described, it can be used to test and apply the methods of Chapter 3 to create and select optimal pathways, which is done in the next chapter.

5. Creation and evaluation of adaptation pathways of the case study

In this chapter, the methods of Chapter 3 are applied to create and select optimal adaptation based on cost for the case study described in Chapter 4. Section 5.1 shows the adaptation pathway maps for the considered combinations of measures. Section 5.2 presents the cost estimations and in Section 5.3 the sensitivity analysis can be found. In Section 5.4, concluding remarks are stated.

5.1. Creation of adaptation pathway maps

Based on the assumed dimensions in section 4.4, the tipping point of the breakwater without any adaptation measures is 0.17 m of sea level rise. This is the starting point for all adaptation pathways. The tipping points of the pathways are calculated with the formulae of Section 2.2, and the changing wave loading due to depth-induced breaking is considered as described in Section 3.1.

All pathways consist of three measures and can at least adapt to 1.29 m sea level rise relative to the 1995-2014 baseline. This value of 1.29 m is the worst scenario considered in this case study, namely the 95th percentile of SSP5-8.5 LC in 2080, which is the assumed end of adaptation lifetime. The tipping points of the measures for all pathways are given in Appendix A. All sea level rise values are relative to the 1995-2014 baseline, consistent with the IPCC data used (Garner et al., 2021).

Because there are 60 possible combinations, including all pathways in one map does not give a clear overview. The pathways are therefore displayed in 5 different maps, one for each starting measure in Figure 5.1 through 5.5. The first map, Figure 5.1, also shows the timing of sea level rise for the median projections of the considered SSP scenarios.

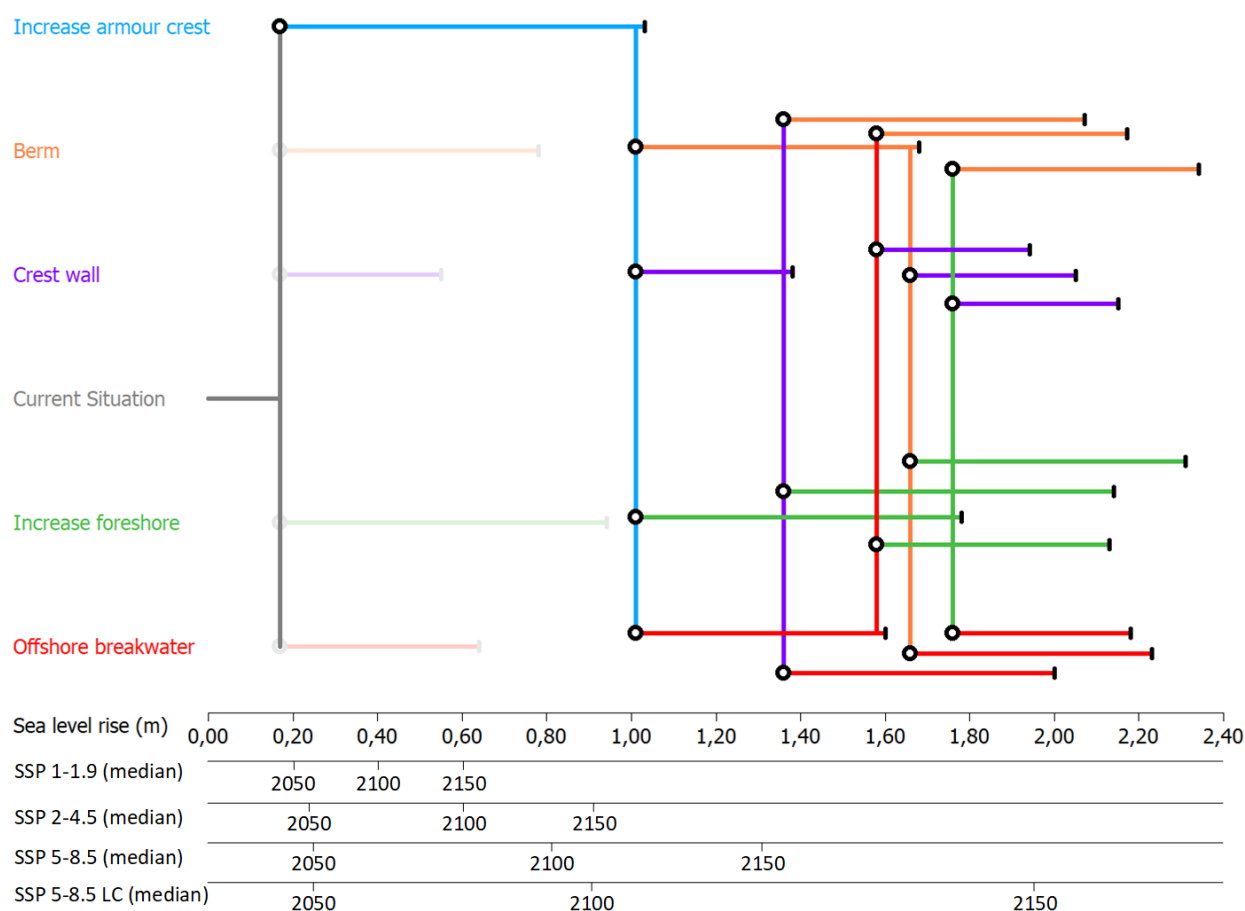Figure 5.1: Adaptation pathways starting with an increase of the armour crest level.
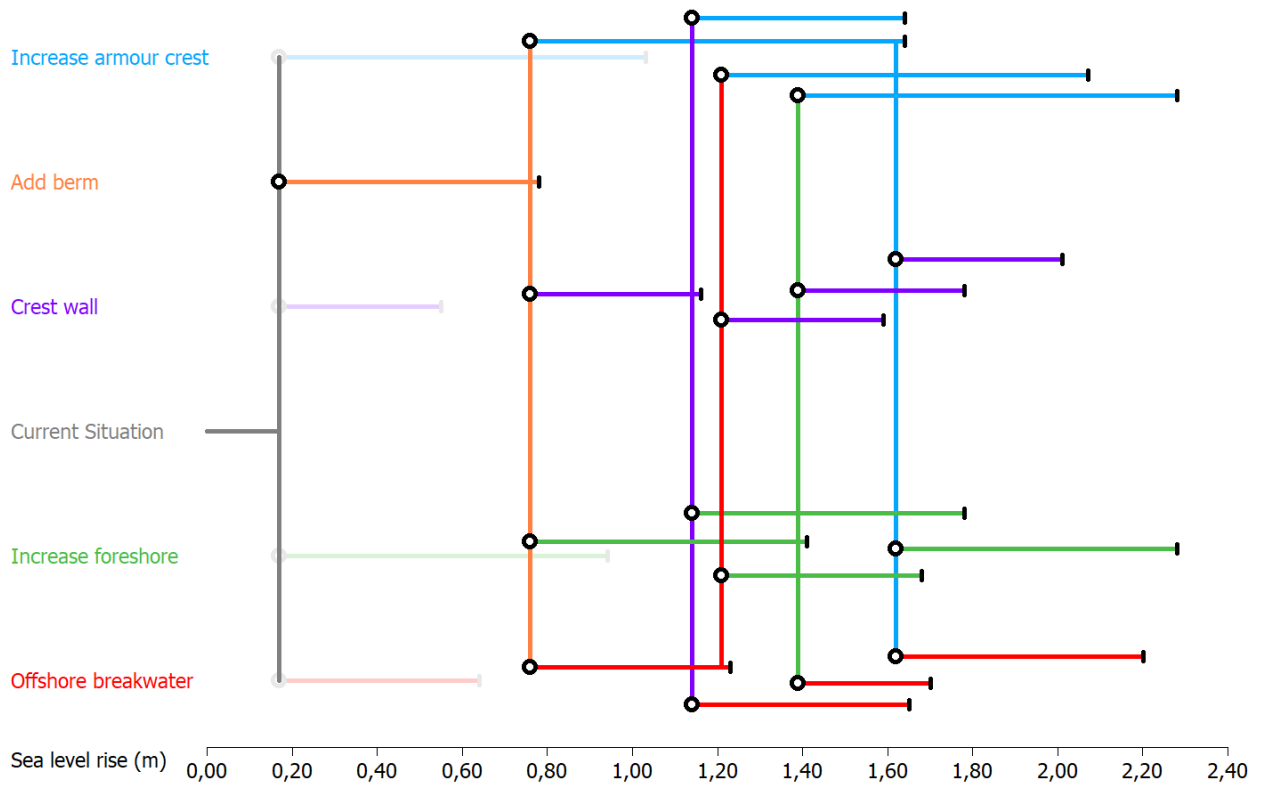
Figure 5.2: Adaptation pathways starting with the addition of a berm.
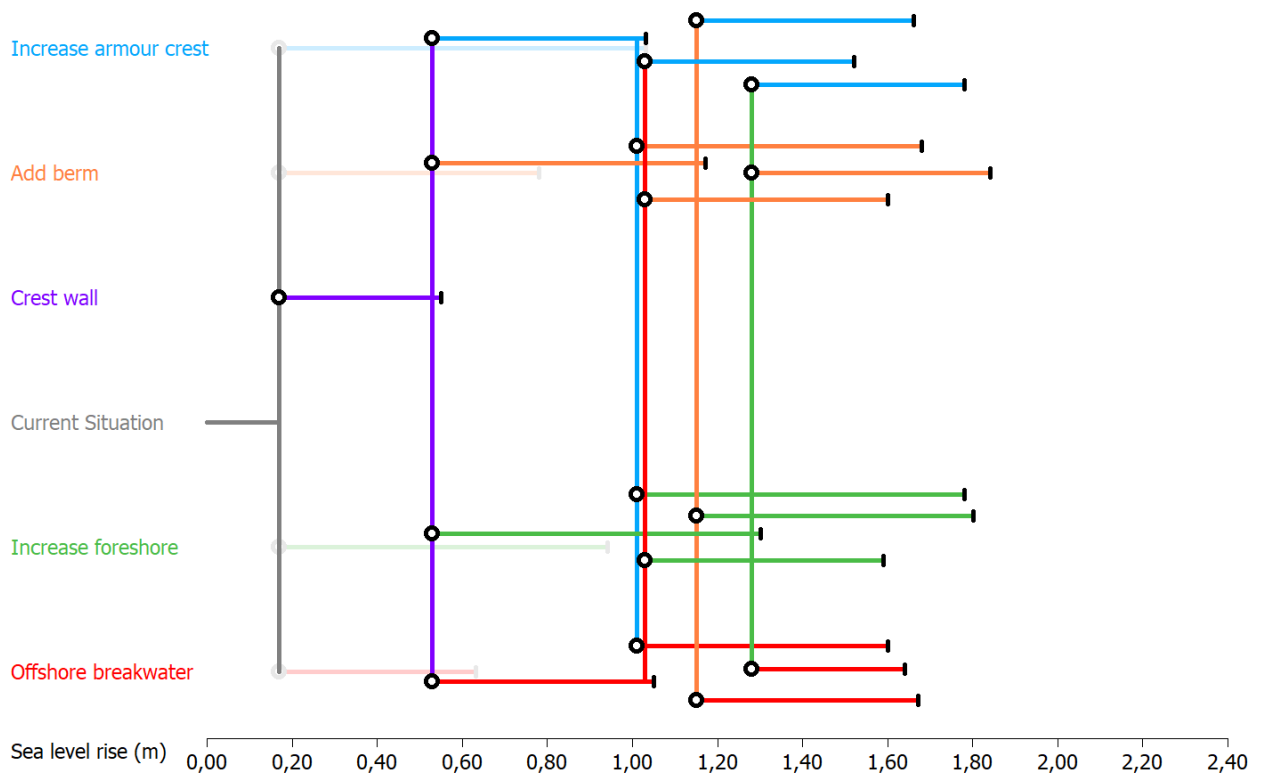
Figure 5.3: Adaptation pathways starting with the addition of a crest wall.
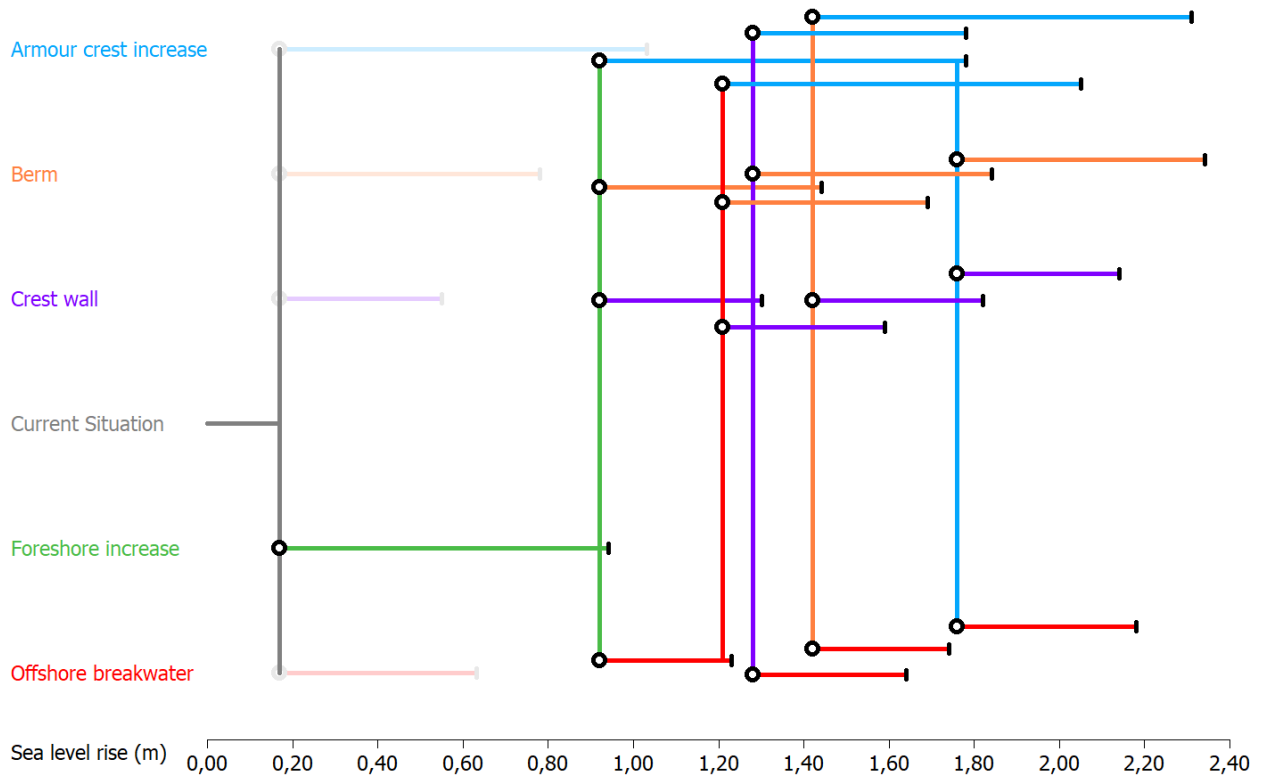
Figure 5.4: Adaptation pathways starting with an increase of the foreshore level.
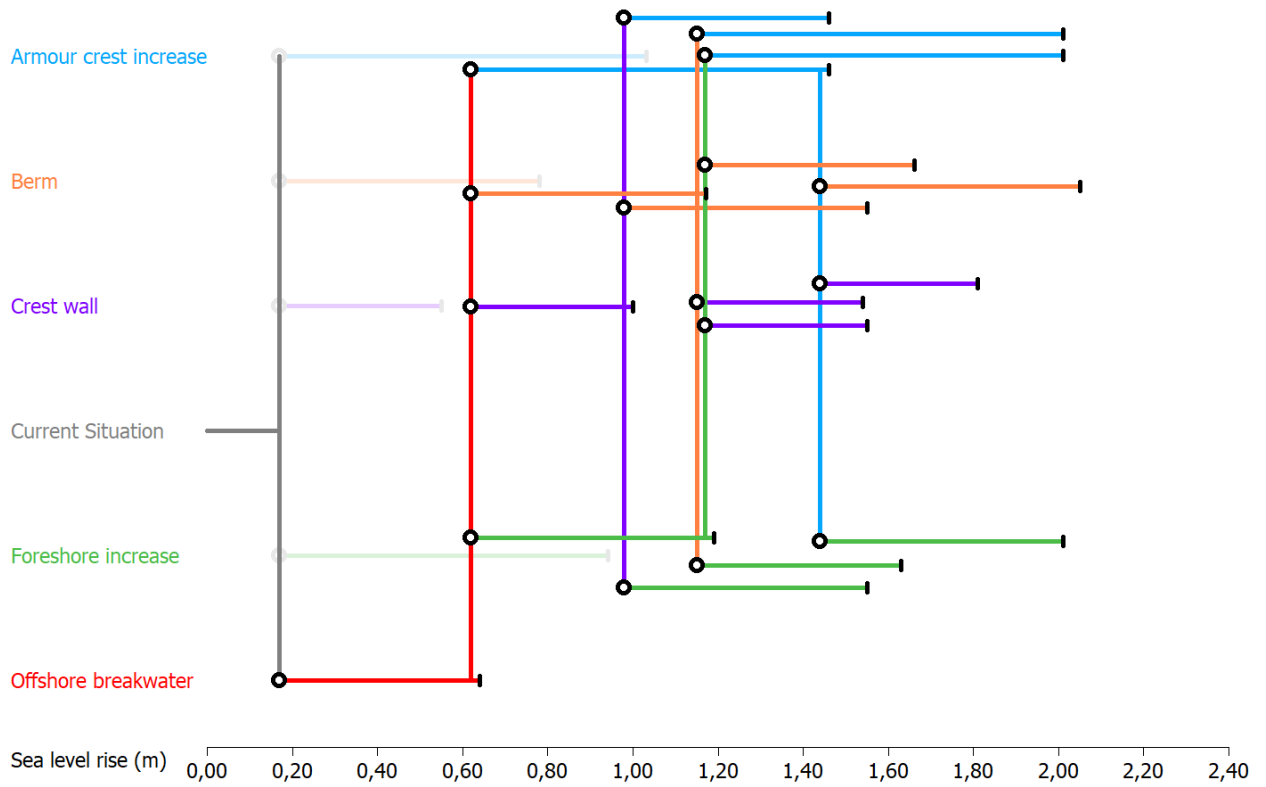
Figure 5.5: Adaptation pathways starting with the placement of an offshore breakwater.

The tipping point of a measure varies based on when the measure is applied and with which other measures it is combined. Below in Table 5.1, the tipping point and adaptation are given for the starting adaptation measures. This means it is applied at the tipping point of the original breakwater (0.17 m of sea level rise) and not combined with any other measure yet. For context, sea level rise values of the considered scenarios are given in Table 5.2, rounded to two decimals (Garner et al., 2021).

Table 5.1: Tipping points and adaptation per starting measure.

Starting adaptation measure	Tipping point (m)	Sea level rise adaptation (m)
Increase of armour crest level	1.01	0.84
Addition of berm	0.76	0.59
Addition of crest wall	0.53	0.36
Increase of foreshore level	0.92	0.75
Placing of offshore breakwater	0.62	0.45

Table 5.2: Sea level rise percentile ranges for each considered scenario: Median (17th - 83rd).

Year	SSP1-1.9	SSP2-4.5	SSP5-8.5	SSP5-8.5 LC
2050	0.20 (0.09 - 0.33)	0.25 (0.16 - 0.35)	0.27 (0.17 - 0.38)	0.27 (0.17 - 0.41)
2080[1]	0.34 (0.17 - 0.55)	0.45 (0.29 - 0.64)	0.55 (0.38 - 0.76)	0.57 (0.38 - 0.91)
2100	0.42 (0.22 - 0.66)	0.60 (0.41 - 0.84)	0.81 (0.57 - 1.12)	0.90 (0.57 - 1.36)
2150	0.61 (0.27 - 1.02)	0.93 (0.58 - 1.40)	1.31 (0.85 - 1.94)	1.96 (0.85 - 5.01)

[1]The assumed end of lifetime of the breakwater.

5.2. Evaluation of adaptation pathways

This section shows the cost evaluation of the pathways presented in Section 5.1. The costs of adaptation measures and pathways are estimated using the assumptions made in Chapter 4. The methods of Section 3.2, 3.3 and 3.4 are used to estimate costs of the pathways. Before these cost estimates are elaborated, the terminology used in this section is explained below. In this same order, these cost estimates are presented in this section.

- Cost. This considers inflation and discount rate, so it represents the present value cost of the pathways. The method of Section 3.3 is applied for the calculation of present value cost.
- Levelised cost. In addition to using present value, levelised cost considers the amount of sea level rise each adaptation measure can adapt to. Levelised cost is the cost per m sea level rise adaptation. The methods of Section 3.3 and 3.4 are both used.
- Expected levelised cost. The expected cost of pathways is determined by using model uncertainty of sea level rise projections. The method of Section 3.2.1 is combined with the methods of present value and levelised cost (Section 3.3 and 3.4).
- Combining all scenarios. All the previous cost estimates can be combined for all sea level rise scenarios, assigning weights to the considered scenarios as discussed in Section 3.2.2.

The complete overview of all adaptation pathway costs is given in Appendix B.

5.2.1. Cost estimation of adaptation measures

Before the costs of pathways are elaborated, the cost of each separate adaptation measure is calculated based on the assumed construction and material costs of Section 4.6.1 and the dimensions of the adaptation measures of Section 4.5.

The costs of the adaptation measures are dependent on the time of application due to inflation and discount rate. The dimensions and hence the cost of the low-crested offshore breakwater and the

berm also depend on the sea level rise at the time of application. The costs of adaptation measures in Table 5.3 are calculated for the year 2022. This corresponds to approximately 0.08 m of sea level rise relative to the 1995-2014 baseline for all considered SSP scenarios (Garner et al., 2021). The values in Table 5.3 are calculated as described in Section 4.6.1 and none of the methods of Chapter 3 are used yet. Because the costs are determined for the year 2022, there is no influence of inflation and discount rate.

Table 5.3: Cost of adaptation measures in 2022 at 0.08 m sea level rise.

Adaptation measure	Symbol	Cost (€/m)
Increase of armour crest level	A	5401
Addition of berm	B	4798
Addition of crest wall	C	1800
Increase of foreshore level	F	1750
Placing of low-crested offshore breakwater	L	3244

As stated in Section 4.6.1, the costs of measures are calculated per meter length of breakwater. The symbols in Table 5.3 will be used throughout this chapter to specify pathways. For example, if a berm is placed first (B), then the foreshore level is increased (F), and lastly the armour crest level is raised (A), the pathway is indicated with B-F-A.

The measures of adding a berm and increasing the armour crest level have much larger cost than the other measures. This is likely due to the high crest level of the breakwater itself. The dimensions and cost of these measures are namely dependent on the size of the original breakwater, while this is not the case for the other measures. In contrast, the relatively low water depth at the case location is beneficial for the cost of the increase of the foreshore level and the low-crested structure. Also noticeable is that the 3 measures consisting of rock material are the most expensive measures.

5.2.2. Cost estimation using present value

Based on the tipping points of Section 5.1 and the method in Section 3.3, the present value costs of all pathways are calculated. The 5 pathways with the lowest costs are presented in Table 5.4.

Table 5.4: The 5 lowest cost pathways based on present value.

Pathway	Cost per scenario (€/m)			
	SSP1-1.9	SSP2-4.5	SSP5-8.5	SSP5-8.5 LC
F-L-C	2564	2635	2965	3210
F-C-L	2652	2722	2978	3272
F-C-A	2713	2783	3041	3351
C-F-L	2796	3128	3295	3513
C-F-A	2857	3189	3358	3592

The pathways which include the cheapest measures (F and C) naturally have the lowest total cost. There are also some other patterns to be seen in Table 5.4, which are caused by the fact that the assumed discount rate (3%) is higher than the assumed inflation (2%):

- It is generally more beneficial to apply cheaper measures early and more expensive ones later. This can be seen when comparing Figure 5.6 and 5.7, in which the cost of pathways A-C-F and F-C-A are displayed. The same measures are applied but in different order. Measure F is much cheaper than measure A, see Table 5.3. The pathway F-C-A applies the cheaper measure first and the most expensive measure last, while A-C-F is the other way around, and this causes A-C-F to be twice as expensive.

- Extremer scenarios with higher sea level rise rates are more expensive than milder scenarios. Due to the faster rise of the sea level, the tipping points of measures are reached sooner, and the discount rate is applied over fewer years. This is especially true for measures applied second or third, which can be seen in Figure 5.7.

If the inflation is higher than the discount rate, the reverse of the above statements would be true.
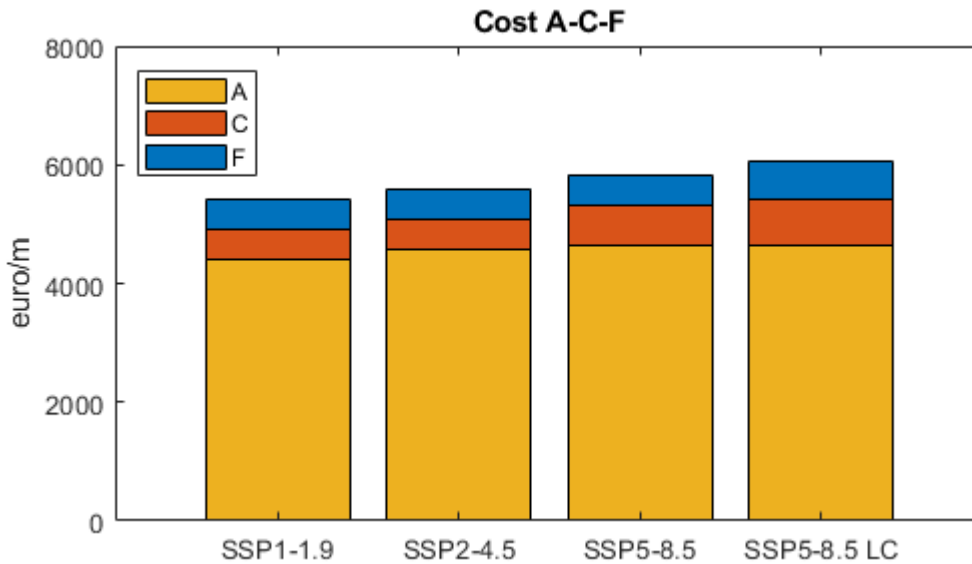
Figure 5.6: Cost per measure of pathway A-C-F for all considered IPCC scenarios.

Figure 5.7: Cost per measure of pathway F-C-A for all considered IPCC scenarios.

5.2.3. Cost estimation using present value and levelised cost

From the adaptation pathway maps, it is clear the pathways adapt to different values of sea level rise. Therefore, the method of Section 3.4 is used to calculate levelised cost of pathways, so a fairer comparison can be made between pathways. In this section it is simply assumed that the difference in sea level rise adaptation between the pathways is not significant, and the pathways can be compared fairly with levelised cost. This assumption is checked with a sensitivity analysis in Section 5.3, as recommended in the method of Section 3.4. In Table 5.5, the 5 lowest levelised cost pathways are presented.

Table 5.5: The 5 pathways with the lowest levelised cost and hence highest cost efficiency.

| Pathway | Levelised cost per scenario (€/m/m) | | | |
	SSP1-1.9	SSP2-4.5	SSP5-8.5	SSP5-8.5 LC
F-C-A	4944	5049	5716	6430
F-A-C	5173	5283	6065	6509
F-C-L	5429	5534	6217	7071
F-L-C	5488	5602	6658	7420
F-A-L	5843	5953	6734	7230

All SSP scenarios have the same top 5 and only SSP5-8.5 LC has a different ranking order, with F-A-L being cheaper than F-L-C. When comparing with the previous results using only present value of Section 5.2.2, relatively similar pathways are present in the top 5. In both this and the previous section, the cheapest pathways are combinations of F, C, A and L.

Based on the sea level rise adaptation of measures (Table 5.1) and the cost of starting measures (Table 5.3), it can be concluded that an increase of the foreshore level (F) has the lowest levelised cost as a starting measure. This is likely the reason every pathway of Table 5.5 starts with F. Figure 5.8 shows the levelised cost of pathway F-C-A for all scenarios. When comparing this to the total cost in Figure 5.7 of the previous section, it can also be seen that the contribution of measure F to the total pathway cost has decreased from approximately 50% to 33% when using levelised cost.

Figure 5.8: Levelised cost per measure of pathway F-C-A for all considered IPCC scenarios.

5.2.4. Cost estimation using present value, levelised cost & model uncertainty

This section adds the model uncertainty into the cost estimation, so the expected costs of pathways are calculated as described in Section 3.2.1. Before the results are presented, two key assumptions for the cost estimation using model uncertainty are repeated:

- 2080 is the end of adaptation lifetime of the breakwater assumed in Section 4.2.
- It is assumed that the trigger value for a new measure is equal to the tipping point of the previous measure. The implementation time needed for the measures of this case study is fairly, as the construction of complete breakwaters can be done in 1-2 years. Therefore, it is assumed the implementation time is negligible and the trigger value for a new measure equals the tipping point of the previous measure.

The range of expected levelised cost is given per starting measure in Table 5.6. Because the expected levelised cost is very dependent on the starting measure, it is chosen to give the results per group of pathways with the same starting measure. The range is given by stating the minimum and maximum expected levelised cost. The top 5 with the lowest expected levelised cost consists of pathways starting with F.

Table 5.6: Range of expected levelised cost per starting measure.

	Minimum and maximum of expected levelised cost per scenario (€/m/m)			
Starting measure	SSP1-1.9	SSP2-4.5	SSP5-8.5	SSP5-8.5 LC
F	1572 - 1578	1930 - 1949	2104 - 2216	2574 - 3019
C	3517 - 3913	4514 - 5504	4986 - 6723	5163 - 7382
A	4310 - 4312	5274 - 5280	5499 - 5548	5620 - 5992
L	5063 - 5261	6372 - 6941	6958 - 8188	7252 - 8838
B	5495 - 5547	6761 - 6914	7197 - 7731	7442 - 8573

The starting measure plays such a large role in the expected cost, because the second and third measures have a much lower probability of being applied before the end of adaptation lifetime, thus the expected cost of these measures is significantly lower or in some cases even negligible. Several factors combined cause this effect:

- The end of (adaptation) lifetime of the breakwater. For the case study, it is assumed that no adaptation measures are applied after 2080, so after approximately 50 years of use. However, the lifetime of a breakwater can also be around 100 years. Logically, a longer lifetime increases the probability of higher sea level rise and thus creates higher probability of two or three measures being necessary.
- The sea level rise scenario. For mild scenarios, the probability that the second or third measure is necessary is very low. The expected cost of a pathway is therefore almost equal to the cost of the first measure. For scenarios with higher sea level rise, it is more likely the tipping point of the first measure is reached before the end of adaptation lifetime and thus the expected cost of pathways increases. This effect is pictured in Figure 5.9 and 5.10, where the expected levelised cost for pathways F-C-A and C-F-A are shown for the different scenarios. The cost variance for pathways with the same starting measure also increases for more extreme scenarios, see Table 5.6.
- The tipping points of the measures. For pathways with starting measures with lower tipping point values, the probability of the second or third measure being applied is higher. This increases the expected cost and the cost variance between the pathways, which can be seen when comparing Figure 5.9 and 5.10. Measure F has a higher tipping point than C, so the probability that a second measure is necessary to apply for pathways starting with C is higher, thus the expected cost of the second measure in pathways starting with C is higher.

Figure 5.9 and 5.10 show that it is very likely only one adaptation measure is necessary for mild scenarios. However, measures adapting for sea level rise values such that likely only one measure is necessary, defeats the purpose of using adaptation pathways to avoid potentially unnecessary costs. So, this is an indication that the measures should be downsized in dimension to get the desired adaptive approach for mild scenarios. On the other hand, downsizing measures might drastically increase the number of measures necessary for extreme scenarios, which would be detrimental for the cost of pathways due to high fixed costs of e.g., construction equipment. Therefore, it is important to optimise the dimensions of the measures for the various sea level rise scenarios in a design or feedback loop. This is not done here but it is recommended for detailed pathway design.
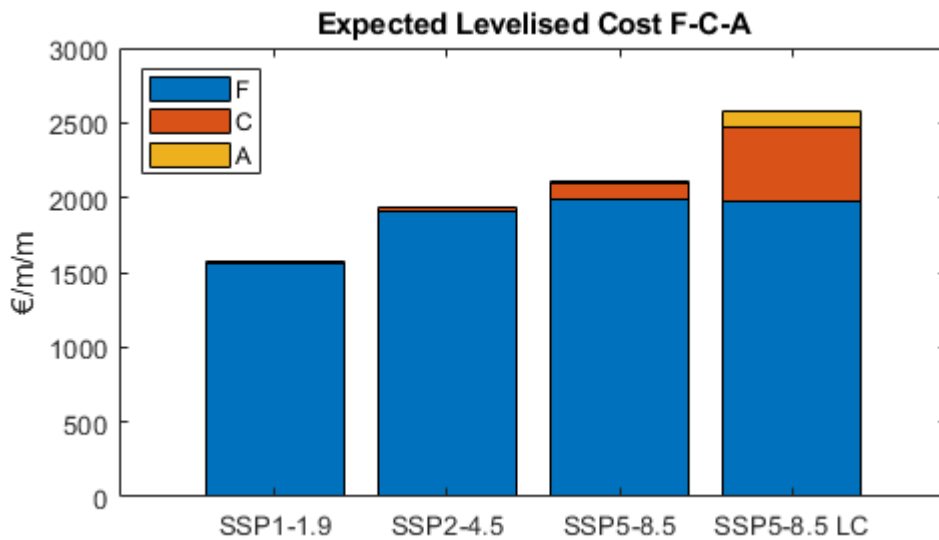
Figure 5.9: Expected levelised cost per measure of pathway F-C-A for all considered IPCC scenarios.

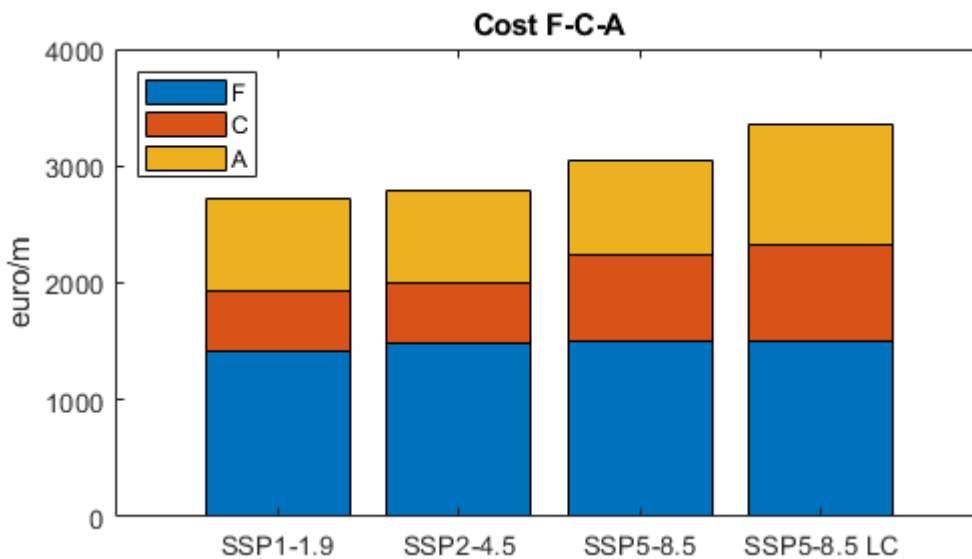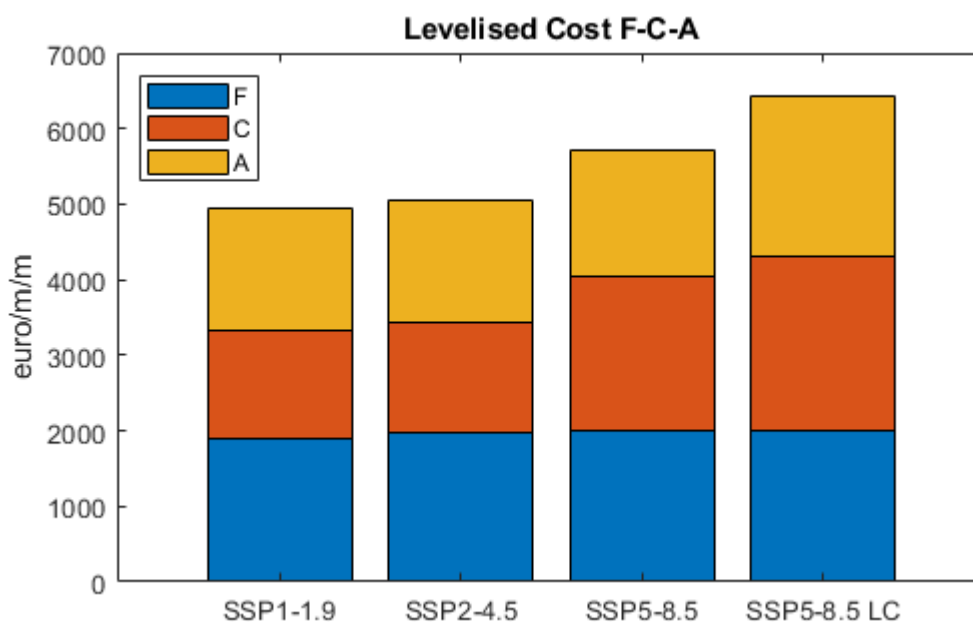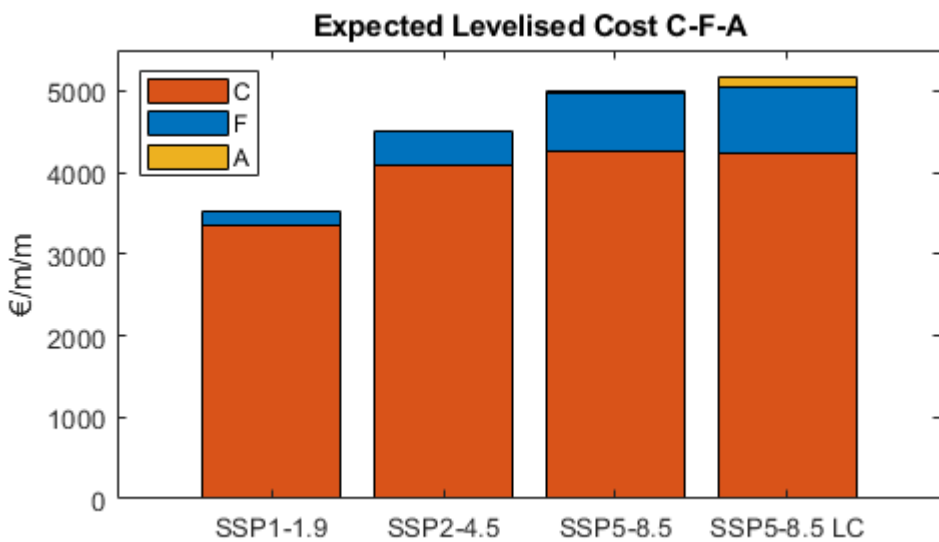Figure 5.10: Expected levelised cost per measure of pathway C-F-A for all considered IPCC scenarios.

5.2.5. Cost estimation using present value, levelised cost, model & scenario uncertainty

Finally, the scenario uncertainty is also included in the cost estimation. The method as described in Section 3.2.2 is used, so weights are assigned to each scenario to determine the cost. In this case study, it is assumed all scenarios have equal weight of 0.25 and thus the average cost is calculated.

Table 5.7 shows top 5 lowest cost pathways when averaging over all scenarios. The cost, the levelised cost and the expected levelised are all presented. This gives an overview of the cost estimation methods of the previous sections, averaged over all scenarios.

Again, pathways including the increase of a foreshore (F) and adding a crest wall (C) together with either the increase of armour level (A) or placing a low-crested offshore breakwater (L) have low costs.

Table 5.7: Top 5 pathways with lowest (expected) levelised cost, averaged over all scenarios.

Pathway	Cost (€/m)	Pathway	Levelised cost (€/m/m)	Pathway	Expected levelised cost (€/m/m)
F-L-C	2844	F-C-A	5535	F-C-A	2045
F-C-L	2906	F-A-C	5758	F-C-L	2054
F-C-A	2972	F-C-L	6063	F-C-B	2063
C-F-L	3183	F-L-C	6292	F-A-C	2064
C-F-A	3249	F-A-L	6440	F-A-L	2064

5.3. Sensitivity analysis of the cost estimation

In this section, a sensitivity analysis is performed to check the influence of several key assumptions on the selection of the optimal pathways. The sensitivity of the cost estimation results is checked for the following assumptions:

- The inflation and discount rate. These values were assumed in Section 4.6.2, but De Ruig et al. (2019) and Haasnoot et al. (2020) stress the importance of a sensitivity analysis.
- The minimum amount of sea level rise pathways can adapt to. In Section 5.1, it is stated that all pathways adapt to at least 1.29 m of sea level rise, but it varies from 1.44 m to 2.32 m. When comparing the pathways based on cost in Section 5.2, it is assumed that the difference in sea level rise adaptation between the pathways is not significant, and the pathways can be compared fairly. However, it can be argued that the difference in sea level rise adaptation is significant. Therefore, a sensitivity analysis is done to see what pathways are preferred for higher adaptation requirements. This is also recommended in the method of Section 3.4.
- The weights assigned to the SSP scenarios. In the method of Section 3.2.2, it is stated to assign equal weights to each considered sea level rise scenario to account for scenario uncertainty as an initial assumption. It is also recommended that the effect of assigning different weights to the considered scenarios on the results is checked with a sensitivity analysis, which will be done in this section.

5.3.1. Ratio of the inflation and discount rate

According to Haasnoot et al. (2020), the assessment of pathways is very sensitive to the discount rate because of the large time frames of adaptation pathways. Therefore, it is important to perform a sensitivity analysis for the assumed discount rate of 3%.

For this sensitivity analysis, only the value of the discount rate is varied, while the inflation is kept constant. For the assumptions of the inflation and discount rate, the most influential part is the ratio between the two factors. This is due to the way the factors are applied to obtain present values. For example, the difference between using 3% discount and 2% inflation opposed to 4% discount and 3% inflation is less than 1% in present value over 50 years. The ratio of the two factors is relatively similar so the resulting present value is similar. Therefore, it is chosen to only vary the discount rate to change the ratio between the inflation and discount rate and see whether this changes the preferred pathways.

Two variations of the discount rate are checked here. The original discount rate of 3% is changed to 2% and 4%. The original values have a ratio of approximately 1.01 (=1.03/1.02). The discount rate of 4% is the value used by De Ruig et al. (2019) and is used here to see how the preferred pathways change for higher discount rates. The ratio of inflation and discount rate is then 1.02 (=1.04/1.02).

For the discount rate of 2%, which is equal to the inflation, the calculation of present value no longer has any effect and postponed measures are not cheaper anymore. This value of 2% is also similar to the value recommended by the Dutch government, see section 4.6.2. For equal inflation and discount rate, the ratio of the factors is simply 1.

Discount rate of 2%

With an inflation and discount rate of 2%, the costs of adaptation measures are not dependent on time. This also means there is no difference in cost between the scenarios. The top 5 lowest cost pathways are presented in Table 5.8.

Certain measures (B, L) do have different dimensions and cost based on the sea level rise value when constructed, but the other measures (A, C, F) cost the same regardless of when they are constructed. This is also the reason why for example the levelised cost of C-A-F, C-F-A and F-C-A are the same.

Table 5.8: Top 5 lowest cost pathways for all scenarios with an inflation and discount rate of 2%.

Pathway	Cost (€/m)	Pathway	Levelised cost (€/m/m)	Pathway	Expected levelised cost (€/m/m)
F-L-C	5732	C-A-F	12960	F-C-A	2628
C-F-L	6040	C-F-A	12960	F-C-L	2649
F-C-L	6040	F-C-A	12960	F-A-C	2660
F-C-A	6251	A-F-C	13628	F-A-L	2661
C-F-A	6251	F-A-C	13763	F-A-B	2663

Discount rate of 4%

The discount rate of 4% is the same value as De Ruig et al. (2019) used for the economic assessment of adaptation pathways. With this higher discount rate, more expensive measures are economically more attractive to apply later. The difference between the cost of pathways for different SSP scenarios is increased and there is larger variation in preference of pathways for different scenarios. Table 5.9 shows the top 5 lowest cost pathways averaged over all scenarios.

Table 5.9: Top 5 lowest cost pathways for all scenarios with an inflation and discount rate of 4%.

Pathway	Cost (€/m)	Pathway	Levelised cost (€/m/m)	Pathway	Expected levelised cost (€/m/m)
F-L-C	1743	F-C-A	2920	F-C-A	1660
F-C-L	1749	F-A-C	2988	F-C-L	1662
F-C-A	1770	F-C-L	3088	F-C-B	1666
F-C-B	2001	F-A-L	3189	F-A-L	1670
C-F-L	2002	F-L-C	3233	F-A-C	1670

Conclusion

For this particular case study, different discount rates do not have a large impact on which pathways are preferred. For all the considered discount rates of 2, 3 and 4%, most of the preferred pathways include the increase of the foreshore level (F) and the addition of a crest wall (C). Even for the different discount rates, pathways F-C-A and F-C-L are still present in almost all top 5 lowest cost rankings. For a 2% discount rate, the increase of the armour crest level (A) is preferred slightly more than in the other cases. The discount rate of 4% causes higher variation in preferred pathways between the different scenarios.

5.3.2. Minimum sea level rise adaptation

In this section, a sensitivity analysis is performed to see what pathways are preferred for higher adaptation requirements. The minimum sea level rise adaptation levels of 1.75 m and 2 m are checked here. The sea level rise adaptation of the 60 pathways ranges from 1.44 m to 2.32 m relative to 1995-2014 baseline. Out of the 60 total pathways, 36 and 20 pathways can adapt to the respective minimum requirement of 1.75 m and 2 m sea level rise. The other pathways that cannot fulfil the requirements, reach the tipping point of the last adaptation measure before the required sea level rise value.

For the minimum adaptation level of 1.75 m, the top 5 lowest cost pathways out of the 36 eligible pathways are presented in Table 5.10. Even with this new requirement, all preferred pathways contain the increase of the foreshore level (F) and often in combination with the addition of a crest wall (C). The increase of the armour crest level (A) is preferred more often, while the low crested offshore breakwater (L) is preferred less than in the results of Section 5.2. Notably, the placing of a berm (B), the measure that was least often preferred in Section 5.2, is present in both top 5 rankings. Table 5.10 also shows that the F-C-A pathway scores best in total cost and in cost efficiency (levelised cost), similar to the results of Section 5.2.

Table 5.10: Top 5 lowest (levelised) cost pathways with minimum of 1.75 m of sea level rise adaptation.

Pathway	Cost (€/m)	Sea level rise adaptation (m)	Pathway	Levelised cost (€/m/m)	Sea level rise adaptation (m)
F-C-A	2972	1.76	F-C-A	4944	1.76
C-F-A	3249	1.76	F-A-C	5173	2.12
C-A-F	3494	1.76	F-A-L	5843	2.16
F-C-B	3694	1.82	F-L-A	5944	2.03
F-B-C	3817	1.8	F-C-B	5994	1.82

For the minimum adaptation level of 2 m, the top 5 lowest cost pathways out of the 20 eligible pathways are presented in Table 5.11. With this added requirement, all the preferred pathways in Table 5.11 contain a combination of F and A, instead of F and C like in Section 5.2 and Table 5.10. Both measures B and L are also present in two of the five preferred pathways. The pathways containing B seem to be a good option for high sea level rise adaptation. Measure C is only present in one of the preferred pathways, but it is the lowest cost pathway F-A-C.

Table 5.11: Top 5 lowest (levelised) cost pathways with minimum of 2 m of sea level rise adaptation.

Pathway	Cost (€/m)	Sea level rise adaptation (m)	Pathway	Levelised cost (€/m/m)	Sea level rise adaptation (m)
F-A-C	3958	2.12	F-A-C	5173	2.12
F-L-A	3996	2.03	F-A-L	5843	2.16
F-A-L	4289	2.16	F-L-A	5944	2.03
F-B-A	4911	2.29	F-A-B	6349	2.32
F-A-B	4921	2.32	F-B-A	6518	2.29

Conclusion

Setting a higher minimum sea level rise adaptation for pathways does have impact on which specific pathways are preferred but increasing the foreshore bed level is still the best measure to implement first. The measure which is most economically preferable to implement second or third, is dependent on the required sea level rise adaptation. The higher adaptation requirement also causes

the measure of increasing the armour crest level to have higher preference. When comparing to the results of section 5.2, it becomes clear that adding a berm is only economically attractive for higher sea level rise adaptation. Most notably, both in Table 5.10 and 5.11 the combination of F, A and C, although in different order, is the most preferable pathway in terms of cost.

5.3.3. Weights of sea level rise scenarios

The cost estimation method in Section 3.2.2 describes how to take into account scenario uncertainty when evaluating adaptation pathways. This method assigns weights to the scenarios to calculate the weighted average cost of pathways. Initially equal weights for all scenarios are used, but the weights should be varied to check the effect on the preferred pathways. Below, this sensitivity analysis is performed.

Before assigning different weights to the scenarios, it is first investigated whether the preferred pathways are significantly different between the sea level rise scenarios. This is checked using the results of Section 5.2.2 and 5.2.3. The cost estimation method that includes present value, levelised cost and model uncertainty is not used here because the difference between pathways is so small it is difficult to select individual preferred pathways, see Section 5.2.4.

The rearranged results of Section 5.2.2 and 5.2.3 in Table 5.12 and 5.13 show that the sea level rise scenarios do not differ significantly in preferred pathways. Moreover, the preferred pathways are identical in terms of ranking when evaluating with present value cost (Table 5.12) and almost identical when using present value and levelised cost (Table 5.13). The only difference in Table 5.13 is that the SSP5-8.5 LC scenario has a different order in ranking the 4th and 5th most preferred pathway compared to the other scenarios, shown bold in Table 5.13.

Table 5.12: Top 5 preferred pathways based on present value cost.

	Preferred pathway per scenario (present value only)			
Rank #	SSP1-1.9	SSP2-4.5	SSP5-8.5	SSP5-8.5 LC
1	F-L-C	F-L-C	F-L-C	F-L-C
2	F-C-L	F-C-L	F-C-L	F-C-L
3	F-C-A	F-C-A	F-C-A	F-C-A
4	C-F-L	C-F-L	C-F-L	C-F-L
5	C-F-A	C-F-A	C-F-A	C-F-A

Table 5.13: Top 5 preferred pathways based on levelised cost with present value.

	Preferred pathway per scenario (present value, levelised cost)			
Rank #	SSP1-1.9	SSP2-4.5	SSP5-8.5	SSP5-8.5 LC
1	F-C-A	F-C-A	F-C-A	F-C-A
2	F-A-C	F-A-C	F-A-C	F-A-C
3	F-C-L	F-C-L	F-C-L	F-C-L
4	F-L-C	F-L-C	F-L-C	**F-A-L**
5	F-A-L	F-A-L	F-A-L	**F-L-C**

Conclusion

The sea level rise scenarios do not differ significantly in pathway preference. Therefore, it can be concluded that giving different weights to the scenarios would not have significant effect on which pathway is preferred. For this case study, the distribution of the weights assigned to scenarios does not have a significant impact on the results.

5.4. Concluding remarks

Optimal adaptation pathways of the case study

In Section 5.2, it can be seen in all different cost estimations, pathways that include the increase of the foreshore level (F) and the addition of a crest wall (C) perform best. These measures can be combined with all other measures to obtain an economically viable pathway. Pathways F-C-A and F-C-L are in the top 3 lowest costs for all different cost estimations. Section 5.3 shows that changing the assumed discount rate and weights assigned to the sea level rise scenarios does not have a significant impact on the results. The required minimum sea level rise adaptation for pathways does influence which pathways are preferred, but similar pathways to those found in Section 5.2 arise as the best options.

The results of Section 5.2 and the sensitivity analysis of Section 5.3 show that for this case study, pathways that combine the increase of the foreshore bed level, the addition of a crest wall, and the increase of the armour crest level are optimal based on cost. Although the preferred order of the adaptation measures is dependent on the minimum required sea level rise adaptation, it is generally optimal to raise the foreshore level as the first adaptation measure.

Reflecting on the methods to implement sea level rise uncertainty in cost estimation

In Chapter 3, the second research sub-question is answered by suggesting two methods, one to include the model uncertainty and one to deal with the different sea level rise scenarios.

The method to include model uncertainty is used in Section 5.2.4. The results of this cost estimation showed very little distinction between pathways with the same first adaptation measure, making it difficult to determine specific optimal pathways. This is due to low probability of the second and third measures being applied, and thus the cost of the first measure having by far the largest contribution to the expected cost. This effect is explained in Section 5.2.4 and is further discussed in Chapter 8. Despite this effect, using the model uncertainty gives insight into the best adaptation measure to start with (raising the foreshore bed) and how likely measures are to be applied, which is valuable for decision-making.

The method to deal with the different sea level rise scenarios is used in Section 5.2.5 and the sensitivity analysis is performed in Section 5.3.3. For this case study, there is almost no difference in preferred pathways between the scenarios. Therefore, applying different probabilities or weights to the scenarios for the weighted average does not change which pathways are preferred. Notably, the previous research by Hogeveen (2021) also found that the same pathways were preferred regardless of the sea level rise scenario.

Next chapters of the thesis

The tipping points of the measures in the case study are determined with estimates and empirical expressions, because numerical and physical models are time-consuming and expensive. However, the expressions of Van Gent et al. (2022) are based on conditions in which no significant wave breaking occurs on the foreshore. Significant wave breaking can occur for the conditions considered here, especially when raising the foreshore bed, so the expressions are used outside of the tested validity range. Furthermore, simple empirical estimates of the method described in Section 3.1 are used to account for depth-induced breaking. Therefore, it is not clear whether the tipping points of the preferred pathways with a raised foreshore bed level are accurately calculated in Section 5.1. For that reason, the accuracy of the empirical estimates for depth-induced wave breaking and overtopping expressions is checked with numerical models in the following chapters to answer the first and third research sub-question. Preferably, physical model tests would be used to check this accuracy, but due to lack of resources numerical models are used instead.

6. Set-up of numerical models for validation of empirical formulae

This chapter describes the numerical models which are used to validate the empirical relations used in the case study. The models are based on the same IJmuiden case. The exact tipping points of the pathways are not determined with the models as that is very time-consuming, but the accuracy of the empirical estimates is checked in a more general approach. First, the choice for the software is explained. The OpenFOAM model used for wave transformation and overtopping, and the XBeach model used for wave transformation are described in Section 6.2 and 6.3, respectively.

6.1. Software choice

The numerical models must be able to compute the wave transformation on the foreshore or the overtopping at the rubble mound breakwater, or both. The choice for each numerical model is elaborated below. Two different numerical model set-ups are used to compare the accuracy of the empirical relations presented in Section 2.2 and Section 3.1:

1. OpenFOAM model. Both the wave transformation on the foreshore and the overtopping at the breakwater are simulated in OpenFOAM.
2. XBeach model. XBeach is used to compute only the wave transformation on the foreshore.

OpenFOAM

OpenFOAM is a Computational Fluid Dynamics (CFD) software, which is based on the Reynolds-Averaged Navier-Stokes equations and the volume of fluid method. OpenFOAM has often been used in recent studies to model wave overtopping at coastal structures (Irías Mata & Van Gent, 2023; Chen et al., 2021; Hogeveen, 2021). Moreover, OpenFOAM can compute wave-structure interaction for porous structures like rubble mound breakwaters (Jensen et al., 2014; Jacobsen et al., 2018).

While multiple studies have used OpenFOAM to compute wave overtopping, the results of Lashley et al. (2020) indicated that OpenFOAM was often less accurate than other models in simulating wave transformation on a foreshore. The OpenFOAM model underestimated significant wave heights due to excessive wave dissipation and overestimated the spectral period compared to physical model tests. In addition, the other used models (SWAN, SWASH, XBeach, BOSZ) required significantly less computational time. Irías Mata and Van Gent (2023) showed that the combination of detailed turbulence models and porous media is not properly solved in OpenFOAM, but detailed turbulence models were not required to obtain accurate results. However, this study specifically investigates wave breaking on the foreshore, which was not the case in the study of Irías Mata and Van Gent (2023), so it is unknown whether accurate results are obtained without detailed turbulence models.

Thus, OpenFOAM can be used for the wave transformation on the foreshore, but the accuracy of the results is unknown, especially because there is no physical model data to compare with. Therefore, another numerical model is used to compare with the wave transformation results of OpenFOAM.

XBeach

There are multiple tools or wave models which are commonly used for wave propagation and transformation in coastal waters, such as SWAN, SWASH or XBeach. Here, XBeach non-hydrostatic (NH) mode is used to compare with the wave transformation results of OpenFOAM. Lashley et al. (2020) concluded that XBeach-NH showed good accuracy for wave transformation on shallow foreshores with reasonable computational demand. The XBeach-NH model of Lashley et al. (2020) accurately reproduced the mean water level, the significant wave height, and spectral period of the physical model tests (within 15% error). Of the considered models, only SWASH and XBeach surf-beat mode had comparable accuracy. Because these models with reasonable accuracy have similar computational time, XBeach-NH is chosen here without any further reasoning.

6.2. OpenFOAM model set-up

6.2.1. General settings

The version of OpenFOAM used for the numerical models includes multiple additional tools and extensions. The waves2foam toolbox developed by Jacobsen et al. (2012) is applied for the generation and absorption of free surface waves by means of relaxation zones. To account for porous structures, the equations of Van Gent (1995a,b) as implemented by Jensen et al. (2014) are used. Lastly, the IsoAdvector method created by Roenby et al. (2016) to improve the sharpness at the water and air interface is included. The specific set-up of the OpenFOAM model is further elaborated in this section.

6.2.2. OpenFOAM test programme

Chapter 5 showed that the optimal pathways for the case study are a combination of the measures F, C, and A. Based on those results, raising the foreshore bed level (F) is the most effective adaptation measure and is thus the focus in the numerical simulations. The addition of a crest wall (C) is also included in the numerical simulation, because it performed well in the evaluation of Chapter 5, and it is commonly used in modern breakwater designs (Van den Bos & Verhagen, 2018). The combination of raising the foreshore bed and adding a crest wall also performed well in the cost evaluation, so it is included in the numerical model. Heightening the armour crest level (A), although it is included in the optimal pathways of Chapter 5, is not researched here.

Table 6.1 shows the parameters that have been varied for the different OpenFOAM model configurations. Most values correspond to the values as presented in the IJmuiden case study of Chapter 4 and 5, but there are some key differences:

- Multiple offshore wave periods are tested. In Section 4.3, only the spectral wave period ($T_{m-1,0}$) of 10.59 s was determined for the offshore wave conditions. The theoretical deep-water ratio T_p / $T_{m-1,0}$ = 1.1 is used to determine the peak period as 11.65 s. This peak period of 11.65 s corresponds to a relatively high wave steepness of 3.5%. A higher peak period of 15.5 s, corresponding to a spectral period of 14.09 s, is also tested, which results in a lower wave steepness of 2.0%. A lower wave steepness is included to see potential effects of the wave steepness on the effectiveness of the measures. The wave conditions with peak period 11.65 s are referred to as high wave steepness, and the conditions with peak period 15.5 s are referred to as low wave steepness.
- The foreshore bed level is also raised with 4 m (F=4 m). The case study only investigated the original bed level of NAP −8 m (F=0 m) and raising the foreshore bed level with 2 m (F=2 m).
- Only the sea level rise values of 0, 1, and 2 m are simulated in OpenFOAM. In the case study, the sea level rise increased in steps of 0.01 m and tipping points for each measure were determined. Finding tipping points for the adaptation measures in the OpenFOAM model would be very time-consuming due to the iterative process of finding tipping points (see Appendix A). Therefore, a more general approach is taken here with only three variations of sea level rise.

Table 6.1: Tested variations for parameters in the OpenFOAM simulations based on the IJmuiden case.

Parameter	Symbol	Tested values	Unit
Peak period	T_p	11.65, 15.5	s
Foreshore toe bed level raise	F	0, 2, 4	m
Crest wall height	C	0, 1	m
Sea level rise	SLR	0, 1, 2	m

The significant wave height is not varied. The offshore significant wave height is calibrated to be approximately 7.35 m, see Section 6.2.6. 18 configurations are tested for the peak period of 11.65 s, but only a subset of 8 simulations have been performed for the peak period of 15.5 s. A full overview of the test programme can be found in Appendix C.

6.2.3. Definition of the numerical flume and grid

Figure 6.1 shows the lay-out of the numerical flume for F=0 m where the bed level at toe of the breakwater is equal to the original level of NAP −8 m. All dimensions and characteristics of the breakwater are equal to those determined in Chapter 4. In total, the model domain is 695 m long and 36 m high.
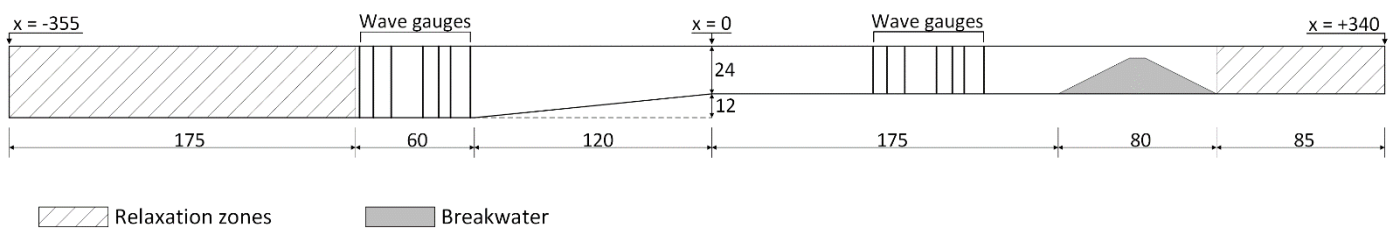
Figure 6.1: OpenFOAM numerical flume lay-out.

The flume bed consists of two horizontal parts connected by a 1:10 slope. At the inlet (left in Figure 6.1), the water depth without sea level rise is approximately three times the significant wave height to avoid wave breaking. The toe water depth at the right horizontal part (without sea level rise and adaptation measures) is equal to 11.95 m as determined in Section 4.3.2. For F=0 m, the length of the horizontal foreshore before the structure is 175 m, which corresponds to one deep-water wavelength based on a spectral period of 10.59 s (high wave steepness). This foreshore length is assumed to be long enough for waves to adjust to the reduced water depth.

When the foreshore is raised as an adaptation measure, the 1:10 slope is continued up until the new raised bed level. This means that if the foreshore is raised with 2 m, the width of the slope is increased with 20 m and the width of the right-hand horizontal part is decreased with 20 m, see Figure 6.2. This means a reduced horizontal foreshore length is applied for shallower foreshores, which can be justified partly by the fact that the local wavelength reduces due to the reduced water depth.
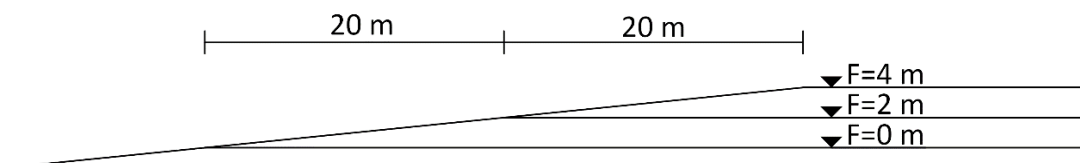
Figure 6.2: Bathymetry of the numerical flume for different foreshore bed levels.

The left relaxation zone and the right relaxation zone are approximately one deep-water wavelength (175 m) and half a deep-water wavelength (85 m) respectively, based on the spectral period of 10.59 s. Furthermore, the position of the wave gauges was determined with a MATLAB script provided by Deltares, based on the modified ELA method of De Ridder et al. (2023). The offshore wave gauges are located from x= −180 m to x= −121.7 m and the wave gauges near the structure are positioned at x=81.7 m to x=140 m. The exact positions are displayed in Table 6.2.

Table 6.2: Positions of the wave gauges in the numerical models.

Gauge #	Offshore gauge x-coordinate (m)	Nearshore gauge x-coordinate (m)
1	-180.00	81.70
2	-171.25	90.45
3	-162.48	99.22
4	-146.55	115.15
5	-138.58	123.12
6	-132.21	129.49
7	-121.70	140.00

The grid in OpenFOAM is made with the utilities blockMesh and snappyHexMesh, with square cells as recommended by Jacobsen et al. (2012). The cell size of the base grid is chosen to be 1x1 m squares. This choice is based on a sensitivity analysis which is elaborated in Section 6.2.5. Further refinements of the grid are made around the water surface, the crest wall, and parts of the foreshore bed.

Previous studies by Jacobsen et al. (2018), Chen et al. (2021), Irías Mata and Van Gent (2023) respectively used 13 to 19 cells per wave height, 9 to 14 cells per wave height and 8 to 11 cells per wave height at the water surface. Here, a similar resolution near the water surface of approximately 15 cells per wave height is used (0.5x0.5 m). An extra level of refinement around the crest wall is added, like Jacobsen et al. (2018) and Irías Mata and Van Gent (2023) did, resulting in 0.25x0.25 m cells. The foreshore bed is refined once at the wave shoaling and breaking area, following the same approach as Irías Mata (2021) who also had a foreshore with changing water depth.

The crest wall, the foreshore and any additional foreshore height are removed from the numerical domain and grid with snappyHexMesh. Slip and zero gradient conditions are applied at all these boundaries.

6.2.4. Modelling of porous media and turbulence

To account for the porosity of the rubble mound breakwater, the porousWaveFoam extension implemented by Jensen et al. (2014) based on Van Gent (1995a,b) is used. This extension applies constant eddy-viscosity outside porous media and a Forchheimer type of equation for dissipation inside porous media. The Forchheimer equation uses two closure coefficients α_F and β_F, which depend on grading and shape of the grains. Here, the coefficients found by Van Gent (1995a,b) are used, so $\alpha_F = 1000$ and $\beta_F = 1.1$. Jacobsen et al. (2018) showed that this is a good estimation for a range of data sets. Furthermore, a porosity value of 0.4 is assumed.

Irías Mata and Van Gent (2023) concluded that using the above method to account for porous media cannot be properly combined with a detailed turbulence model. The added turbulence model results in extra resistance in the porous media flow, causing higher water levels in the structure and larger overtopping discharges. Therefore, no turbulence closure model is added.

6.2.5. Sensitivity analysis and selection of the grid size

Three grid sizes are examined to check whether the results of the model are dependent on grid size, and to decide which grid size should be used. A coarse, medium and fine grid are used, corresponding to base cell sizes in x and y direction of 2 m, 1 m, and 0.5 m respectively. The medium grid size corresponds to the grid size described in Section 6.2.3. Because there are no physical model tests to use as a reference and to test the accuracy of the results, this analysis only checks the convergence of the results.

The main comparison between the grid size is made with the water surface elevation, significant wave height, the spectral wave period and overtopping volume. The cumulative overtopping volume over time is displayed in Figure 6.3. The water surface elevation, wave height and period are compared using unseparated wave signals of 141 uniformly spaced wave gauges from x= −245 m to x= 175 m. Figure 6.4 shows the minimum, mean and maximum water surface elevation at all wave gauges for the three grid sizes. In Figure 6.5 and Figure 6.6, the significant wave height and spectral period are shown respectively.

The overtopping volume in Figure 6.3 clearly displays large differences and even divergence of results when refining the grid. However, the fine grid is already very computationally demanding, so no further refined grid sizes are investigated.
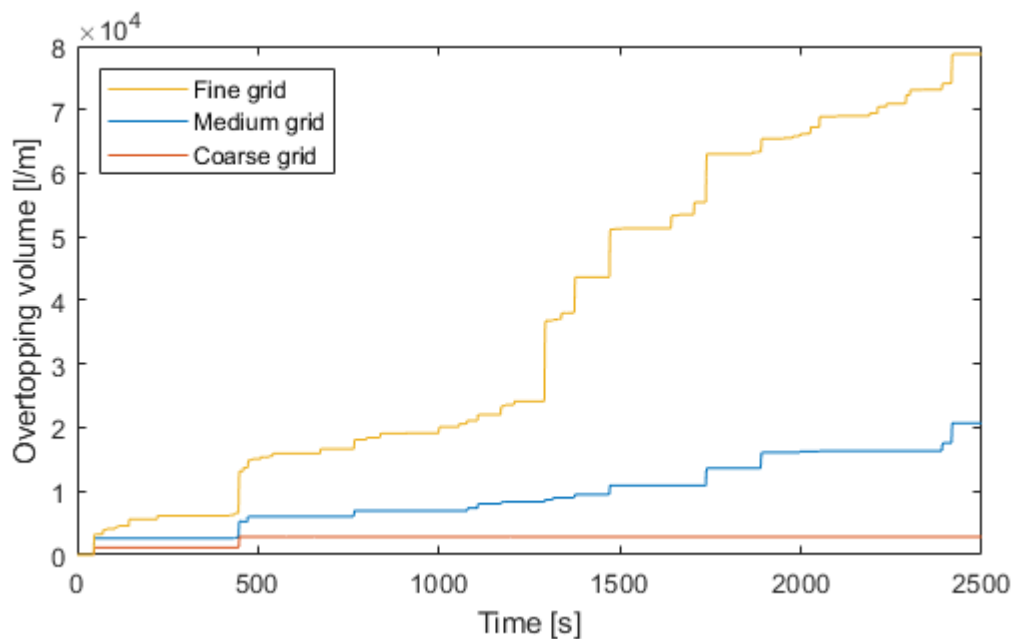
Figure 6.3: Cumulative overtopping volume over the total simulation time.
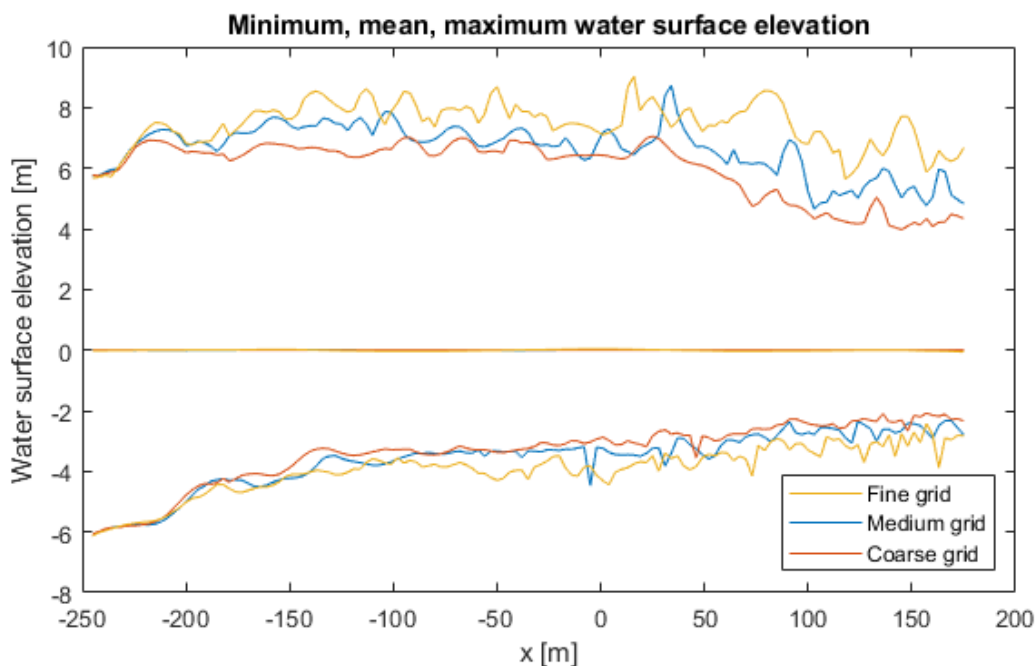
Figure 6.4: Minimum, mean, maximum surface elevation from x=−245 m to x=175 m.

53
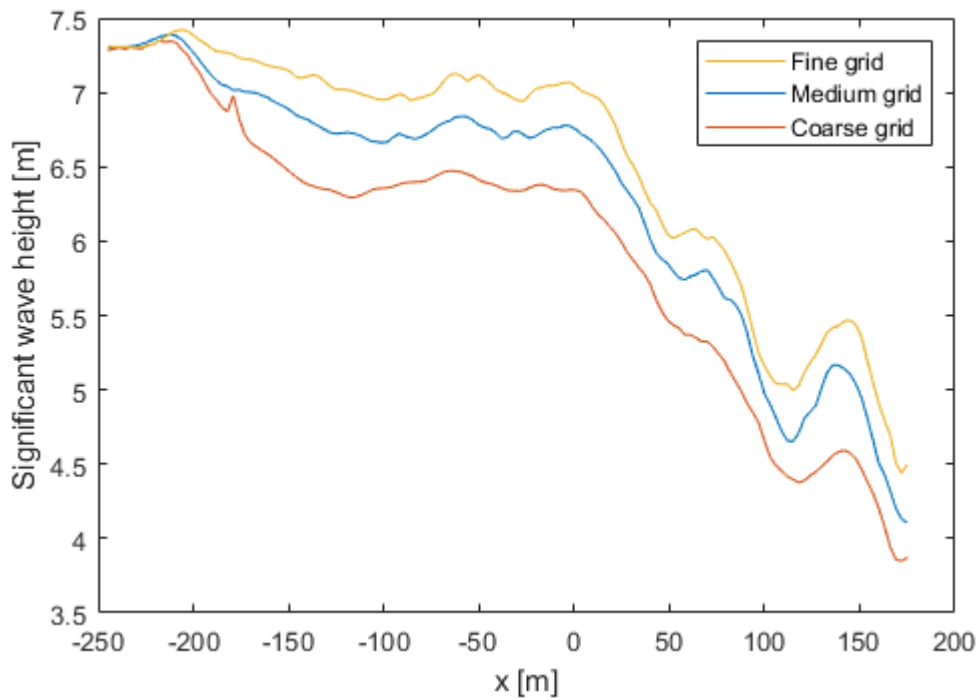
Figure 6.5: Significant wave height from x=−245 m to x=175 m.
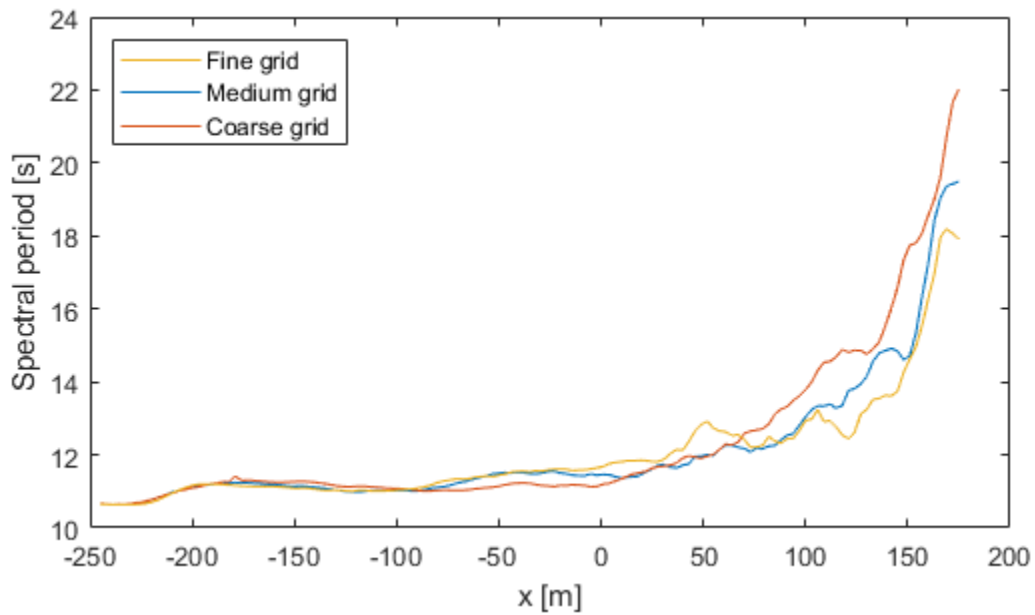
Figure 6.6: Spectral period from x=−245 m to x=175 m.

The water elevation data, significant wave height and spectral period show a reasonable similarity but there is no clear convergence of the results. However, the significant wave height is already different for the different grid sizes at the end of the relaxation zone at x=−180. To create a fair comparison, the input significant wave height in the models with medium and coarse grid is increased with a factor, the so-called gain factors. This is done to have approximately the same wave height for each model at the end of the relaxation zone and the start of the computed domain at x=−180 m.

Figures 6.7 and 6.8 show the comparison between the models with and without gain factors, levelised based on the wave height of the model with the fine grid. Although, the significant wave height still differs between the grid sizes at the end of the relaxation zone, the difference is now less than 2%. With gain factors, there is still no convergence for the significant wave height. However, the difference between the fine and medium grid is less than 10% at the toe of the breakwater. Notably, numerical instability seems to occur in and at the end of the relaxation zone for the coarse grid.
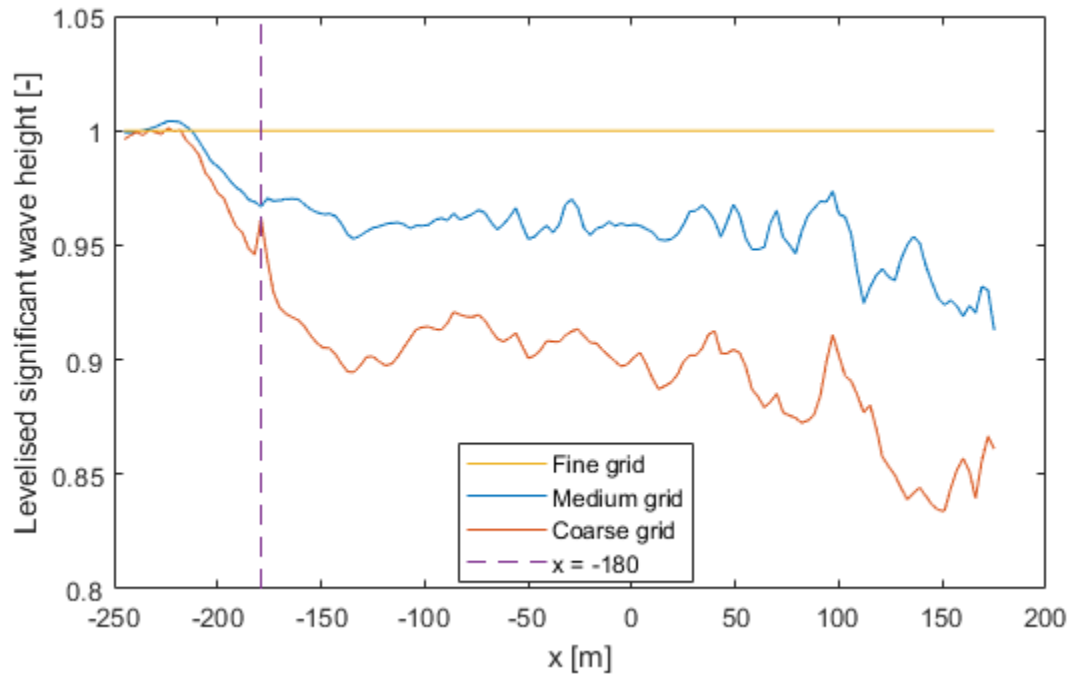
Figure 6.7: Significant wave height levelised based on the fine grid.
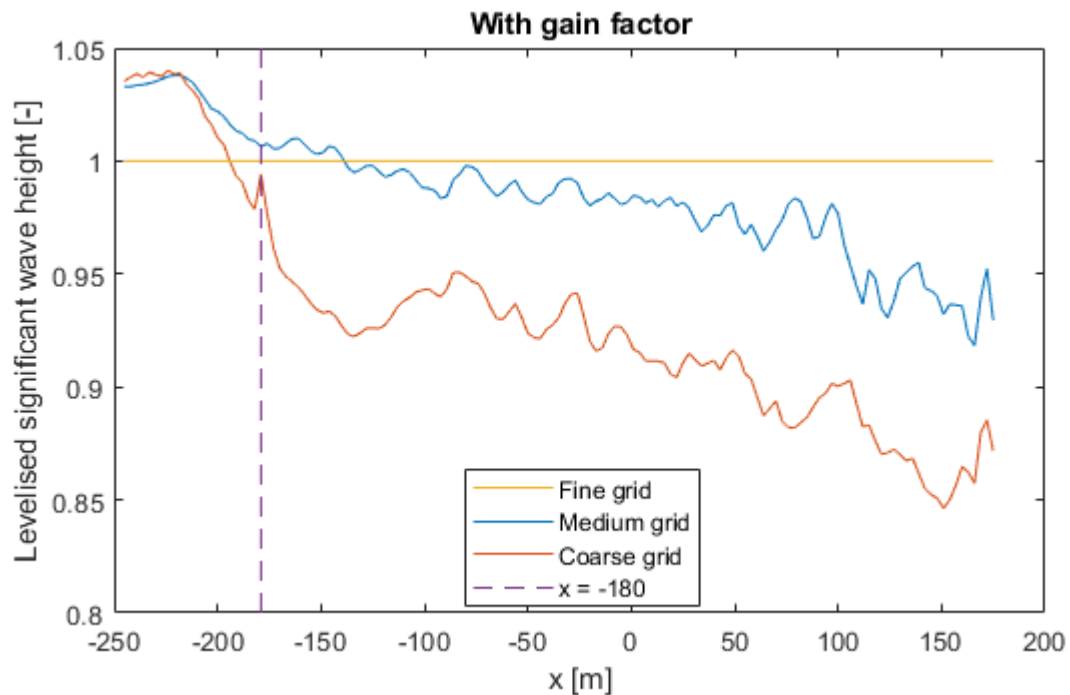
Figure 6.8: Significant wave height levelised based on the fine grid, including gain factors for the coarse and medium grid.

Conclusion

The overtopping discharge is dependent on the chosen grid size. The water surface elevation varies less due to the grid size but still shows no convergence when refining the grid. Furthermore, finer grids show less wave energy dissipation, which agrees with previous work using waves2Foam (Conde, 2019). The fine grid has very high computational demand and the coarse grid seems to show numerical instability in the relaxation zone (Figure 6.5, 6.7, 6.8). A trade-off between accuracy and computational time is reached with the medium grid size, which is selected to use in the OpenFOAM model. The grid size dependency is important context for the numerical results of Chapter 7, especially for the wave overtopping. It should be noted that the results with a fine grid, which is assumed to be closer to reality, can lead to wave heights at the toe of the structure that are about 7% higher than those obtained with the applied medium grid.

6.2.6. Calibration of the wave input

For all simulations, approximately 1000 waves are generated to obtain a representative average overtopping discharge for the chosen wave conditions. The incoming waves are generated using the external forcing 'irregularFast' (Jacobsen, 2017). This allows wave input in the form of a JONSWAP spectrum. The most important parameters to define the spectrum are the peak wave period (T_p), significant wave height (H_{m0}) and peak enhancement factor (γ). A typical value of 3.3 is used for the peak enhancement factor. The offshore significant wave height of 7.35 m was determined in Section 4.3. As elaborated in Section 6.2.2, peak periods of 11.65 s and 15.5 s are tested, corresponding to deep-water spectral periods of 10.59 s and 14.09 s, respectively.

Normally, when using numerical models as an addition to physical experiments, wave conditions in the numerical model are calibrated based on the measurements of the physical model. Here, the calibration of the wave conditions is done with the deep-water wave conditions as stated above. The objective is to have the significant wave height equal to 7.35 m and spectral period equal to 10.59 s or 14.09 s at the end of the inlet relaxation zone (x= −180 m). The calibration is performed based on the offshore wave gauges from x= −180 m to x= −121.7 m. The wave signal is separated using the modified ELA method of De Ridder et al. (2023). Only the case with no sea level rise or adaptation measures is calibrated and this calibrated input is used for the other cases as well.

Calibration high wave steepness

First, the significant wave height is calibrated. An initial input significant wave height of 7.35 m results in a significant wave height of 6.375 m of the incoming wave signal at x= −180 m. The gain factor to obtain 7.35 m is 1.1529 (=7.35/6.375). The new input of the significant wave height is then 8.474 m. With this new input, the new incoming significant wave height is 7.241 m. This is only a 1.5% difference compared to the target of 7.35 m and thus no further iterations are performed for this calibration.

For a peak period of 11.65 s, the spectral period is 10.93 s for the incoming wave signal at x= −180 m. Because this is already relatively close to the target spectral period of 10.59 s, with a deviation of approximately 3%, no calibration is performed.

Calibration low wave steepness

Based on the wave calibration with the high wave steepness conditions, an initial input of 8.474 m for the significant wave height is tested. The corresponding incoming wave height of 7.54 m is too high. An input significant wave height of 8.15 m results in a wave height of 7.27 m, which is considered satisfactorily close to the target of 7.35 m (1% difference).

For a peak period of 15.5 s, the spectral period at the offshore wave gauges is equal to 14.21 s. This deviates less than 1% from the target spectral period of 14.09 s, so the peak period is not changed.

6.3. XBeach model set-up

6.3.1. General settings

Arguably the most important setting of an XBeach model is the chosen hydrodynamic option. As stated in Section 6.1, the XBeach model used for wave transformation on the foreshore, will be used in the non-hydrostatic (NH) mode. Using NH mode in XBeach allows to model the propagation and dissipation of individual waves by using the non-linear shallow water equations with a pressure correction term (XBeach User Manual, 2020). Specifically, the two-layer non-hydrostatic mode (NH+) is implemented here to improve the dispersive behaviour. Because the model is used for wave transformation only, morphological changes and sediment transport are not modelled. More information on the shallow water equations, the non-hydrostatic pressure correction, and the reduced two-layer model can be found in the XBeach User Manual (2020).

The XBeach model is made using an XBeach MATLAB toolbox called Open Earth Tools (OET). With the MATLAB functions of OET, the text files necessary to run XBeach are created. For many settings, the default values of XBeach (version 1.23.5526, XBeachX release) are used, thus no further explanation on these parameters is given. Non-default input, for example the chosen bathymetry and wave input, are elaborated in this section.

6.3.2. XBeach test programme

The XBeach model is used to check only the wave transformation. Therefore, only the parameters that affect the wave transformation are relevant for the XBeach simulations. The breakwater and consequently the crest wall are not simulated in XBeach. Other than this change, the tested variations for XBeach given in Table 6.3 are identical to the OpenFOAM programme. Similar to the OpenFOAM simulations, only an offshore significant wave height of approximately 7.35 m is tested. A full overview of the test programme can be found in Appendix C.

Table 6.3: Tested variations for parameters in the XBeach simulations based on the IJmuiden case.

Parameter	Symbol	Tested values	Unit
Peak period	T_p	11.65, 15.5	s
Foreshore toe bed level raise	F	0, 2, 4	m
Sea level rise	SLR	0, 1, 2	m

6.3.3. Numerical flume and grid

The numerical flume is very similar to the flume modelled in OpenFOAM. However, because the XBeach model only computes the wave transformation and not the overtopping discharge at the breakwater, the breakwater is omitted in XBeach. This has the advantage that the XBeach flume has no wave reflection from wave interaction with the breakwater.

For the bathymetry in the XBeach models, two slightly different set-ups are used for high and low wave steepness simulations. The reason for this difference is based on the wave calibration and is further explained in Section 6.3.4. Below, the bathymetry for the XBeach simulations is elaborated.

For the high wave steepness simulations, the first part of the bathymetry of the XBeach model is equal to the bathymetry of the OpenFOAM model described in Section 6.2.3. The difference between the numerical flumes is that the numerical flume in XBeach is extended with a horizontal part of 200 m and a 1:50 slope which stops at 1 m above the initial water level. The 1:50 slope functions as a beach to dissipate wave energy and prevent reflection, because the standard

absorbing-generating boundary condition (abs_1d) does not work properly for the non-hydrostatic mode.

Figure 6.9 shows the bathymetry of the XBeach model for high wave steepness, with the original bed level at the toe and 0 m sea level rise, in which y=0 m equals NAP −20 m. The bathymetry of the simulations with low wave steepness is only slightly different. The starting point of the model is changed from x=−355 m to x=−210 m. This only shortens the horizontal part on the left-hand side of the bathymetry. The reason behind this change is explained in Section 6.3.4.
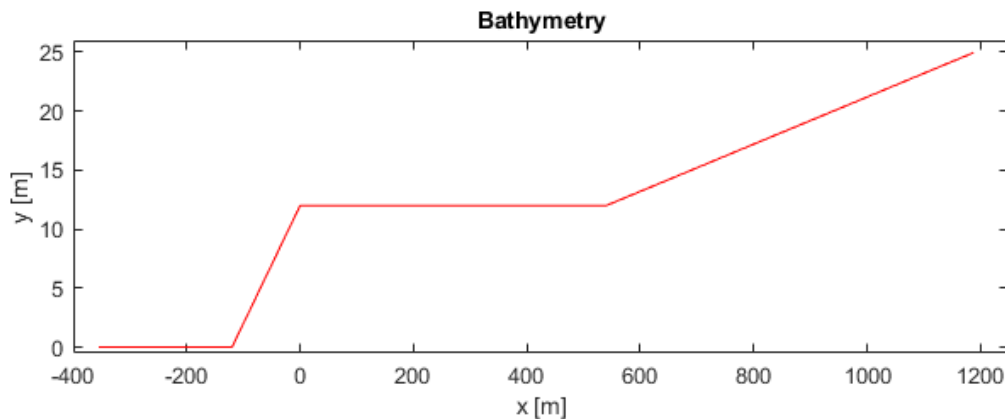
Figure 6.9: Bed level for XBeach model with high wave steepness, original bed level and 0 m sea level rise.

The model grid is made using the xb_grid_xgrid function of OET, which creates a model grid based on the bathymetry and additional parameters such as the Courant number and the incident short wave period. Non-default input for this function are the Courant number of 0.55, and the corresponding water level and wave period for each simulation. It is also specified in the grid function that the simulation is non-hydrostatic. Figure 6.10 shows the cross-shore grid resolution for the model with original bed level at the toe and 0 m sea level rise. For the grid cell sizes, no distinction is made between the high and low wave steepness simulations.
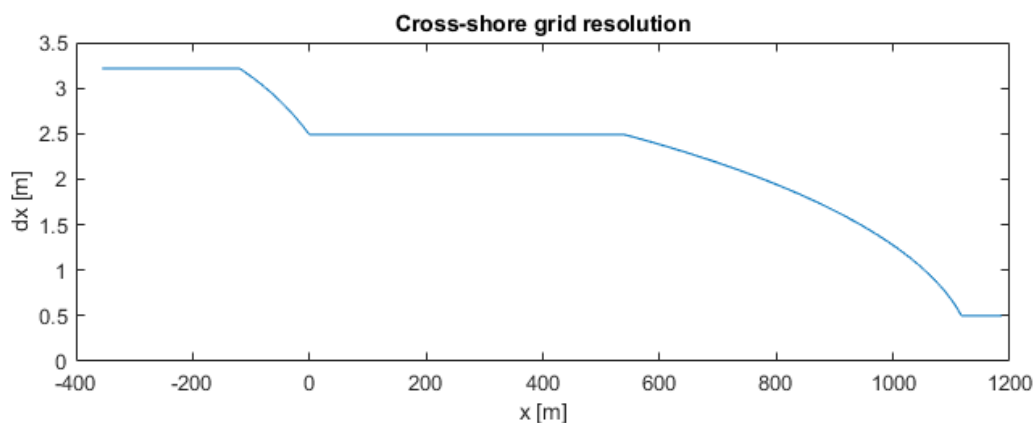
Figure 6.10: Cell size (dx) along the flume for the model with original bed level at the toe and 0 m sea level rise.

The output point locations in XBeach are chosen to contain the same locations as the wave gauges placed in OpenFOAM. The same wave signal separation method of De Ridder et al. (2023) is used to fairly compare the wave conditions at these locations.

6.3.4. Calibration of the wave input

The wave input type used in XBeach is the same as in OpenFOAM. Again, a JONSWAP spectrum with a shape factor of 3.3, a significant wave height of 7.35 m and peak period of 11.65 s or 15.5 s is used for the initial wave input. However, to get a fair comparison between the wave transformation in XBeach and OpenFOAM, it is important that the offshore wave conditions are equal or at least similar. Therefore, the offshore wave gauges (x= −180 m to x= −121.7 m) are used to calibrate the offshore wave conditions of XBeach to those of OpenFOAM. Identical to the procedure in Section 6.2.6, the calibration is performed for the case with 0 m sea level rise and no adaptation measures, and this newly found input is applied to every case.

Calibration high wave steepness

First, the significant wave height is calibrated. The initial input of 7.35 m results in an incoming wave height of 6.849 m. Therefore, a gain factor of 1.073 (=7.35/6.849) is applied to get a new input of 7.89 m. This new input results in an incoming wave height of 7.255 m, comparable to the 7.241 m of OpenFOAM. This is a deviation from the target wave height of 7.35 m of approximately 1% and thus no further calibration is done for the significant wave height.

Next, the spectral and peak wave periods are calibrated. The initial input peak period of 11.65 s results in an incoming spectral period of 11.84 s. This differs significantly from the target spectral of 10.59 s. However, to decrease the $T_{m-1,0}$ towards the target value, the input T_p would have to be decreased. The result would be that the offshore JONSWAP spectra of the OpenFOAM and XBeach models have significantly different energy distributions. Having similar wave spectra is considered to be more important than having a similar spectral period, thus no calibration factors are applied to the input peak period.

Figure 6.11 below shows the spectra of the incoming wave signal at x=−180 m for the XBeach and OpenFOAM simulations with 0 m sea level rise and no adaptation measures applied. This shows reasonable similarity for the wave input of both models for the high steepness waves.
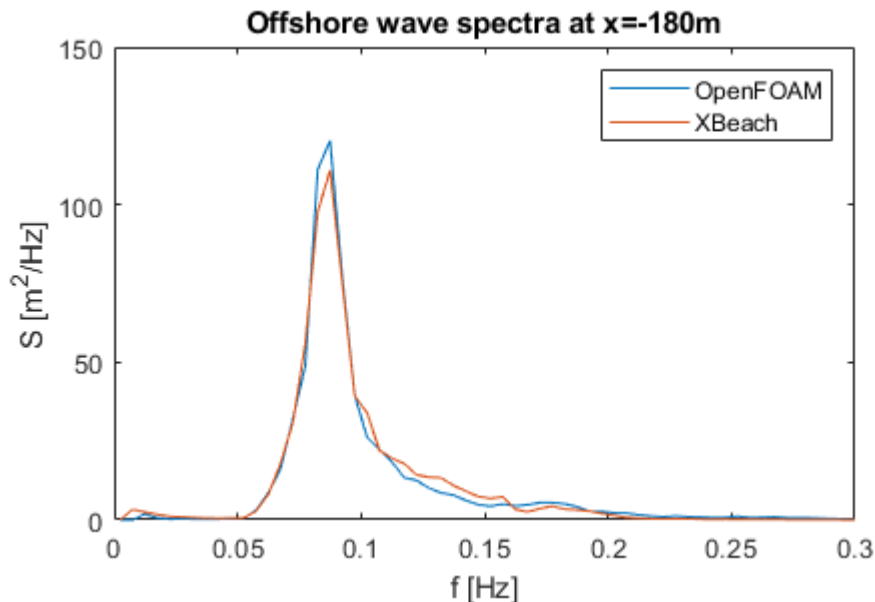
Figure 6.11: Wave spectra for 0 m sea level rise, original bed level, and a peak period of 11.65 s.

Calibration low wave steepness

For the XBeach simulations with low wave steepness, the offshore wave spectrum at x=−180m already shows a shift in wave energy to the higher frequency at approximately twice the peak frequency. Furthermore, there is also an additional small energy peak below 0.02 Hz in the XBeach wave spectrum. Due to this shift in energy in the XBeach wave spectra, the offshore wave spectra of the XBeach and OpenFOAM simulations differ significantly for the low-steepness waves, see Figure 6.12.
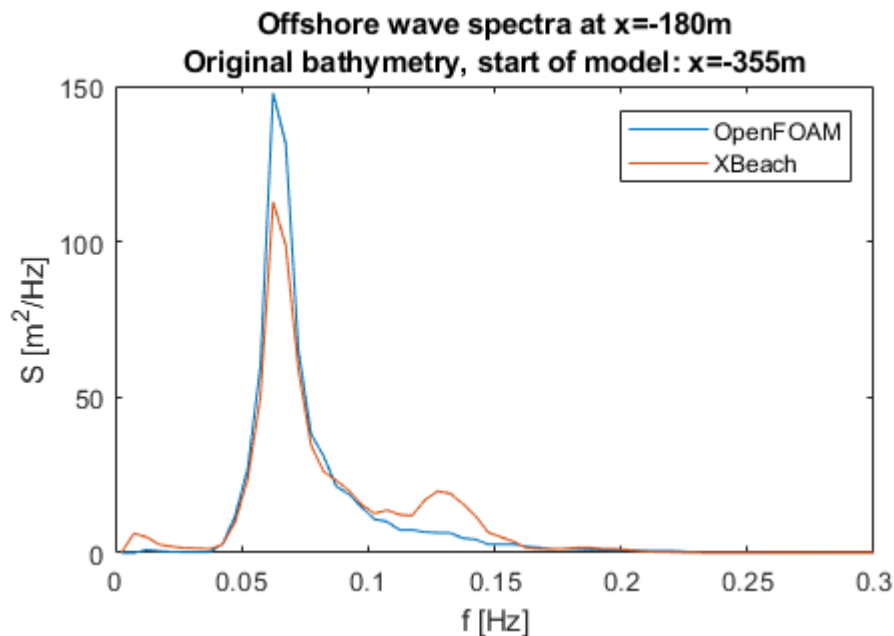
Figure 6.12: Wave spectra comparison of the low wave steepness conditions, with the original XBeach bathymetry.

To obtain better similarity between the offshore wave spectra and consequently a better comparison between the wave transformation of the two models, the XBeach model bathymetry is changed slightly. The starting point of the model is changed from x=−355m to x=−210 m, shortening the offshore horizontal bed before the slope. In Figure 6.13, the wave spectrum for the changed XBeach bathymetry is compared to the OpenFOAM wave spectrum, which shows better similarity between the spectra. The difference at the twice the peak frequency is now negligible, but the difference below 0.02 Hz is still present. It should be noted that the XBeach wave spectra at x=−180 m strongly depend on the length of the deep-water section (water depth approximately equal to three times the offshore wave height), which physically seems unrealistic.

There are two important remarks regarding this calibration in XBeach by means of changing the bathymetry. The first is that while the offshore wave spectra in Figure 6.12 and 6.13 are significantly different, the nearshore wave height and spectral period differ less than 2% between the two XBeach simulations. The second is that the XBeach input of the significant wave height for Figure 6.12 is 7.5 m, while it is 7.6 m for Figure 6.13, which contributes to the similarity between the peaks of the spectra in Figure 6.13.
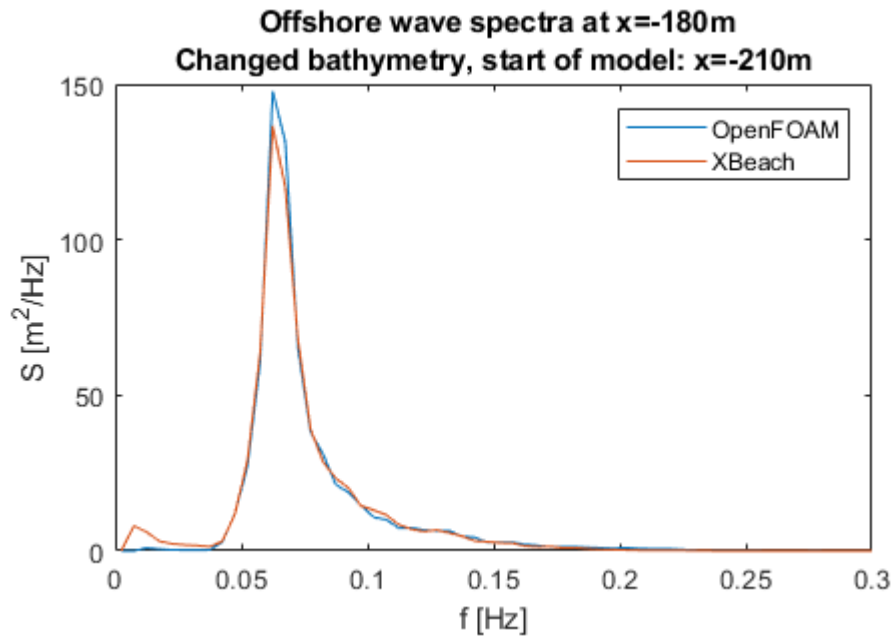
Figure 6.13: Wave spectra comparison of the low wave steepness conditions, with the changed XBeach bathymetry.

For the changed bathymetry of the low wave steepness simulations, the same procedure to calibrate the wave input is performed. The calibrated inputs lead to the XBeach spectrum shown in Figure 6.13.

A significant wave height input of 7.6 m results in an incoming offshore wave height of 7.28 m. This simulated wave height is similar to those in the previously performed wave calibrations of both XBeach and OpenFOAM. The deviation between all calibrated cases is around 1%, thus no further calibration is performed for the wave height.

For the wave period, the peak period of 15.5 s is used as input, as was done for the OpenFOAM simulations with low wave steepness. The incoming spectral period is 16.59 s, thus significantly different from the 14.21 s in the OpenFOAM simulations. This difference can already be seen in the low frequencies of the wave spectra in Figure 6.13. However, the only way to calibrate the spectral period would be to change the peak period, which in turn creates a larger difference between the wave spectra of XBeach and OpenFOAM. Therefore, the deviation in spectral period cannot be avoided, and no calibration is performed for the spectral period. This difference in the wave input of the models, and its influence on the spectral periods at the toe needs to be considered in Chapter 7.

7. Validation of the empirical formulae with numerical models

In this chapter, the empirical estimates of Section 3.1 and the empirical formulae of Van Gent et al. (2022), used in the case study to determine the tipping points, are validated with the numerical models described in the previous chapter. As explained previously in Section 3.1, finding the exact tipping points of pathways with numerical models is time-consuming (compared to using empirical relations). Instead, a more general approach is used to validate the empirical estimates, which also gives an indication on the accuracy of the tipping points calculated in the case study of Chapter 5.

First, the estimates for depth-induced breaking are validated with XBeach and OpenFOAM, related to research sub-question 1. Then, sub-question 3 is answered by validating the empirical expressions of Van Gent et al. (2022) with the overtopping discharges obtained in OpenFOAM. Lastly, a reflection on the results of this chapter is given. An overview of the numerical results is given in Appendix C.

7.1. Comparison of depth-induced breaking on the foreshore

7.1.1. Empirical and numerical wave conditions

Significant wave height

For the method of Section 3.1, the significant wave height at the toe of the breakwater is estimated with a rule of thumb, which states that the maximum significant wave height at the toe of the breakwater is equal to half the water depth at the toe. In Figure 7.1, this rule of thumb is compared with the numerical wave transformation results. The incoming significant wave heights near the breakwater ($H_{m0,t}$) are determined with the method of De Ridder et al. (2023) and the wave gauges at x=81.7 m to x=140 m, which are plotted against the water depths at the toe of the structure (h_t). Both are made dimensionless with the incoming offshore wave heights ($H_{m0,o}$), determined with the method of De Ridder et al. (2023) using the wave gauges at x= −180 m to x= −121.7 m.
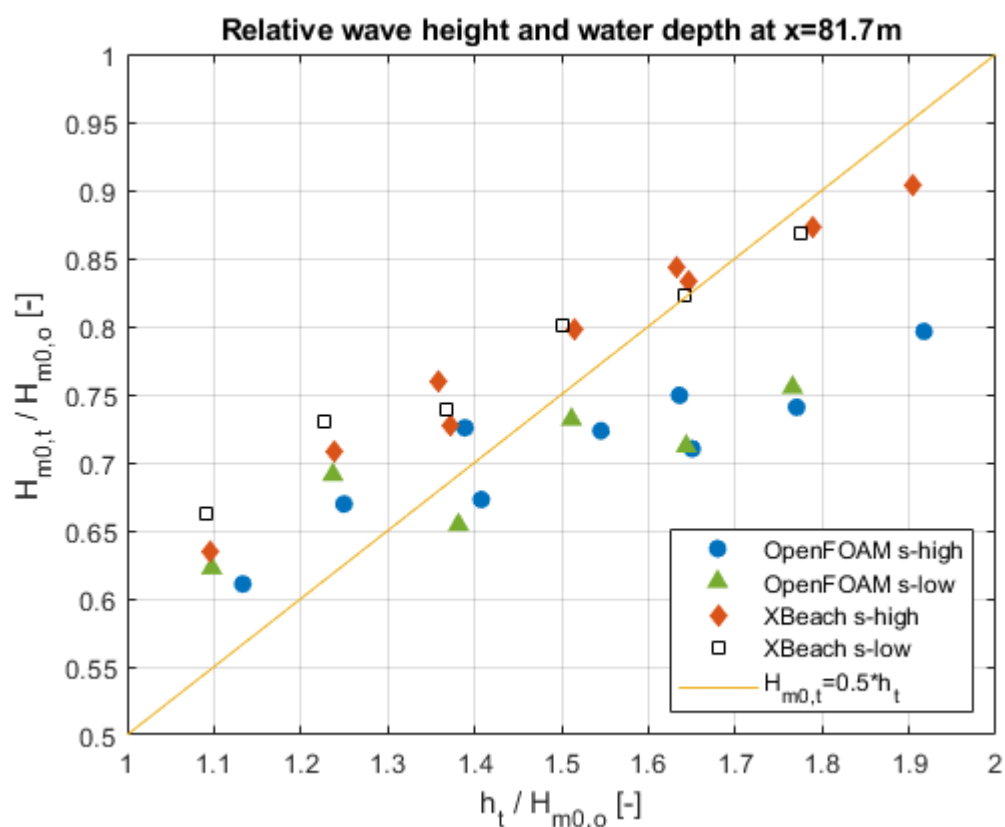
Figure 7.1: Comparison of the rule of thumb with the numerical results for the significant wave height.

The agreement between the numerical results and the empirical rule of thumb varies significantly. For high wave steepness conditions, the XBeach model is mostly within 5% of the empirical estimate for the larger water depths, but the wave height is 16% larger for the lowest tested water depth. The low wave steepness results in XBeach are similar to the high steepness results, although the difference with the empirical estimate is even larger, up to 21% for lower water depths. The largest absolute difference is 0.85 m between the wave height computed with XBeach and the rule of thumb. The wave heights computed using XBeach are generally higher than those obtained with the rule of thumb.

In contrast to XBeach, the OpenFOAM high wave steepness results deviate less than 9% for lower water depths, but the biggest difference with the rule of thumb is for the highest water depth, approximately 17%. For low steepness conditions, the relative wave height is similar to those with high steepness, but the deviation from the empirical estimate for lower water depths is up to 13% instead of 9%. The largest absolute difference between OpenFOAM and the rule of thumb is 1.18 m. For the lower water depths, the results obtained using OpenFOAM are relatively close to those to those obtained with XBeach, while for larger water depths the computed wave heights are clearly lower than those obtained using XBeach or the rule of thumb.

Notably, for both XBeach and OpenFOAM, the low wave steepness conditions show slightly higher wave heights than the high wave steepness conditions for the two lowest water depths, although it is only a 5% difference. For the larger water depths, this difference is less than 3%.

Figure 7.2 displays the results for high wave steepness only, but parameter F (foreshore bed level raise) is specified for each result. It shows that the relative wave height increases more for increasing water depths for F=4 m than F=0 m, indicating that the relation between wave height and water depth differs for the different bathymetries and water depths. This is both seen in the XBeach and OpenFOAM results. As an example, the OpenFOAM results are used here. The wave height increase from 0 m to 2 m sea level rise is 0.65 m, 0.72 m, and 0.91 m for F=0 m, F=2 m and F=4 m, respectively. This corresponds to a relative increase of 13% for F=0 m, 15% for F=2 m and 21% for F=4 m. So, both in absolute and relative terms, the relation between wave height and water depth is different.

Furthermore, for almost equal water depth but different foreshore bed levels, the relative wave height can vary significantly when comparing within the XBeach results and within the OpenFOAM results themselves. This is especially visible for the OpenFOAM results. For example, the OpenFOAM results at $h_t/H_{m0,o} \approx 1.4$ show very different relative wave height.

One possible contribution to this difference is how the foreshore bed level is raised in the numerical flume. Because the 1:10 slope is extended to the raised bed level, the slope increases and the horizontal foreshore length decreases. Therefore, the foreshore length at which the water depth is equal to h_t significantly reduces for higher bed levels. For F=0 m, the horizontal foreshore length up to the wave gauges is 81.7m, while it is reduced to 61.7 and 41.7 m for F=2 m and F=4 m, respectively. This could be one of the reasons that the higher bed levels result in higher significant wave height for the same water depth.

Notably, these cases with similar water depth but different wave height have very similar wave steepness values, with only around a 3% to 6% difference. In OpenFOAM, the simulations with higher wave height (and higher bed level) have slightly higher wave steepness, although the spectral period is also slightly higher. So, a difference in local wave steepness is not likely to be the cause of the wave height differences.
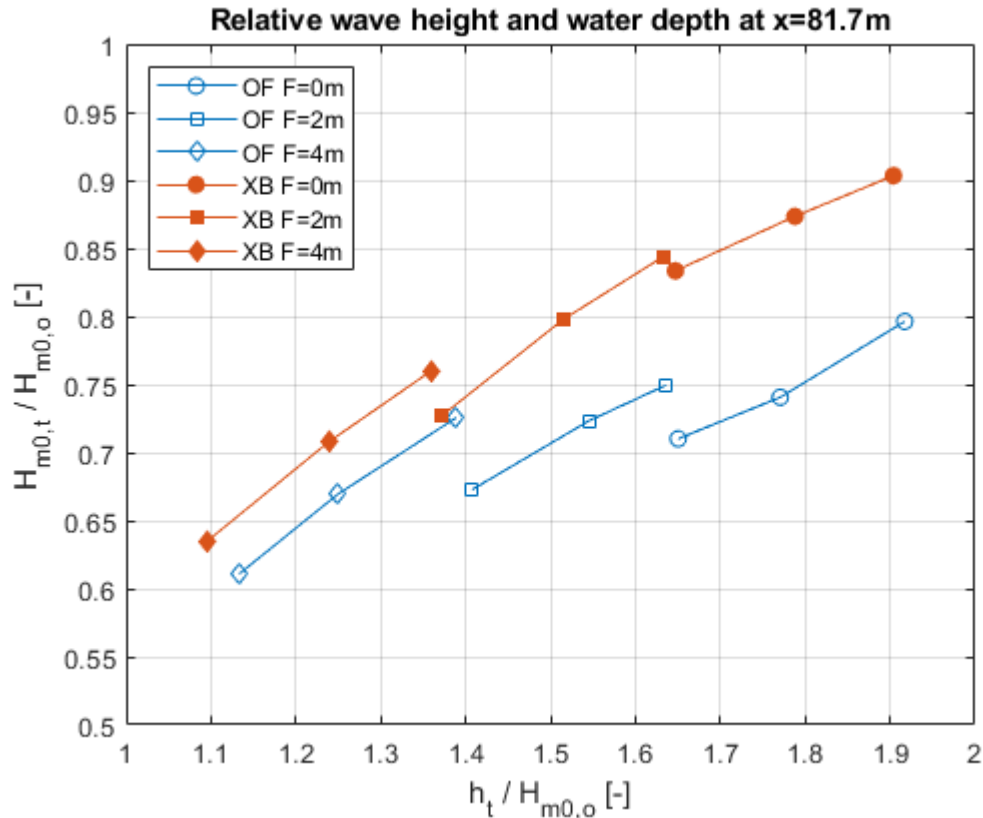
Figure 7.2: Significant wave height of the numerical models near the breakwater.

For the water depth to wave height ratios and assumed bathymetry of the case study, the significant wave height calculated with the rule of thumb maximally deviates 21% compared to the numerical results. Based on the observed differences, it can be said that the rule of thumb served as a reasonable first estimate for the case study presented in Chapter 5. However, it is apparent that numerical modelling is necessary for further detailed calculations, because the accuracy of the rule of thumb is highly variable. The bathymetry (i.e., foreshore length and slope) and wave steepness influence the wave height in the numerical models, which is not considered in the rule of thumb. It must be noted that there is also significant disagreement between numerical models themselves, which is discussed further in Section 7.1.2.

Spectral period

Another empirical estimate is used in the method of Section 3.1, namely that the spectral period does not change from offshore to nearshore for $h_t/H_{m0,o} > 1$. Based on the ratio of the initial water depth to the offshore wave height of 1.6 and the results of Hofland et al. (2017), it was assumed that the change in spectral period is insignificant for the depths used in the case study. This assumption is compared to the numerical results below.

Figure 7.3 shows the spectral period at the toe ($T_{m-1,0,t}$) relative to the offshore spectral period ($T_{m-1,0,o}$), plotted against the water depth (h_t) over the offshore wave height ($H_{m0,o}$). The assumption of the case study is that the ratio $T_{m-1,0,t}/T_{m-1,0,o}$ equals 1, which is the deep-water limit.
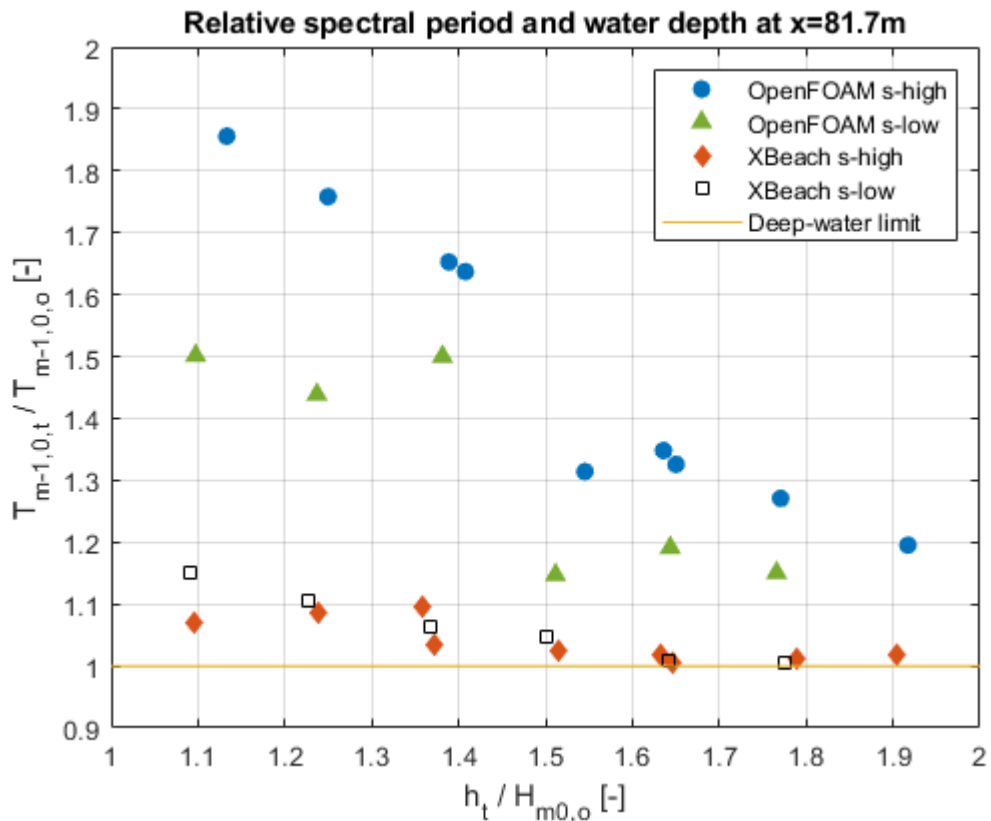
Figure 7.3: Relative spectral wave period as function of relative water depth.

The XBeach model results are very close to the assumed deep-water limit, regardless of the tested wave steepness. While the OpenFOAM results show a significant increase in the spectral period for lower water depths, this increase is smaller for low wave steepness conditions. Notably, the relative spectral period in OpenFOAM seems to increase significantly for a relative water depth smaller than 1.5. XBeach shows a maximum deviation of 15% from the assumed deep-water limit, while OpenFOAM results show a minimum increase of 15% and maximum increase of 85% of the spectral period from offshore to nearshore.

When comparing the results of Figure 7.3 with Figure 7.4 of Hofland et al. (2017), no clear conclusion can be drawn either. The data of Van Gent (1999) and Chen et al. (2016) used in Hofland et al. (2017) only has one clump of data between relative water depth of 1 and 2, which seems to be between the results of the OpenFOAM and XBeach models used here.

So, depending on which numerical model is deemed accurate, the assumption for the spectral period is either reasonable or not. In the next section, the XBeach and OpenFOAM wave transformation results are compared in more detail to determine the sources of these differences.
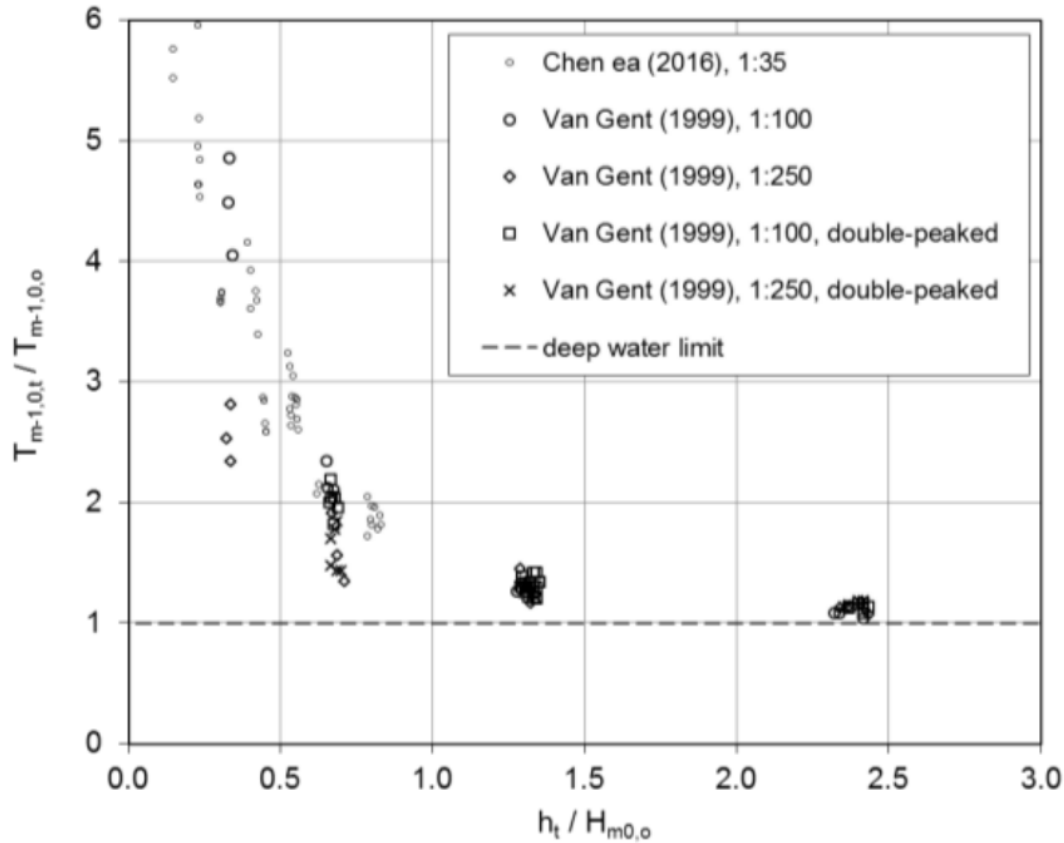
Figure 7.4: Relative spectral wave period as function of relative water depth obtained from Hofland et al. (2017).

7.1.2. XBeach and OpenFOAM wave conditions

The results presented in previous sections showed significant differences between the XBeach and OpenFOAM models. For the same model configuration, OpenFOAM simulations consistently produce lower significant wave heights and higher spectral periods. These results seem to agree with previous work of Lashley et al. (2020). Compared to an XBeach NH model and physical model tests, the OpenFOAM model of Lashley et al. (2020) underestimated the significant wave height and overestimated the spectral period due to excessive energy dissipation and too much energy shifting to low frequencies, respectively. Chen et al. (2021) also found that the spectral period is overestimated in OpenFOAM compared to physical model experiments, although to a lesser extent than found here.

Another important difference between the XBeach and OpenFOAM models is stated in Section 6.3.4. For the offshore wave conditions in the low wave steepness simulations, there is already a shift in wave energy to the higher frequencies in XBeach, while this is not the case for OpenFOAM. The XBeach model was changed to have a shorter flume offshore, to prevent this shift and have more similar offshore wave spectra, but it is very important to note this difference. It might be that XBeach shows changes in the wave spectrum at larger water depths than OpenFOAM. Notably, this difference was only significant for the low steepness conditions, and not for high steepness conditions.

To understand the differences in wave transformation between the OpenFOAM and XBeach models, the wave spectra at the nearshore wave gauges are compared. Wave spectra of a small selection of simulations is shown in Figure 7.5 to 7.8, which give a good representation of the general differences between the XBeach and OpenFOAM results. The main differences in the wave spectra are:

- The total energy in the wave spectrum. For the same input parameters, the XBeach model produces larger nearshore significant wave heights than the OpenFOAM model. The difference could already be seen in the comparison of the significant wave heights in Figure 7.1 and 7.2, which is up to 17.6% for the largest relative water depth.
- The energy peak at $2 \cdot f_p$. The XBeach wave spectra show higher energy peaks around two times the peak frequency. This is still the case when normalising the spectra with the total energy.
- The energy in the lower frequencies. Even though the total wave energy in the OpenFOAM simulations is lower, they generally show higher energy in the frequencies below 0.05 Hz. The exception is the simulation with low wave steepness and F=0 m (Figure 7.7), where the low energy peak is slightly higher in XBeach. However, this low energy peak in the XBeach wave spectrum is already present in the offshore conditions. This peak can be seen in Figure 6.13 in Section 6.3.4, and has the same peak value of approximately 10 m^2/Hz.
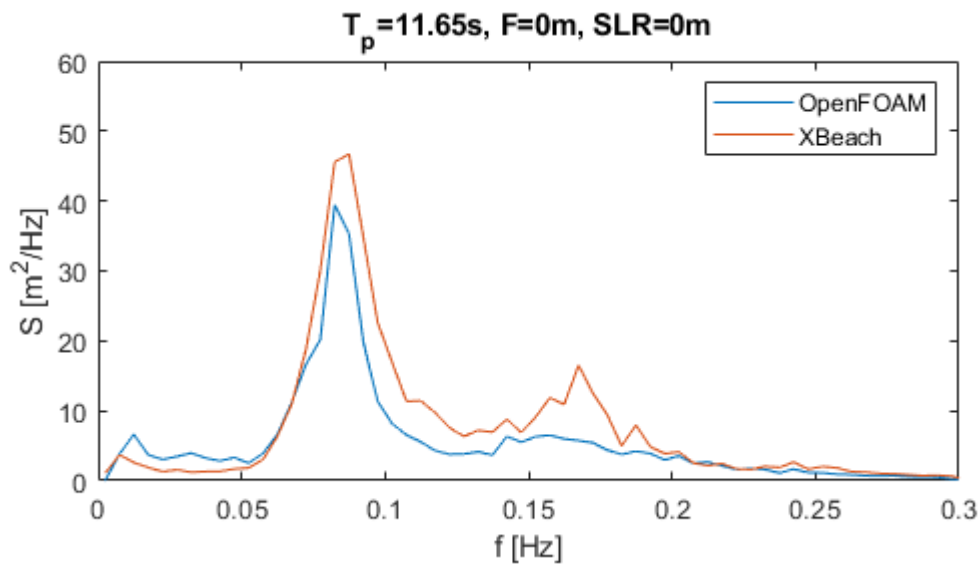
Figure 7.5: Wave spectra at x=81.7m with high wave steepness, original bed level and no SLR.
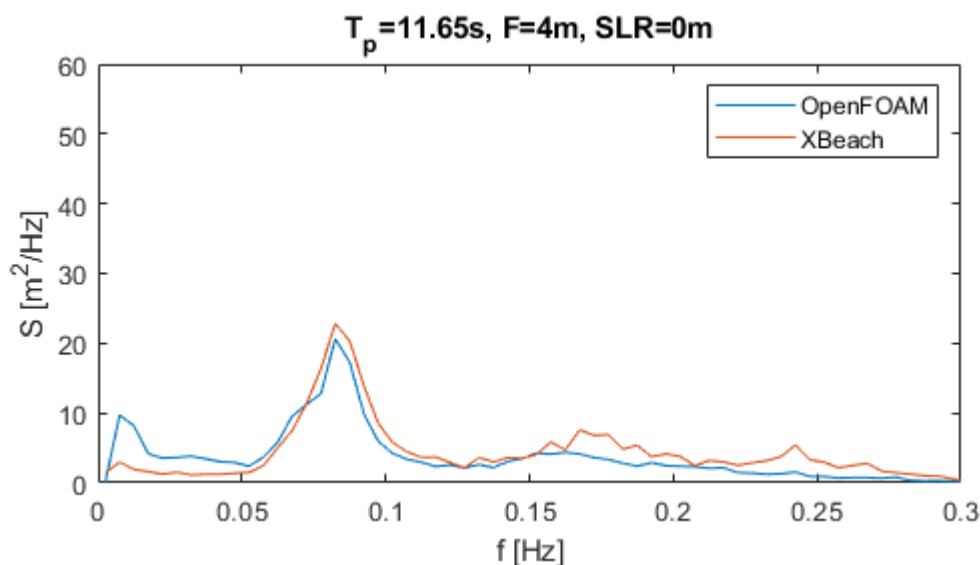
Figure 7.6: Wave spectra at x=81.7m with high wave steepness, bed level raised with 4 m and no SLR.
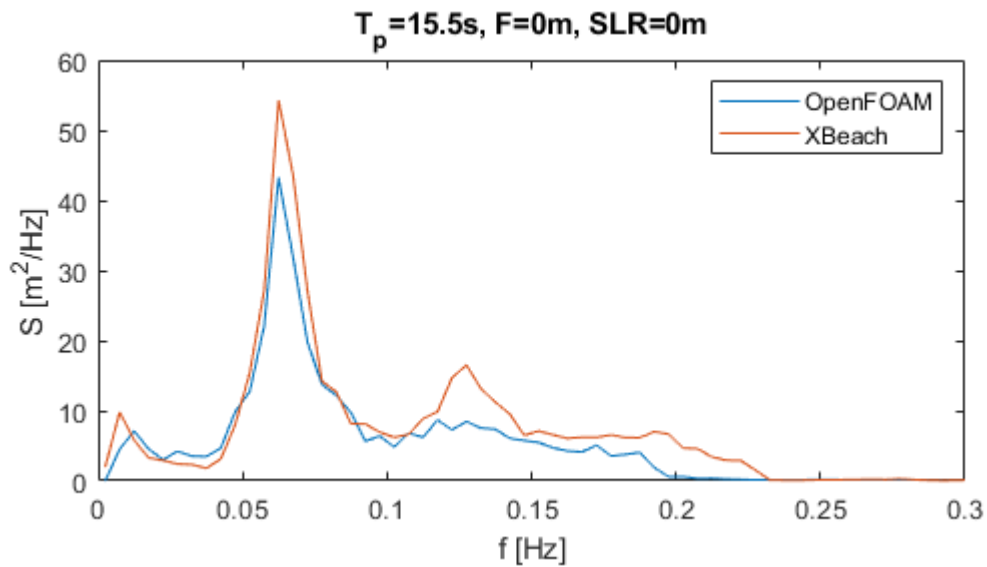
Figure 7.7: Wave spectra at x=81.7m with low wave steepness, original bed level and no SLR.
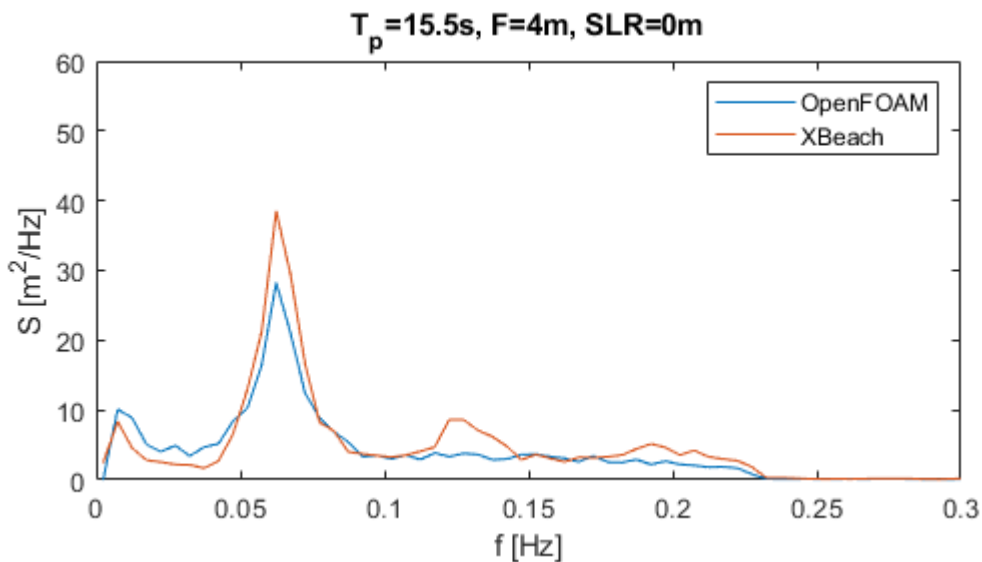
Figure 7.8: Wave spectra at x=81.7m with low wave steepness, bed level raised with 4 m and no SLR.

Other than the inherent differences between the numerical models, the difference between the XBeach and OpenFOAM results might also be partially caused by other factors.

One possible factor is the presence of the breakwater in OpenFOAM, while it is not included in XBeach. The OpenFOAM numerical flume contains the breakwater which causes wave reflection due to wave-structure interaction. If this reflection is not perfectly filtered out of the wave signal, this can already create a difference between the computed incoming wave signals of XBeach and OpenFOAM simulations. This can be checked by running OpenFOAM simulations without the breakwater for comparison, which is briefly done here for two simulations. Figure 7.9 and 7.10 show the comparison for a simulation with F=4 m, SLR=0 m, and both high and low wave steepness. Based on these figures, it can be concluded that differences between the OpenFOAM and XBeach wave spectra are not caused by the presence of the breakwater.
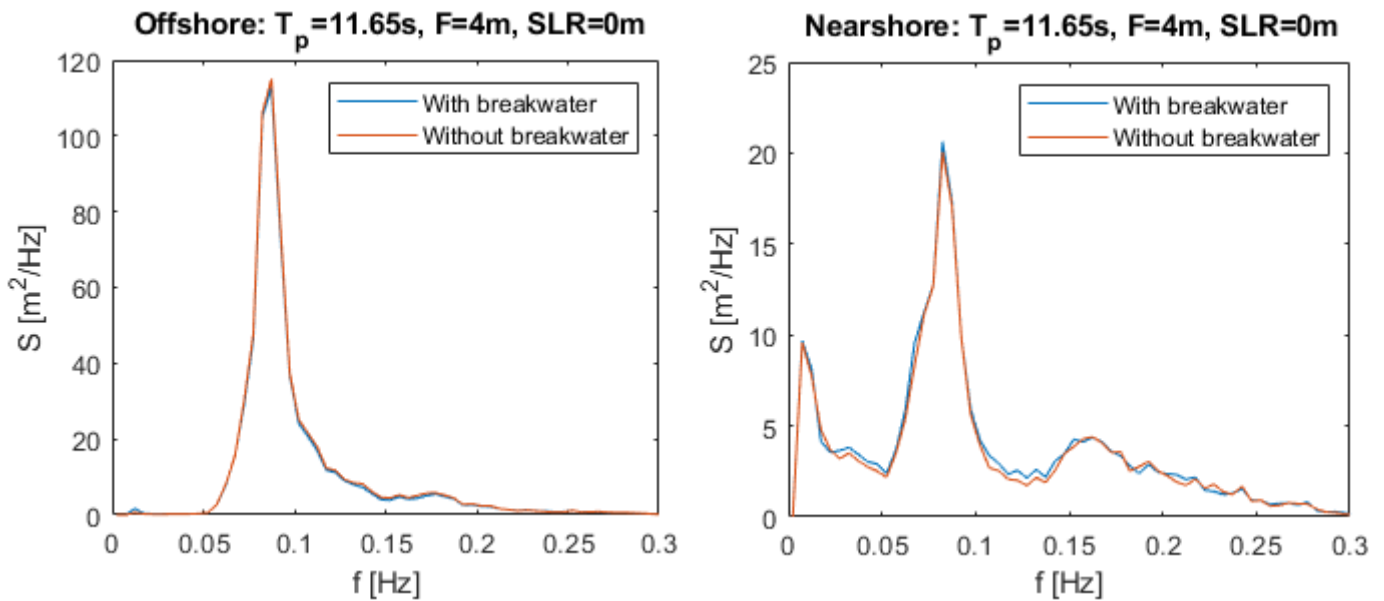
Figure 7.9: OpenFOAM high steepness wave spectra with and without breakwater at x=−180 m (left side) and x=81.7 m (right side).
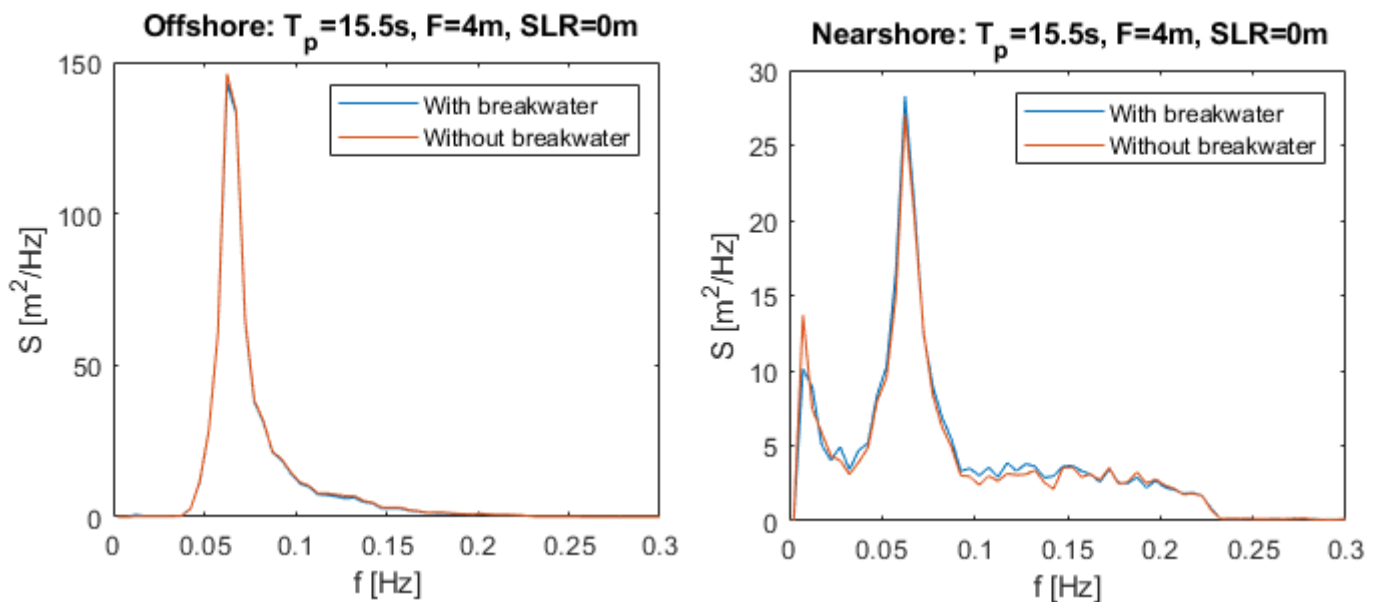
Figure 7.10: OpenFOAM low steepness wave spectra with and without breakwater at x=−180 m (left side) and x=81.7 m (right side).

Another potential cause of difference between XBeach and OpenFOAM regards the low frequency peaks in the wave spectra. In the unfiltered wave spectra of the numerical simulations, there is an energy peak at frequencies below 0.02 Hz, which is much larger in OpenFOAM than in XBeach. The size of these energy peaks varies based on the foreshore bed level and on whether there is a crest wall on the breakwater or not. This already indicates that this wave energy is not generated with the JONSWAP wave spectrum, but that it might be caused by wave reflection or wave breaking. Notably, these low frequency peaks are still present in the simulations without breakwater. Furthermore, these low frequencies correspond to deep-water wave lengths which cannot be accurately identified with the used spacing between the wave gauges. Further research should be done on the cause of this low frequency energy, but it falls outside the scope of this thesis. However, it causes an increase in the low frequency energy of the wave spectra and the spectral period of the OpenFOAM results,

69

which is important to keep in mind when viewing the results. Especially because the spectral period results are significantly different between the OpenFOAM and XBeach models (see Section 7.1.1).

A general source of inaccuracy in the wave signal separation and consequent calculation of the wave spectra is the breaking and changing of the waves at the nearshore wave gauges. The wave gauges near the breakwater are placed less than 1 deep-water wavelength after the 1:10 slope. The waves are therefore breaking at the position of the wave gauges, causing the waves to change between the first and the last wave gauge. In turn, the wave signals at the wave gauges are inherently different, which likely results in inaccuracies of the signal separation. A simple solution would be to lengthen the horizontal foreshore in front of the breakwater. The wave gauges can then be placed further from the slope, so waves do not break at the wave gauges. However, a longer numerical flume is more computationally demanding and could result in too much numerical dissipation, especially in OpenFOAM. This is not researched further in this thesis.

Specifically for the low wave steepness simulations, there may be additional inaccuracies. The set-up of the numerical flume, for example the length of the relaxation zones (only OpenFOAM) and the positioning of the wave gauges (XBeach and OpenFOAM), is determined based on the wave length of the high steepness conditions. Based on the spectral period, the deep-water wave length of the high steepness wave conditions is 175 m while the corresponding wave length for the low steepness conditions is 310 m. Because the waves are much longer, the generation and damping of waves in the relaxation zones and the signal separation of the wave gauge measurements might be less accurate.

7.2. Comparison of wave overtopping at the breakwater

7.2.1. Numerical wave overtopping results

In all of Section 7.2, a relative comparison of the overtopping discharge is done, because the analysis in Section 6.2.5 showed that the wave overtopping of the OpenFOAM model is grid size dependent. Therefore, the absolute values of the overtopping cannot be compared to the absolute values computed with the empirical expressions of Van Gent et al. (2022). Instead, the overtopping discharges are compared relatively, by normalising with overtopping values of other (model) configurations. For example, to see the influence of the crest wall, the overtopping discharge with a crest wall is divided by the overtopping discharge of the same configuration without a crest wall. This gives the relative reduction of wave overtopping by adding a crest wall, which can be compared between the numerical and empirical results. The absolute overtopping results are presented in Appendix C.

Before the OpenFOAM overtopping results are compared against the empirical expressions of Van Gent et al. (2022) in Section 7.2.2, the numerical results are presented and compared between each other here. Figure 7.11 shows the relative overtopping results for all high wave steepness simulations for all tested values of sea level rise (SLR). All overtopping discharges are normalised with the discharge of the model configuration without any adaptation measures applied (q_0), so with the original bed level (F=0 m) and without crest wall.

Based on Figure 7.11, several observations are made for the high steepness results:

- The adaptation measures of adding a crest wall of 1 m and raising the foreshore bed level with 2 m show similar reduction of the overtopping discharge. This can be seen when comparing F=0 m with wall and F=2 m without wall, but also F=2 m with wall and F=4 without wall. Although the effects are similar, raising the foreshore bed with 2 m reduces overtopping slightly more than adding a crest wall of 1 m.
- The adaptation measures cause relatively less reduction in overtopping discharge for higher sea level rise and water levels. The effectiveness of the measures might be correlated to the amount of overtopping discharge, where the effectiveness decreases for higher discharges.
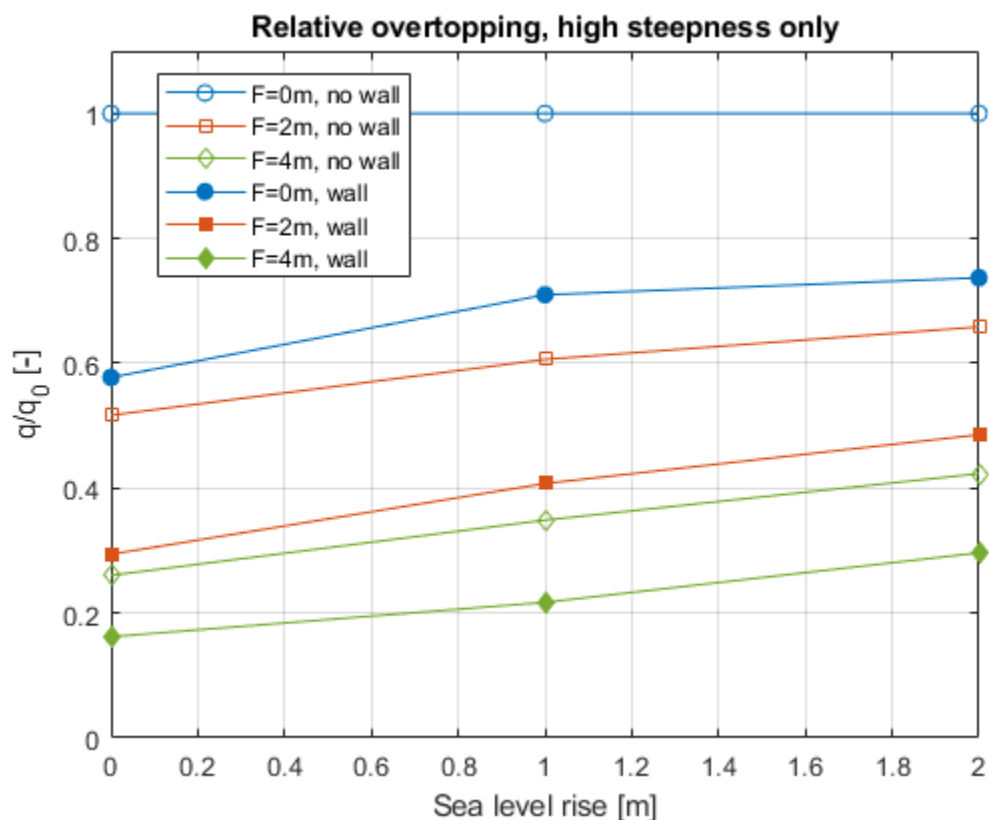
Figure 7.11: OpenFOAM relative overtopping discharge with q_0: F=0 m, no wall, high steepness.

The low wave steepness overtopping discharges (s-low) are compared to the high steepness counterparts (s-high) in Figure 7.12. Again, the configuration with F=0 m, without crest wall, and high steepness is used to normalise the overtopping discharges. It can be seen that low wave steepness consistently leads to more wave overtopping than the high steepness conditions with the same model configuration. This agrees with the results of Van Gent et al. (2022).
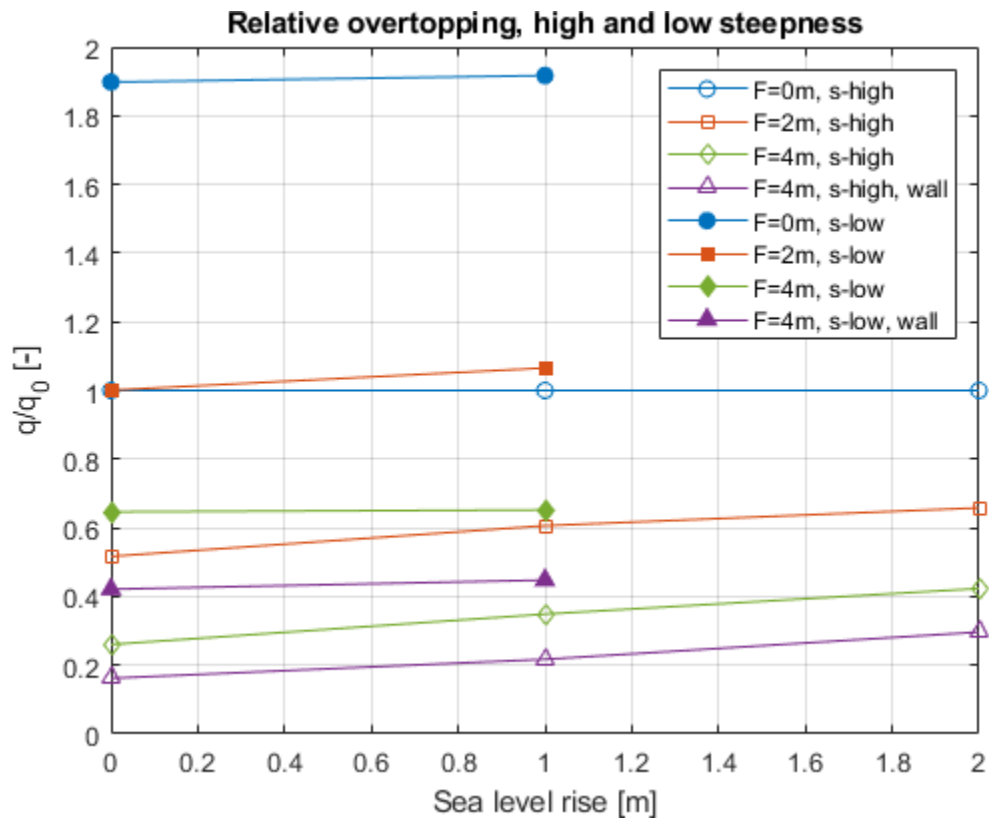
Figure 7.12: OpenFOAM relative overtopping discharge with q_0: F=0 m, no wall, high steepness.

In Figure 7.13, again the low wave steepness overtopping discharges (s-low) are compared to the high steepness counterparts (s-high). However, the discharge that is used to normalise (q_0) is different. The high steepness results are again normalised with the discharge of the configuration with high steepness, F=0 m, and no wall. The low steepness results are now normalised with the discharge for low steepness, F=0 m, and no wall. By normalising the high steepness results with the high steepness case without measures, and the low steepness results with the low steepness case without measures, it can be seen whether the effectiveness of the adaptation measures is influenced by the wave steepness.

Based on Figure 7.13, the effectiveness of the measures to reduce overtopping is similar for high and low wave steepness. Still, there is a noticeable difference for the simulations with F=4 m at 0 m sea level rise. For the case without a crest wall (green), low steepness results in a value of 0.34 and high steepness in a value of 0.26 at SLR=0 m. The case with a crest wall (purple) has values of 0.22 and 0.16 for low and high steepness, respectively. Additionally, the relative overtopping (q/q_0) does not seem to increase with sea level rise as much for low steepness cases, compared to the high steepness results.
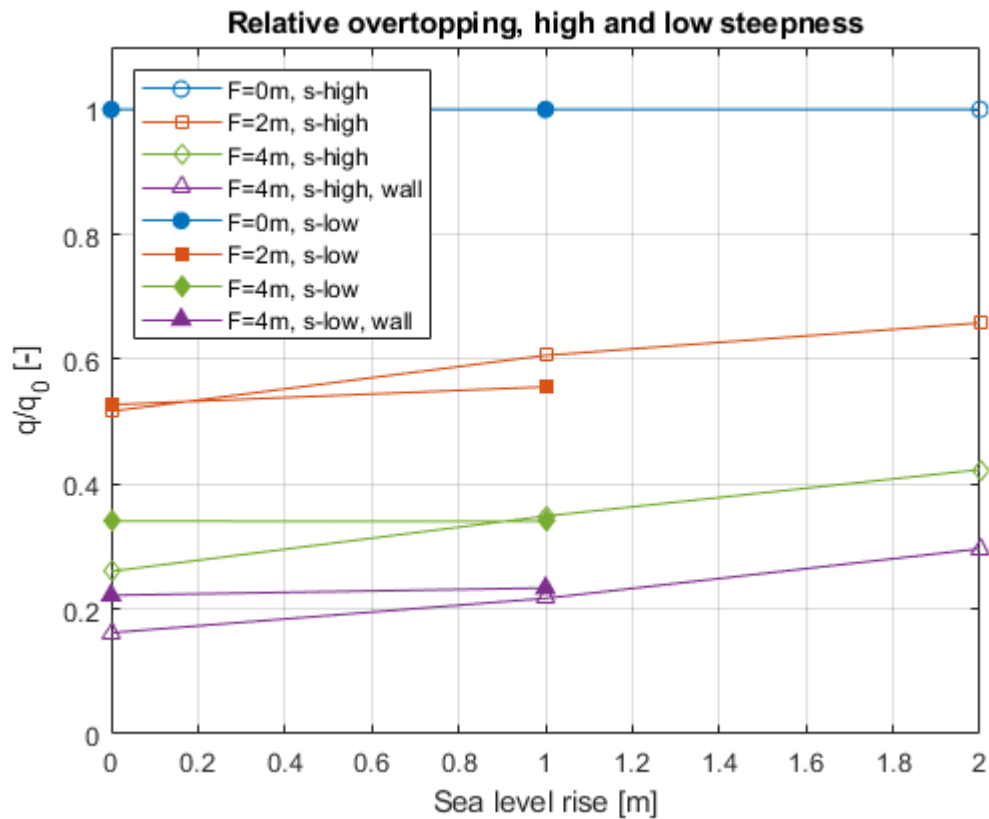
Figure 7.13: OpenFOAM relative overtopping discharge with q_0: F=0m, no wall, and low and high steepness for low and high steepness results respectively.

7.2.2. Comparison of empirical and numerical wave overtopping

In this section, the overtopping discharge computed with the OpenFOAM model are compared to the discharge computed with the empirical expressions of Van Gent et al. (2022). These expressions are used in the case study to determine the tipping points of the adaptation measures, and thus the effectiveness of the measures. However, as previously explained in Section 1.2 and 5.4, these expressions were used outside of the known validity ranges. For this reason, the overtopping expressions are compared to the OpenFOAM model results.

Section 7.1 shows that the empirical estimates for the significant wave height and spectral period of the method of Section 3.1 have varying levels of agreement with the numerical model results. Thus, in addition to using the empirical estimates as input for the overtopping expressions, the nearshore wave conditions as computed with the numerical models are also used as input in the empirical overtopping expressions.

Influence of the foreshore

The influence of raising the foreshore bed level is checked here by looking at the relative reduction in overtopping. So, it is investigated how much the overtopping discharge computed for the original bed level (F=0 m) reduces by raising the foreshore with 2 or 4 m (F=2 m or 4 m).

First, the overtopping expressions in combination with the empirical estimates (denoted with RoT, short for rule of thumb) are compared to the numerical results. As a reminder: The empirical estimates are that the significant wave height is equal to half the water depth at the toe, and the spectral period at the toe of the structure is the same as the offshore value.

Figure 7.14 shows the reduction of the overtopping due to raising the foreshore bed level, relative to the simulation with the original bed level, so q_0 is the simulation with F=0 m. Although the trends are similar (the reduction of overtopping decreases with sea level rise), the empirical expressions estimate much larger overtopping reduction by raising the foreshore bed level.

Figure 7.14: OpenFOAM and empirical (empirical estimates with Van Gent et al. (2022)) relative overtopping reduction $(q_0-q)/q_0$ with q_0: F=0 m, no wall, high steepness.

As stated in the beginning of this section, the significant wave height and spectral period determined with the empirical estimates can deviate significantly from the numerical models. Therefore, the nearshore significant wave height and spectral period obtained in OpenFOAM are used as input for the empirical formulae. The relative reduction in overtopping is compared in Figure 7.15, for high wave steepness conditions and without a crest wall. OpenFOAM is shortened to 'OF' in the legend of Figure 7.15.

In Figure 7.15, the empirical and numerical reduction is similar at 0 m sea level rise, but the empirical overtopping reduction rapidly decreases for increasing sea level rise. At 1 m and 2 m sea level rise, the reduction with F=4 m is even smaller than F=2 m for the empirical results. The overtopping reduction is even negative for F=4 m compared to q_0 (F=0 m) at 2 m sea level rise. It is a combination of two effects that cause the empirical expressions to significantly differ from the numerical results for higher sea level rise:

- In OpenFOAM, the wave height for F=4 m and F=2 m increases more with sea level rise than for F=0 m. This trend between wave height and water depth was also presented in Figure 7.2 of Section 7.1.1 and is more prominent for F=4 m than F=2 m. For higher sea level rise, the difference in wave height between F=0 m, 2 m, 4 m decreases. Additionally, the relatively small differences in wave heights for varying water depths in OpenFOAM also contribute to the trends seen in Figure 7.15.

- In OpenFOAM, the spectral periods increase significantly for lower water depths and higher foreshore bed levels, as concluded in Section 7.1.1. In general, a larger spectral period and thus lower wave steepness causes larger overtopping discharges.

Figure 7.15: OpenFOAM and empirical (OpenFOAM wave conditions with Van Gent et al. (2022)) relative overtopping reduction $(q_0-q)/q_0$ with q_0: F=0 m, no wall, high steepness.

In Section 7.1, a significant difference in the nearshore wave conditions between the XBeach and OpenFOAM models is found, especially in the spectral period. As stated previously, this can have a significant impact on the calculation of overtopping with the empirical formulae. For comparison, XBeach wave conditions are used as input for the empirical overtopping expressions by Van Gent et al. (2022) in Figure 7.16. XBeach is shortened to 'XB' in the legend of Figure 7.16.

Figure 7.16 shows much better agreement between the empirical and numerical results than in Figure 7.14 and 7.15. The empirical overtopping reduction of F=4 m is positive and larger than the reduction of F=2 m for every sea level rise value, in contrast to Figure 7.15. The empirical and numerical reduction show similar trends, although the decrease with sea level rise is steeper for the empirical lines. At 0 m sea level rise, the largest difference between empirical and numerical is found for both F=2 m and F=4 m.

Figure 7.14, 7.15 and 7.16 all show the high steepness results. The low wave steepness conditions show identical trends and are not shown here for brevity and clarity of the figures, but these low steepness results can be found in Appendix C.

Figure 7.16: OpenFOAM and empirical (XBeach wave conditions with Van Gent et al. (2022)) relative overtopping reduction $(q_0-q)/q_0$ with q_0: F=0 m, no wall, high steepness.

Influence crest wall

To see the influence of adding the crest wall, the overtopping discharge with a crest wall (q) is compared to the overtopping discharge of the same configuration without a crest wall (q_0). Specifically, the relative reduction of wave overtopping by adding a crest wall ($q_0-q)/q_0$ is compared between the numerical and empirical results.

Figure 7.17 shows the first comparison between the overtopping equations and the numerical results. For input in the empirical equations, the rule of thumb is used for the significant wave height and the spectral period is assumed to be equal to the offshore value. Similar to the influence of the foreshore, this combination of the rule of thumb and overtopping expressions predict higher overtopping reduction, and both the numerical and empirical results show lower reduction for higher sea level rise. The foreshore bed level also influences the effectiveness of the crest wall, with higher bed level corresponding to higher overtopping reduction. This effect can be explained for the empirical results when looking at the Equation 2.1 of Section 2.2.2, repeated below.

$$\frac{q}{\sqrt{g \cdot H_{m0}^3}} = 0.016 \cdot s_{m-1,0}^{-1} \cdot \exp\left(-\frac{2.4 \cdot R_c}{\gamma_f \cdot \gamma_b \cdot \gamma_\beta \cdot \gamma_v \cdot \gamma_p \cdot H_{m0}}\right) \tag{2.1}$$

The influence factor of the crest wall (γ_v) is larger than 1 when a protruding crest wall is applied. This means that for the same crest level and freeboard (R_c), a rubble mound structure with a protruding crest wall leads to more overtopping than for a rubble mound structure where the armour layer is extended to the same crest level. In Equation 2.1, it can be seen that γ_v is multiplied with the

76

significant wave height (H_{m0}). So, for higher H_{m0}, the factor γ_v has a larger influence. Because γ_v has an increasing effect on the overtopping discharge, adding a crest wall is more effective for smaller H_{m0} with the same R_c. Based on the rule of thumb, a higher foreshore bed level and consequently smaller water depth results in smaller significant wave height. Thus, a higher foreshore bed level results in higher effectiveness of adding the crest wall for the empirical equations. Similarly, higher sea level causes higher wave height and thus lower effectiveness of adding a crest wall. Although for the relation with sea level rise this may not be the only cause, as the lower effectiveness for higher sea level was also observed for the influence of the foreshore. These effects also seem to be present for the numerical results, but the effect is not as clear and the difference between the foreshore bed levels is smaller.

Notably, the wave steepness does not have an effect for the empirical results in Figure 7.17, but it does for the numerical results, where the reduction is smaller for lower wave steepness. For the numerical results, the high and low wave steepness conditions also show a similar trend for F=4 m, as the overtopping reduction is similar for 0 m and 1 m sea level rise.
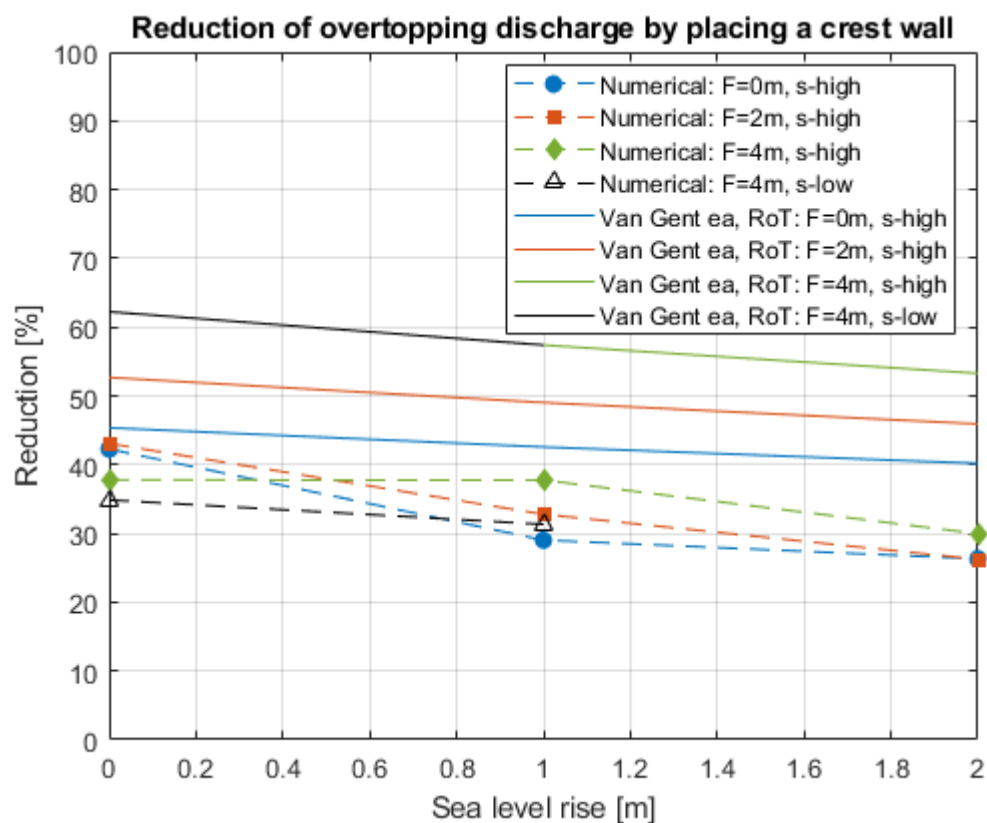
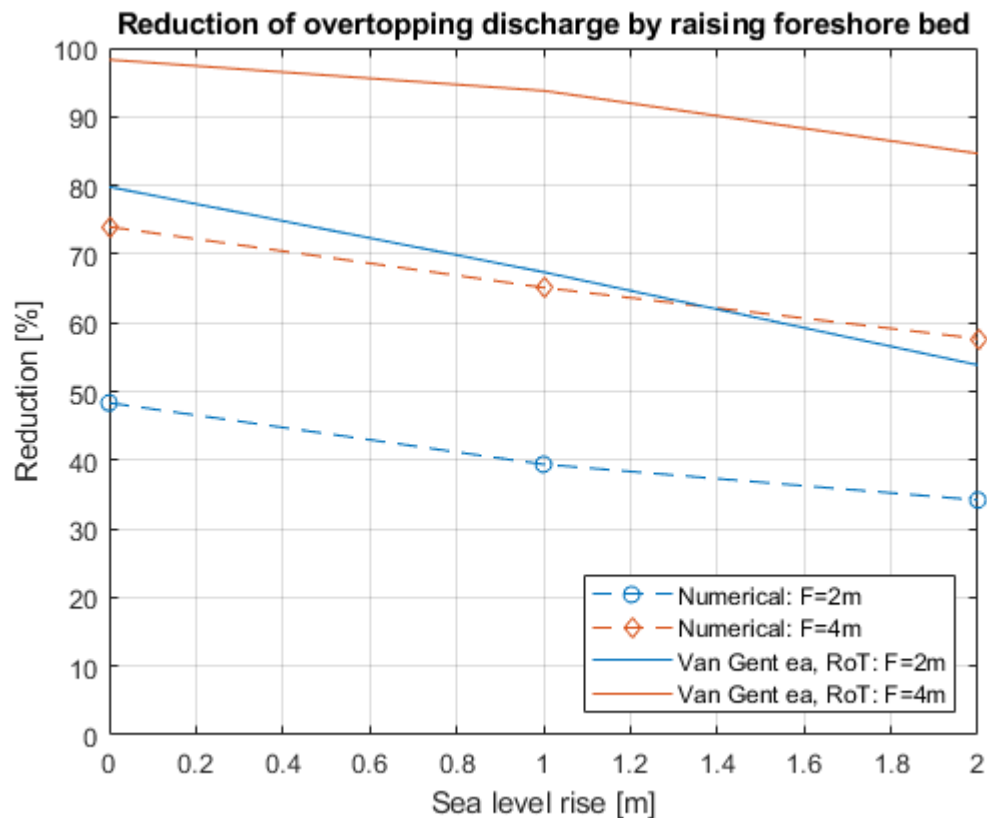Figure 7.17: OpenFOAM and empirical (rule of thumb with Van Gent et al. (2022)) relative overtopping reduction (q_0-q)/q_0 with q_0 having the same F and wave steepness but without crest wall

Figure 7.18 shows the empirical overtopping reduction when using the OpenFOAM wave conditions as input for the formulae. To calculate the overtopping with and without crest wall using the empirical expressions, the OpenFOAM nearshore wave conditions for the simulations without a crest wall are used. There are slight differences in incoming wave parameters between the simulations with and without a crest wall. Using the same input for the overtopping calculations with and without crest wall is necessary to get a good representation of the overtopping reduction based on the empirical formulae of Van Gent et al. (2022). Note that using the simulations with crest wall as input gives almost identical overtopping reduction percentages to using the simulations without crest wall as input (less than 2% difference). The latter are used and presented in Figure 7.18.

Compared to the empirical lines in Figure 7.17, there are several small differences when using the OpenFOAM wave conditions in the empirical expressions:

- The difference in reduction of overtopping between the foreshore bed levels is smaller. This seems to agree with the explanation that the difference in wave height for the varying bed levels causes this, since the wave heights in OpenFOAM differ less for varying bed levels than in the rule of thumb.
- The empirical lines of F=0 m and F=2 m show higher reduction and thus differ more from the corresponding numerical lines, while the opposite is true for the high and low steepness cases of F=4 m (lower reduction, closer to numerical lines compared to Figure 7.17).
- The low wave steepness and high steepness results are different for F=4 m. The crest wall is less effective for low wave steepness, which is also the case in the numerical results.
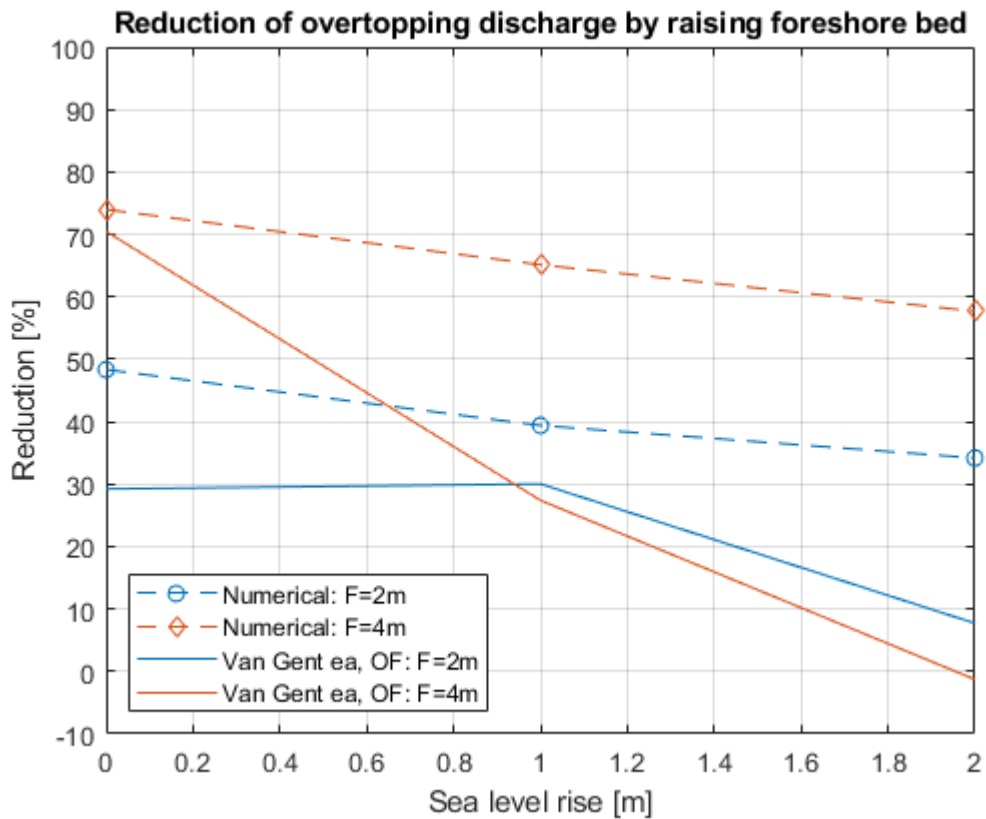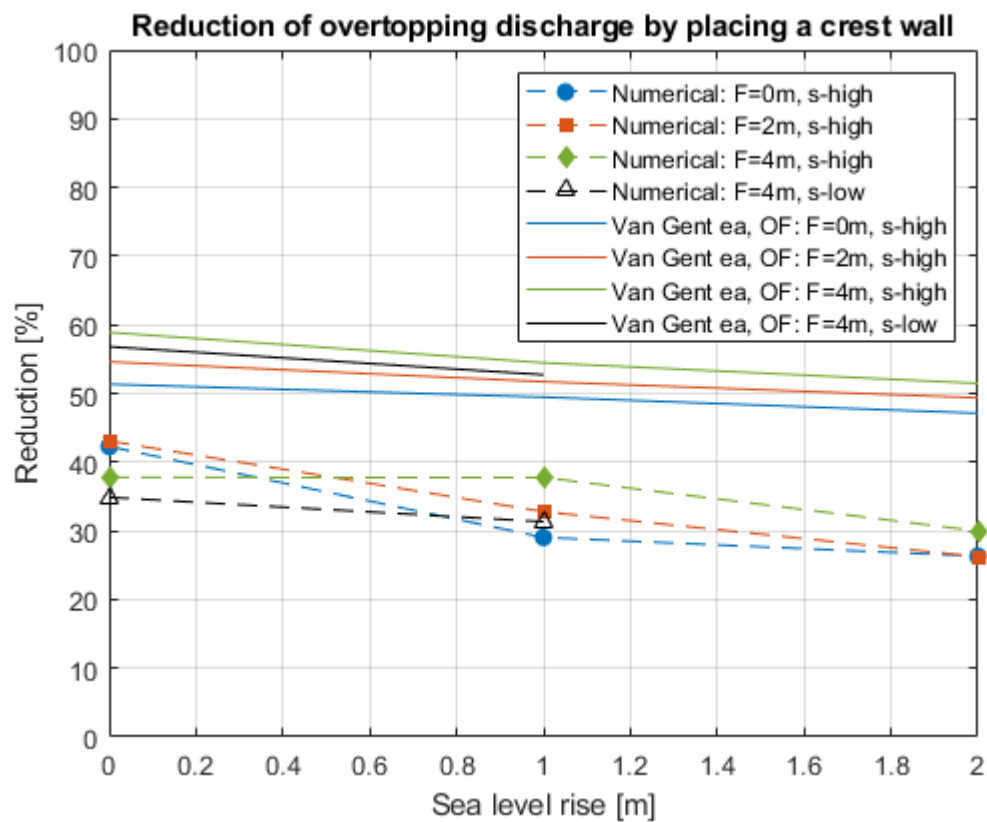

Figure 7.18: OpenFOAM and empirical (OpenFOAM wave conditions with Van Gent et al. (2022)) relative overtopping reduction $(q_0-q)/q_0$ with q_0 having the same F and wave steepness but without crest wall

The XBeach wave conditions are used as input in the overtopping expressions in Figure 7.19. There is better agreement between the empirical and numerical reduction than in the previously used inputs for all bed levels and wave steepness. The differences between the empirical lines are smaller than in Figure 7.17 which uses the rule of thumb, but larger than in Figure 7.18 where the OpenFOAM wave parameters are used. Furthermore, the low wave steepness case shows lower reduction than the corresponding high wave steepness case of F=4 m, which is also the case in Figure 7.18 but not in Figure 7.17.

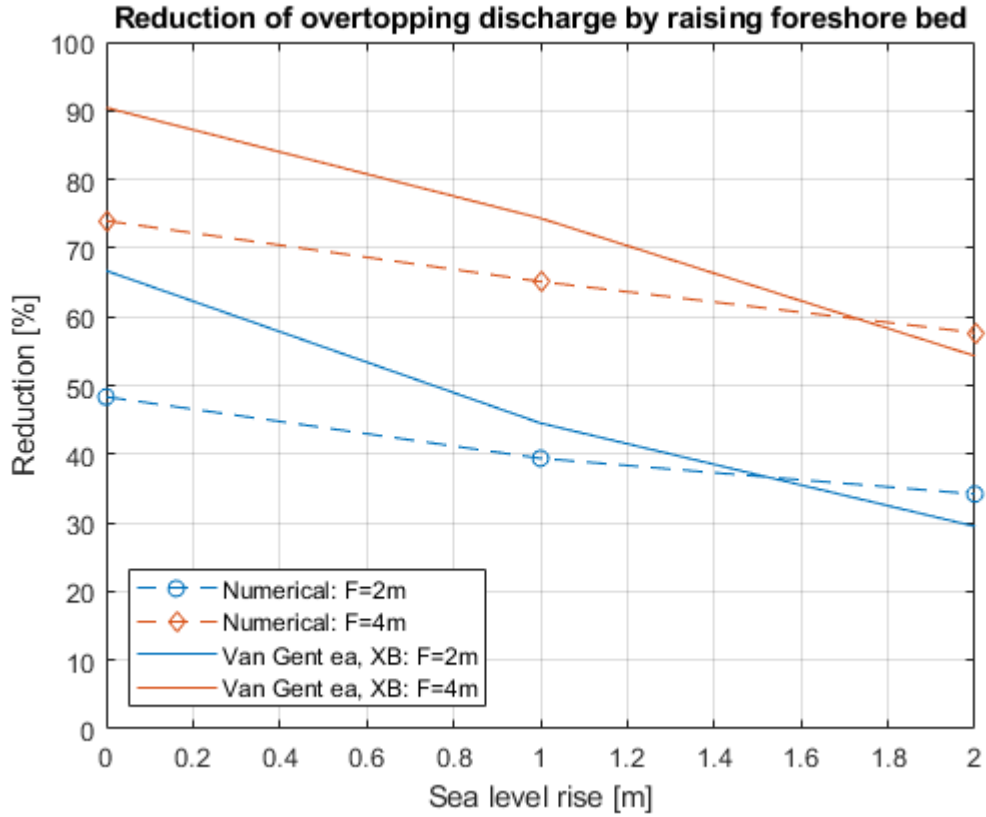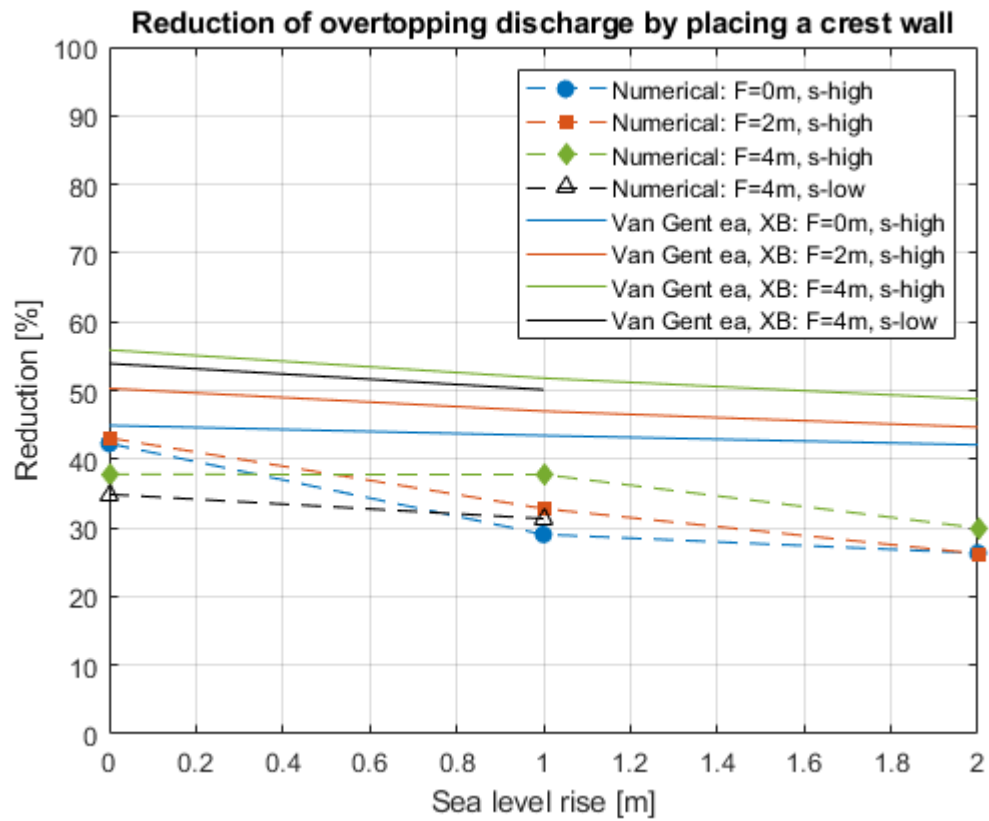Figure 7.19: OpenFOAM and empirical (XBeach wave conditions with Van Gent et al. (2022)) relative overtopping reduction $(q_0-q)/q_0$ with q_0 having the same F and wave steepness but without crest wall.

General trend

In Figure 7.20, the numerical and empirical dimensionless overtopping discharges are compared.
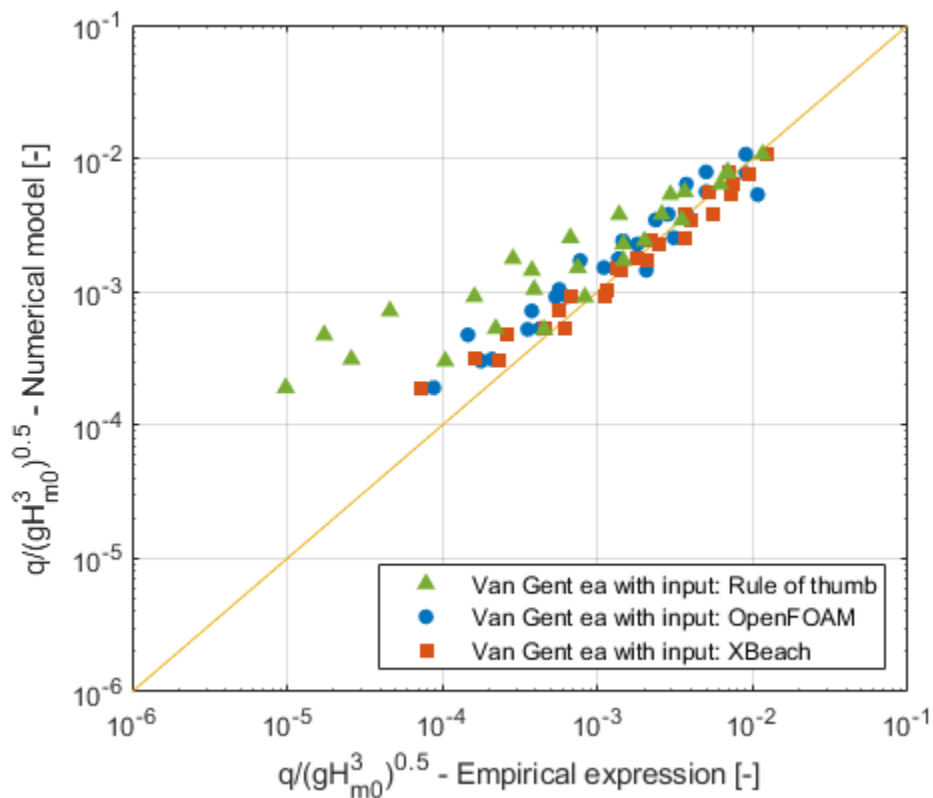
Figure 7.20: Dimensionless overtopping of OpenFOAM model versus empirical expression with various inputs.

In the beginning of this section, it is explained that the discharges are only compared relatively, because the OpenFOAM overtopping discharge is grid size dependent. The comparison in Figure 7.20 is a comparison of absolute values, but it is mostly used to look at the general trend of the dimensionless overtopping discharges.

The agreement between the numerical and empirical dimensionless overtopping is rather good, especially for higher discharges. The results computed with the rule of thumb show larger spreading and a diverging trend for lower discharges. The overtopping based on the OpenFOAM wave conditions in the empirical expression has a consistent and good agreement with the numerical OpenFOAM results. However, the best comparison with the numerical model results is the empirical expressions with XBeach wave conditions as input, although the spreading does slightly increase for lower discharges.

As a quantification of the agreement between the numerical and empirical dimensionless overtopping, the RMSE is used as defined in Equation 7.1. The RMSE is 0.596 when using the rule of thumb, 0.216 when using the OpenFOAM wave parameters, and 0.138 when using the XBeach wave parameters as input for the empirical expressions. These RMSE values should only be compared mutually. The RMSE values indicate relatively small deviations when comparing to values mentioned in e.g., Irías Mata and Van Gent (2023), but it is an unfair comparison. This is because the current research contains mostly data for relatively high overtopping which are generally computed more accurately.

The RMSE is also computed for the actual (dimensional) overtopping discharge, without making it dimensionless by using the wave height and gravitational acceleration like in Equation 7.1. Using the XBeach results as input for the empirical overtopping expressions has a slightly higher RMSE (0.155), but it is still better than using OpenFOAM (0.216) or the empirical estimates using the rule of thumb (0.623). Note that when using OpenFOAM wave parameters, the RMSE is identical whether it is used for dimensionless or regular overtopping discharges, as the significant wave height is identical for the numerical and empirical case.

$$RMSE = \sqrt{\frac{\sum_{i=1}^{n_{tests}} \left(\log \left(q_{num}/\sqrt{gH_{m0}^3} \right) - \log \left(q_{emp}/\sqrt{gH_{m0}^3} \right) \right)^2}{n_{tests}}} \tag{7.1}$$

7.3. Concluding remarks

In this chapter, empirical estimates and empirical formulae are validated with the XBeach and OpenFOAM models to help answer research sub-questions 1 and 3.

Wave transformation and depth-induced breaking on the foreshore

In the case study, two empirical estimates of the suggested method in Section 3.1 are used regarding the wave transformation and wave breaking on the foreshore:

- The significant wave height at the toe is computed with a rule of thumb for depth-induced breaking.
- The spectral period at the toe is assumed to be equal to the offshore value.

Based on the validation, it can be said that the empirical estimates served as a reasonable first estimate for the case study of Chapter 5. However, it is apparent that more accurate methods are necessary for detailed calculations because the accuracy of the assumptions (i.e., the wave heights

are equal to half the water depth and there are no changes in wave period) varies significantly based on the relative water depth and shows slight dependency on the bathymetry and wave steepness.

Wave overtopping at the breakwater

Together with the assumptions for the wave transformation, the case study used the overtopping expressions of Van Gent et al. (2022) to compute the tipping points and thus effectiveness of the adaptation measures. The reduction in overtopping obtained with the measures is compared between the OpenFOAM overtopping results and the expressions of Van Gent et al. (2022) with three sources of wave parameter input. Figure 7.21 shows the average reduction in overtopping for the tested measures (averaged over the sea level rise values and the wave steepness conditions).
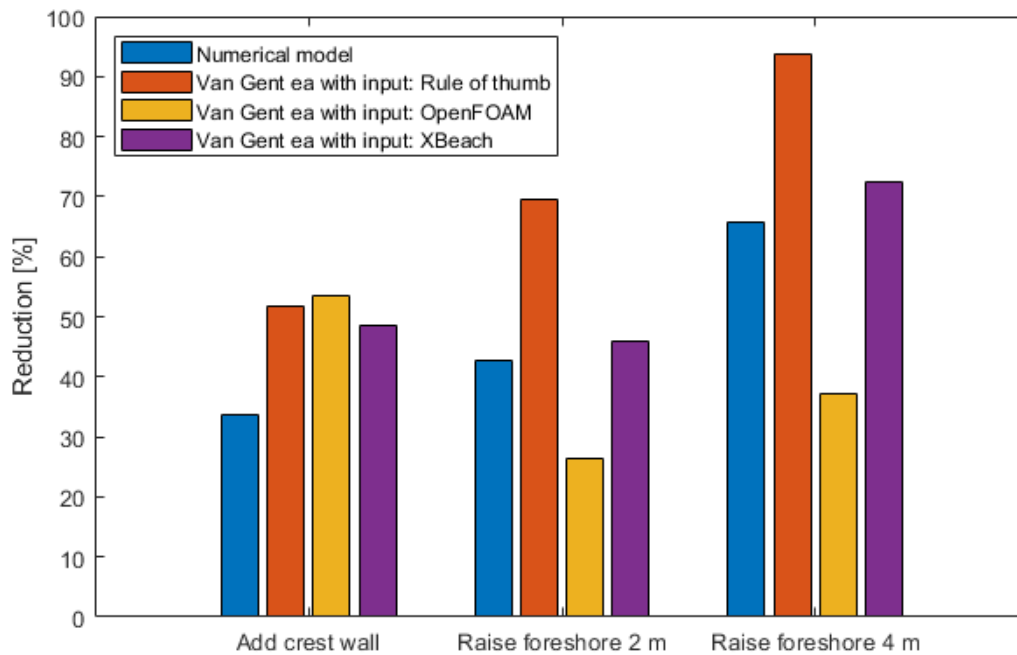
Figure 7.21: Overtopping reduction of adaptation measures in OpenFOAM compared to empirical expressions.

Based on the comparison, the expressions of Van Gent et al. (2022) can predict overtopping results with reasonable accuracy when the wave parameters obtained with XBeach are used as input. However, due to the sensitivity of the numerical model results to the grid and foreshore length, inaccuracies in the numerical models, and the limitations of the validity of the empirical overtopping expressions, firm conclusions with respect to the effectiveness of the adaptation measures cannot be obtained. Dedicated physical model tests including wave breaking on the (nourished) foreshore would be necessary to draw firm conclusions on the effectiveness of the adaptation measures.

Reflecting on the optimal pathway of the case study

The adaptation measures of adding a crest wall and raising the foreshore bed level are part of the optimal pathways determined in Chapter 5. In the case study, the crest wall of 1 m could compensate for 0.53 m of sea level rise and raising the foreshore with 2 m could compensate for 0.92 m of sea level rise. The numerical results indicate that the crest wall is not as effective as determined in the case study, which is even more so for raising the foreshore bed level. The tipping points of the optimal pathway are thus reached earlier, and the pathway can adapt to less sea level rise than expected if the numerical results are accurate. It is also likely that raising the foreshore bed level is not preferred as much over the crest wall as a first measure, as the effectiveness is more similar in the numerical model. No further conclusions can be made regarding optimal pathways of the case study, because the other adaptation measure of raising the armour crest, adding a berm to the breakwater, and placing a low crested structure are not investigated in the numerical model.

8. Discussion

In this chapter, the applicability of the methods (Section 8.1), the key assumptions and limitations of the case study (Section 8.2), and the numerical validation results (Section 8.3) are discussed.

8.1. Applicability of the methods

In Chapter 3, methods are proposed to incorporate changes in depth-induced breaking in the creation of adaptation pathways and incorporate uncertainty of sea level rise in the selection of optimal adaptation pathways. Then, in Chapter 5 the applicability of the methods is tested with a case study. Although this is only a single test case, it is deemed sufficient to prove the applicability of the methods. Different cases (i.e., different boundary conditions, breakwater design, adaptation measure characteristics, costs, economic factors, etc.) might have different tipping points and cost of adaptation pathways, which changes the input and output values for the methods, but this does not affect the applicability of the proposed methods. However, it must be noted that the method to incorporate depth-induced breaking is only recommended for shallow foreshores ($h_t/H_{m0,o} > 1$).

Nevertheless, it is still beneficial to apply the methods for more cases to gain more insight into the accuracy of the method for depth-induced breaking and the benefits of applying the methods to select optimal pathways, and potentially to find points for improvement of the proposed methods.

8.2. Assumptions and limitations of the case study

Creation of adaptation pathways

As stated in the scope of the research, and in Section 3.1 and Section 4.3, a simplified approach is taken regarding climate change and the consequent changes in the hydraulic boundary conditions:

- The (potential) change of wave climates due to climate change is not considered. However, for coastal structures in depth-limited conditions, the impact of increasing offshore wave heights is likely insignificant.
- It is assumed that the increase of the design still water level is equal to the local sea level rise. If the design water level does not increase as much as the average sea level, smaller or less measures would be necessary in the adaptation of breakwaters. Naturally, the reverse is also true, which is important in the planning of sea level rise adaptation and creating adaptation pathways. The effect of climate change on extreme wave conditions and water levels is a current research topic e.g., Fox-Kemper et al. (2021), so further research might provide new knowledge to incorporate in the method suggested in Section 3.1.

Furthermore, multiple assumptions regarding the design of the rubble mound breakwater and the adaptation measures have been made, of which the following are considered most important:

- After the tipping point of a measure is reached, an entirely different measure is applied but adaptation measures could also be expanded or extended instead. For example, extending the crest wall, raising or widening the berm, or raising the crest of the low-crested structure. This can potentially be used for smaller amounts of sea level rise adaptation towards the end of the structural lifetime, giving additional flexibility for decision-making. Additionally, expanding on the existing measure might be cheaper than applying different measures. This can also be done if certain measures are already used in the original design of the breakwater.
- The dimensions and characteristics of the adaptation measures are assumed based on examples in Section 4.5, which determines the tipping points of the measures. However, in Section 5.2.4 it is observed that it is very likely only one adaptation measure is necessary for mild scenarios. Measures adapting for sea level values such that likely only one measure is

necessary, defeats the purpose of using adaptation pathways to avoid potentially unnecessary costs. So, this is an indication that the measures should be downsized in dimension to get the desired adaptive approach for mild scenarios. On the other hand, downsizing measures might drastically increase the number of measures necessary for extreme scenarios, which would be detrimental for the cost of pathways due to high fixed costs of e.g., construction equipment. These aspects must be considered to create optimal adaptation pathways for all considered sea level rise scenarios.

Evaluation of adaptation pathways

While a sensitivity analysis is performed for several assumptions regarding the cost evaluation of pathways in Section 5.3, there are also other aspects which have not been analysed or considered in the case study:

- Values for material and construction cost are assumed in Section 4.6. In a more detailed analysis, variations in these values should be checked to see whether different pathways are preferred. These values are also very location dependent, based on availability of equipment and cost of labour.
- Operation and maintenance cost have not been considered. These costs are especially important for raising the foreshore bed level, depending on how often nourishments must be done to maintain the desired bed level, which makes it less attractive to apply this measure first. Also costs like long-distance transport of materials or more detailed construction costs are not considered, which could also influence the evaluation.
- In the sensitivity analysis of the discount rate, relatively mild changes are checked. For a more elaborate analysis, more extreme changes in the inflation and discount rate values must be considered, as was done by for example Haasnoot et al. (2020).
- The case study only investigated the location of IJmuiden, but the cost of measures might be very different at other locations for different breakwater size, water depth and wave climate. Naturally the dimensions of all measures are somewhat dependent on for example the water depth, but some are likely more dependent than others.
- As explained in Section 5.2.4, the probability of a second or third adaptation measure being needed is increased for longer structural lifetimes. Other values than the assumed 50 years have not been analysed, so the effect on the preferred pathways is not known. It is noted that structures may be designed for e.g., 50 years, but that these structures are likely to be present for a longer period. This increases the importance of adaptation pathways for sea level rise scenarios over longer periods.
- For the evaluation of the pathways, the amount of sea level rise adaptation pathways provide is an important criterion. However, the previous and next section highlight how much uncertainty surrounds the calculation of tipping points. It is important to consider this when viewing the evaluation of pathways and the selection of optimal pathways, as different calculation methods might result in different optimal pathways.
- For the method to include model uncertainty in the cost estimation, the probability of a measure being necessary is simplified to either applying the measure or not. In reality, this decision is more complex. It can also be decided to apply the measure with larger or smaller dimensions based on the desired remaining lifetime of the structure, as the structures are likely to be present for longer than the initially assumed lifetime.

As stated in the scope of the research, the thesis focuses on the reduction of overtopping discharge at the breakwater. However, measures can also have added value on other aspects which can be considered when selecting optimal pathways, for example:

- Measures like the low-crested structure and foreshore nourishment are also beneficial for the armour stability of the breakwater because the incoming wave height is reduced.
- The low-crested structure can also be an artificial reef or reef-like structure as shown by Buis (2022), thus it can provide additional ecological value.
- Raising the armour crest level can be combined with replacing the armour units with units that can withstand larger waves, for stability purposes.
- In general, aspects like durability and sustainability can also be considered when deciding which pathway is optimal.

8.3. Numerical models and the validation of empirical formulae

In Chapter 7, the numerical model results are presented and compared with the empirical formulae used in the case study. The possible inaccuracies and inconsistencies of these results are discussed in this section.

Wave transformation and depth-induced breaking

The XBeach and OpenFOAM results showed a significant difference in the spectral period for decreasing water depths. A potential source of this discrepancy are the low frequency energy peaks in the OpenFOAM wave spectra, which are often much smaller in the XBeach spectra. The wave lengths corresponding to these frequencies are such that realistically it cannot be accurately determined with the chosen spacing between the wave gauges, nor can it be generated with the JONSWAP input and relaxation zone. The low frequency peaks also change based on the presence of the crest wall and increase with increasing foreshore bed level, so it might be related to reflection or wave breaking. The peaks are still present in the simulations without the breakwater, thus it cannot only be attributed to wave-structure interaction and reflection.

While OpenFOAM has been used to accurately predict overtopping (Irías Mata & Van Gent, 2023; Chen et al., 2021), it has not been used often to compute significant wave breaking on the foreshore. Both Lashley et al. (2020) and Chen et al. (2021) found that OpenFOAM overestimates the spectral period compared to physical model tests, although this overestimation was less than 10% for Chen et al. (2021). Lashley et al. (2020) even specifically found that a XBeach non-hydrostatic model showed better agreement with physical model tests. Based on the findings in Section 7.1, the unexplained low frequency peaks discussed above, and these previous findings in literature, the spectral periods produced by the XBeach model are considered more accurate than those computed with the OpenFOAM model. Therefore, the conclusion on the change of the spectral period due to depth-induced breaking in the next chapter is based on the XBeach results.

A general source of inaccuracy for the computed nearshore wave conditions of the numerical models is the breaking and subsequent changing of waves throughout the set of wave gauges. The signal decomposition method assumes that the wave signal does not change between the wave gauges, so it is likely that this causes inaccuracies in the separation of the incoming and reflected wave signals.

Irías Mata and Van Gent (2023) showed that detailed turbulence models were not required to obtain accurate wave propagation results in OpenFOAM. However, the OpenFOAM model in this thesis specifically investigates wave breaking on the foreshore, which was not the case in the study of Irías Mata and Van Gent (2023). Therefore, it is unknown whether accurate results can be obtained for foreshores with severe wave breaking without detailed turbulence models.

The numerical models, especially OpenFOAM, showed deviations of up to 10% between wave heights for the same water depth at the toe but for different bed levels. A possible reason for this

difference is how the foreshore bed level is raised in the numerical flume. Because the 1:10 slope is extended to the raised bed level, the slope width increases and the horizontal foreshore length decreases. Therefore, the foreshore length at which the water depth is equal to water depth at the toe significantly reduces for higher bed levels. If the wave gauges are placed further from the slope, the significance of this effect might be reduced, because the waves can break before they reach the gauges.

The comparison between the empirical rule of thumb and numerical models is only done for a relative water depth ($h_t/H_{m0,o}$) between 1 and 2. The differences between the numerical models and the rule of thumb might be very different for very or extremely shallow foreshores with relative water depth below 1. Also, only a simplified bathymetry with a horizontal offshore bed, 1:10 transition slope and horizontal bed at the breakwater is tested. For a more complete comparison, different bathymetries should be tested.

The water surface elevation, significant wave height and spectral period in OpenFOAM all showed grid dependency in Section 6.2.5. However, the difference between the finest mesh and the chosen mesh size is less than 10%, with the significant wave height being higher and spectral period lower. The differences between the computed wave conditions in OpenFOAM and those computed with the rule of thumb and XBeach would still be similar, although smaller. Therefore, the trends observed in the OpenFOAM wave parameters and differences in the comparison with the rule of thumb and XBeach are not caused by the grid dependency of the OpenFOAM model.

Wave overtopping
The empirical overtopping expressions with the nearshore wave conditions of OpenFOAM as input and the overtopping computed in OpenFOAM showed very different overtopping reduction for the adaptation measure of raising the foreshore bed. This difference could be caused by the fact that the empirical expressions are used outside the known validity range, regarding the breaking of waves on the foreshore. However, it could also be caused by the wave parameter input taken from OpenFOAM, because there are potential sources of inaccuracy in these wave parameters, as discussed previously. Specifically, the unexplained low frequency peaks in OpenFOAM could be a factor, which cause significant increase of the spectral period. These peaks are much smaller in the XBeach wave spectra and using XBeach wave parameters in the empirical expressions does give similar results to the numerical overtopping. Therefore, it seems likely that the largest contribution to the difference in overtopping lies with the wave parameters computed in OpenFOAM and not the empirical expressions.

The empirical overtopping expressions predict higher effectiveness of the crest wall for each tested wave parameter input compared to the OpenFOAM model. This could be indication that the crest wall influence factor of Van Gent et al. (2022) is slightly inaccurate for conditions with significant wave breaking on the foreshore. However, the difference in crest wall effectiveness might not even be significant. The empirical and numerical (dimensionless) overtopping results show reasonable agreement when using XBeach wave parameter input, even though the overtopping reduction differs 15 percentage points. Also, based on the potential inaccuracies of the OpenFOAM model mentioned previously, and the fact that the expressions of Van Gent et al. (2022) are based on much more data from physical model tests, it is difficult to assess whether the OpenFOAM model can be trusted enough to conclude that the expressions are slightly inaccurate. Further testing, preferably physical model testing, could give more insight into the influence of the crest wall for conditions with breaking waves on the foreshore.

9. Conclusions and recommendations

9.1. Conclusions

In Chapter 1, the objective of the thesis is specified and formulated in the form of the main research question:

> **How can an optimal adaptation pathway for rubble mound breakwaters be determined based on cost and uncertainty of sea level rise, aiming to limit wave overtopping when considering changes in depth-induced wave breaking?**

To answer this main research question, three research sub-questions were formulated and are addressed below. All answers to the sub-questions combined give the answer to the main research question.

1. **How can changes in depth-induced breaking be considered when determining tipping points of adaptation pathways for rubble mound breakwater?**

To account for changes in depth-induced breaking, a method is proposed that uses two estimates for the significant wave height and the spectral period, which can then be used in empirical overtopping expressions to determine tipping points:

- The significant wave height can be determined using a common rule of thumb, in which the significant wave height at the toe of the breakwater is at maximum equal to half the water depth at the toe.
- The spectral period at the toe can be assumed to be equal to the deep-water spectral period for shallow foreshores (definition based on the relation of water depth and offshore wave height; $h_t/H_{m0,o} > 1$).

The accuracy of these estimates to account for wave transformation and depth-induced breaking is checked by comparing them to XBeach model results, based on a case study for the location of IJmuiden, the Netherlands. Two conclusions are drawn with respect to the suggested method:

- The rule of thumb can be used estimate the significant wave height with an average deviation of 8% and a maximum of 21% compared to numerical model results. The largest differences were found for the lowest water depths, for which the rule of thumb underestimates the wave height.
- The estimate that the spectral period does not change from offshore to the toe can be used for the tested relative water depths ($1 < h_t/H_{m0,o} < 2$) within error of 15% compared to the numerical results. The largest increase in spectral period from offshore to nearshore was observed for the lowest water depths in the numerical results.

Based on the results stated above, it is concluded that the suggested method serves as a reasonable first estimate, but numerical models are necessary to determine wave loading more accurately and subsequently to calculate tipping points of adaptation pathways more accurately.

2. **How can uncertainty of sea level rise projections be accounted for in the cost assessment of adaptation pathways for rubble mound breakwaters?**

Two methods are proposed in this thesis that can be used to account for sea level rise uncertainty in the cost assessment of adaptation pathways, one for the model uncertainty and one for the scenario uncertainty:

- The first method uses model uncertainty percentile ranges of a scenario to approximate a gaussian probability distribution of the sea level rise at the end of the lifetime of the breakwater. With this probability distribution, the probability of sea level rise exceeding the tipping point of an adaptation measure can be determined, which is the probability that the next adaptation measure needs to be applied. Multiplying the probability of a measure being applied with the cost of the measure gives a simple risk evaluation and the expected value of the cost (expected cost in short) of one adaptation measure, and the sum for the measures in a pathway gives the expected cost of the adaptation pathway.
- The second method computes the weighted average of all considered scenarios for the cost of pathways to deal with scenario uncertainty. Because the likelihoods or probabilities of sea level rise scenarios are often unknown, the suggested method is to first use the average of all scenarios and then assign different weights to the scenarios in a sensitivity analysis to see how this affects the results.

The methods were used in the case study, which lead to the following conclusions:

- The method to include model uncertainty showed very little distinction between pathways with the same first adaptation measure, making it difficult to determine specific optimal pathways. Despite this effect, using the model uncertainty gave insight into the best adaptation measure to start with and how likely measures are to be applied, which is valuable for decision-making.
- For this case study, there is no significant difference in preferred pathways between the scenarios. Therefore, applying different probabilities or weights to the scenarios for the weighted average does not change which pathways are preferred. Notably, the previous research by Hogeveen (2021) also found that the same pathways were preferred regardless of sea level rise scenario.

3. **How do adaptation measures influence wave overtopping discharge in a numerical model compared to empirical formulae for conditions with significant wave breaking on the foreshore?**

The numerical overtopping results from the numerical OpenFOAM model are compared to the empirical overtopping expressions of Van Gent et al. (2022) with three sources of wave parameter input. Only two adaptation measures are tested, namely raising the foreshore bed level and adding a protruding crest wall.

Based on the comparison with numerical results, the expressions of Van Gent et al. (2022) can predict (the influence of adaptation measures on) overtopping with reasonable accuracy, even for conditions with significant wave breaking on the foreshore. For this study, this is specifically the case when the wave parameters obtained from the XBeach model are used as input for the overtopping expressions, with a root mean square error of 0.1381 for the comparison of dimensionless overtopping with the numerical results.

Nevertheless, due to the sensitivity of the numerical model results to the grid and foreshore length, inaccuracies in the numerical models, and the limitations of the validity of the empirical overtopping expressions, firm conclusions with respect to the effectiveness of the adaptation measures cannot be obtained. For more accurate adaptation pathways (i.e., tipping points of adaptation measures), more accurate methods are necessary to determine (the effect of measures on) the wave loading and overtopping discharge for conditions with significant wave breaking on the foreshore.

9.2. Recommendations

Creating and evaluating adaptation pathways

Regarding the process of creating and evaluating adaptation pathways, there are several recommendations:

- To consider depth-induced wave breaking when creating adaptation pathways and determining tipping points, the rule of thumb and the offshore spectral period can be used as a first estimate for shallow foreshores ($1 < h_t/H_{m0,o} < 4$). It is recommended to validate the accuracy of these estimates for more cases. Moreover, applying the formula of Hofland et al. (2017) to determine the spectral period is probably more accurate within its range of validity.
- For more detailed creation of adaptation pathways, it is recommended to use a numerical solver which can model the propagation and decay of individual waves like the XBeach model used in this thesis. The output of this model can then be used in the empirical expressions of Van Gent et al. (2022) or the modified expressions of Irías Mata and Van Gent (2023). For the water depths ($1 < h_t/H_{m0,o} < 2$) and adaptation measures (crest wall, foreshore nourishment) tested in this thesis, this method generated very similar overtopping results to the OpenFOAM model, but the computational time is drastically lower.
- Incorporate expansion of existing features of the rubble mound breakwater or already applied adaptation measures when creating adaptation pathways for rubble mound breakwaters. Both in this thesis and the work of Hogeveen (2021), this has not been considered. However, this could improve the flexibility and adaptability of the pathways and potentially save costs.
- To gain more insight into the usefulness (for decision makers) of the proposed method to incorporate sea level rise uncertainty in the selection of pathways, the method should be applied to more cases. Furthermore, it should also be compared to a full probabilistic assessment in further stages of adaptation planning, for example with a Monte Carlo simulation as used by Trommelen (2022). This can give a more detailed overview of the possible cost variation and can also include uncertainty of other factors, such as inflation, discount rate, and material cost.
- Based on the evaluation, a feedback loop should be done for detailed adaptation plans to optimise the pathways and characteristics of the measures. This can be done for example by using the methods of levelised cost and expected cost of pathways. The optimisation must also consider the different sea level rise scenarios and how many measures are likely necessary per scenario when deciding the characteristics and dimensions of the measures. An optimum must be found between the case in which the mild scenarios only need one measure, and the case in which the extreme scenarios need an inefficient number of measures.

Numerical and physical modelling

Numerical and/or physical modelling are required to determine accurate adaptation pathways. To increase the accuracy of wave loading and wave overtopping predictions for this purpose, the following recommendations are given with respect to numerical and physical modelling:

- The expressions of Van Gent et al. (2022) should be tested further for conditions with significant wave breaking on the foreshore, preferably with physical models. The expressions have yielded similar results to the OpenFOAM model. Although it produces logical and consistent overtopping results, this numerical model contains several potential sources of inaccuracy, for example the grid dependency of the overtopping, significant numerical

dissipation, and unexplained low frequency wave energy. Further investigation could focus on the validation of the numerical results presented in this research. For example, the effectiveness of the adaptation measures of raising the foreshore bed level and adding a crest wall. In addition, physical model tests could also be used to validate the numerical results of the wave transformation on the foreshore, as the OpenFOAM and XBeach models showed significant differences.

- If physical model testing is not feasible, further research could be performed in numerical models to compare the effectiveness of the adaptation measures with the empirical expressions for conditions with significant wave breaking on the foreshore. For example, different bathymetry set-ups can be tested, varying the slope and how the nourishment is applied on the foreshore to see how it affects the wave transformation and overtopping. The foreshore is raised evenly in the simulations performed here, but the nourishment can also be distributed differently. More tests could be done with varying wave steepness, since the number of low wave steepness tests in this thesis is limited. The effectiveness of other adaptation measures, which were not researched here, could also be investigated and compared to the empirical formulae. Further research could also focus on even shallower foreshores, as the wave conditions deviate even more for lower water depth to offshore wave height ratios compared to the tested conditions by Van Gent et al. (2022).

- It is advised to investigate the coupling of XBeach and OpenFOAM, for numerical modelling of the conditions with significant wave breaking on the foreshore. The wave transformation and wave breaking from offshore to the depth at the toe of the breakwater can be computed with XBeach and converted to a wave spectrum. This wave spectrum can then be used as input for the OpenFOAM model to compute the overtopping at the breakwater. This plays to the strengths of both models, and potentially saves a lot of computational time. The implementation of the XBeach wave spectrum as input for the OpenFOAM model is the main source of difficulty. Most importantly, the accuracy of the results produced by this coupling of XBeach and OpenFOAM should be investigated.

- The influence of detailed turbulence modelling in OpenFOAM could be researched. Irías Mata and Van Gent (2023) showed that detailed turbulence models were not required to obtain accurate wave propagation results in OpenFOAM. However, the study of Irías Mata and Van Gent (2023) did not have significant wave breaking on the foreshore. Including detailed turbulence models might alter the wave transformation results when significant depth-induced wave breaking occurs in the model.

References

Appelquist, L.R., & Halsnæs, K. (2015). The Coastal Hazard Wheel system for coastal multi-hazard assessment & management in a changing climate. *Journal of Coastal Conservation, 19,* 157-179. https://doi.org/10.1007/s11852-015-0379-7

Asariotis, R. (2021). *Climate change impacts on seaports: A growing threat to sustainable trade and development.* United Nations Conference on Trade and Development (UNCTD). https://unctad.org/news/climate-change-impacts-seaports-growing-threat-sustainable-trade-and-development

Briganti, R., van der Meer, J. W., M.Buccino, & Calabrese, M. (2003). Wave transmission behind low-crested structures. *ASCE 2003*. https://doi.org/10.1061/40733(147)48

Buis, L. (2022). *Wave transmission over artificial reefs. A physical model study* [Master's thesis, Delft University of Technology]. http://resolver.tudelft.nl/uuid:f98b4e33-e512-424a-a7ab-671f2f85e8b7

Buurman, J., & Babovic, V. (2016). Adaptation Pathways and Real Options Analysis: An approach to deep uncertainty in climate change adaptation policies. *Policy and Society, 35-2,* 137-150. https://doi.org/10.1016/j.polsoc.2016.05.002

Chen, X., Hofland, B., & Uijttewaal, W. (2016). Maximum overtopping forces on a dike-mounted wall with a shallow foreshore. *Coastal Engineering*, *116*, 89-102. https://doi.org/10.1016/j.coastaleng.2016.06.004

Chen, W., van Gent, M.R.A., Warmink, J.J., & Hulscher, S.J.M.H. (2020). The influence of a berm and roughness on the wave overtopping at dikes. *Coastal Engineering, 156*, 103613. https://doi.org/10.1016/j.coastaleng.2019.103613

Chen, W., Warmink, J. J., Van Gent, M. R. A., & Hulscher, S. J. M. H. (2021). Numerical modelling of wave overtopping at dikes using OpenFOAM®. *Coastal engineering, 166*, 103890. https://doi.org/10.1016/j.coastaleng.2021.103890

CIRIA, CUR, CETMEF. (2007). *The Rock Manual. The use of rock in hydraulic engineering (2nd 550 edition)*. 551 C683, CIRIA, London

Conde, J. M. P. (2019). Comparison of different methods for generation and absorption of water waves. *Revista de Engenharia Térmica*, *18*(1), 71-77.

d'Angremond, K., van der Meer, J. W., & de Jong, R. J. (1996). Wave transmission at low-crested structures. *ASCE Chapter 187*. https://doi.org/10.1061/9780784402429.187

Dassanayake, D.M.D.T.B., Kumuthini, S., Galappatti, R., Wootton, D., & Mendis, M. (2008). Hydraulic model study to the breakwater design for Colombo south harbour. *PIANC-COPEDEC VII*. https://www.researchgate.net/publication/331258178_HYDRAULIC_MODEL_STUDY_TO_THE_BREAKWATER_DESIGN_FOR_COLOMBO_SOUTH_HARBOUR

Den Bieman, J. P., van Gent, M. R. A., & van den Boogaard, H. F. P. (2020). Wave overtopping predictions using an advanced machine learning technique. *Coastal Engineering, 166,* 103830. https://doi.org/10.1016/j.coastaleng.2020.103830

De Ridder, M.P., Kramer, J., den Bieman, J.P., Wenneker, I. (2023). Validation and practical application of nonlinear wave decomposition methods for irregular waves. *Coastal Engineering, 183,* 104311. https://doi.org/10.1016/j.coastaleng.2023.104311

De Ruig, L.T., Barnard, P.L., Botzen, W.J.W, Grifman, P., Hart, J.A.F., De Moel, H., Sadrpour, N., & Aerts, J.C.J.H. (2019). An economic evaluation of adaptation pathways in coastal mega cities: An illustration for Los Angeles. *Science of The Total Environment, 678,* 647-659. https://doi.org/10.1016/j.scitotenv.2019.04.308

De Vries, H., Katsman, C., & Drijfhout, S. (2014). Constructing scenarios of regional sea level change using global temperature pathways. *Environmental Research Letters*, *9*(11), 115007. https://doi.org/10.1088/1748-9326/9/11/115007

EurOtop. (2018). *Manual on wave overtopping of sea defences and related structures. An overtopping manual largely based on European research, but for worldwide application*. Van der Meer, J.W., Allsop, N.W.H., Bruce, T., De Rouck, J., Kortenhaus, A., Pullen, T., Schüttrumpf, H., Troch, P. and Zanuttigh, B., www.overtopping-manual.com.

Fox-Kemper, B., Hewitt, H.T., Xiao, C., Aðalgeirsdóttir, G., Drijfhout, S.S., Edwards, T.L., Golledge, N.R., Hemer, M., Kopp, R.E., Krinner, G., Mix, A., Notz, D., Nowicki, S., Nurhati, I.S., Ruiz, L., Sallée, J.-B., Slangen, A.B.A., & Yu, Y. (2021). *Ocean, Cryosphere and Sea Level Change*. In Climate Change 2021: The Physical Science Basis. Contribution of Working Group I to the Sixth Assessment Report of the Intergovernmental Panel on Climate Change. Cambridge University Press, Cambridge, United Kingdom and New York, NY, USA, pp. 1211–1362. https://www.ipcc.ch/report/ar6/wg1/chapter/chapter-9/

Gallo, A. (2014). *A refresher on net present value*. Harvard Business Review. https://hbr.org/2014/11/a-refresher-on-net-present-value

Garner, G.G., Hermans, T., Kopp, R.E., Slangen, A.B.A., Edwards, T.L., Levermann, A., Nowicki, S., Palmer, M.D., Smith, C., Fox-Kemper, B., Hewitt, H.T., Xiao, C., Aðalgeirsdóttir, G., Drijfhout, S.S., Golledge, N.R., Hemer, M., Krinner, G., Mix, A., Notz, D., … , Pearson, B. (2021). IPCC AR6 Sea-Level Rise Projections. Version 20210809. PO.DAAC, CA, USA. Dataset accessed 03-10-2022 at https://sealevel.nasa.gov/ipcc-ar6-sea-level-projection-tool?psmsl_id=9&info=true.

Haasnoot, M., Kwakkel, J.H., Walker, W.E., & ter Maat, J. (2013). Dynamic adaptive policy pathways: A method for crafting robust decisions for a deeply uncertain world. *Global Environmental Change, 23-2,* 485-498. https://doi.org/10.1016/j.gloenvcha.2012.12.006

Haasnoot, M., Brown, S., Scussolini, P., Jimenez, J.A., Vafeidis, A.T., & Nicholls, R.J. (2019). Generic adaptation pathways for coastal archetypes under uncertain sea-level rise. *Environmental Research Communications, 1,* 071006. https://doi.org/10.1088/2515-7620/ab1871

Haasnoot, M., van Aalst, M., Rozenberg, J., Dominique, K., Matthews, J., Bouwer, L. M., Kind, J., & Poff, N.L. (2020). Investments under non-stationarity: economic evaluation of adaptation pathways. *Climatic change, 161(3),* 451-463. https://doi.org/10.1007/s10584-019-02409-6

Hofland, B., Chen, X., Altemare, C., & Oosterlo, P. (2017). Prediction formula for the spectral wave period $T_{m-1,0}$ on mildly sloping shallow foreshores. *Coastal Engineering, 123 (2017) 21-28*. https://doi.org/10.1016/j.coastaleng.2017.02.005

Hogeveen, K.P.J. (2021). *Climate Adaption of Rubble Mound Breakwaters; A Study to the Accuracy of Overtopping Formulas for Combination of Solutions* [Master's thesis, Delft University of Technology]. http://resolver.tudelft.nl/uuid:3a6ec8ac-0b81-4d32-adf1-6d7b4f842ceb

IPCC. (2021). *Summary for Policymakers*. In: Climate Change 2021: The Physical Science Basis. Contribution of Working Group I to the Sixth Assessment Report of the Intergovernmental Panel on Climate Change. Cambridge University Press, Cambridge, United Kingdom and New York, NY, USA, pp. 3–32, doi:10.1017/9781009157896.001.

Irías Mata, M. (2021). *Numerical estimation of wave loads on crest walls on top of rubble mound breakwaters using OpenFOAM* [Master's thesis, Delft University of Technology]. http://resolver.tudelft.nl/uuid:36b66c90-dfdb-41d0-b1f2-1253d3f87b4c

Irías Mata, M., & Van Gent, M.R.A. (2023). Numerical modelling of wave overtopping discharges at rubble mound breakwaters using OpenFOAM®. *Coastal Engineering, 180,* 104274. https://doi.org/10.1016/j.coastaleng.2022.104274

Jacobsen, N.G., Fuhrman, D.R., & Fredsøe, J. (2012). A wave generation toolbox for the open-source CFD library: OpenFOAM®. *International Journal for Numerical Methods in Fluids, 70(9)*, 1073-1088. https://doi.org/10.1002/fld.2726

Jacobsen, N.G. (2017). Waves2Foam Manual.

Jacobsen, N.G., van Gent, M.R.A., Capel, A., & Borsboom, M. (2018). Numerical prediction of integrated wave loads on crest walls on top of rubble mound structures. *Coastal Engineering, 142*, 110124. https://doi.org/10.1016/j.coastaleng.2018.10.004

Jensen, B., Jacobsen, N.G. and Christensen, E.D. (2014). Investigations on the porous media equations and resistance coefficients for coastal structures. *Coastal Engineering, 84*, 56-72. https://doi.org/10.1016/j.coastaleng.2013.11.004

Kind, J.M., Baayen, J.H., & Botzen, J.W. (2018). Benefits and Limitations of Real Options Analysis for the Practice of River Flood Risk Management. *Water Resources Research, 54-4,* 3018-3036. https://doi.org/10.1002/2017WR022402

KNMI. (2021). *Ook de hoogste en laagste scenario's voor de uitstoot van broeikasgassen doen er toe.* https://www.knmi.nl/over-het-knmi/nieuws/ook-de-hoogste-en-laagste-scenario-s-voor-de-uitstoot-van-broeikasgassen-doen-er-toe

Krom, J.C. (2012). *Wave overtopping at rubble mound breakwaters with a non-reshaping berm* [Master's thesis, Delft University of Technology]. http://resolver.tudelft.nl/uuid:984bc5e5-8c04-4d35-b34a-2b871f636fa1

Kuiper, C., & Van Gent, M.R.A. (2006). *Havendammen IJmuiden: 2D modelonderzoek naar mogelijke schademechanismen Proevenserie A*.

Kwakkel, J.H. (2020). Is real options analysis fit for purpose in supporting climate adaptation planning and decision-making? *WIREs Climate Change, 11-3,* e638. https://doi.org/10.1002/wcc.638

Lashley, C. H., Zanuttigh, B., Bricker, J. D., Van der Meer, J., Altomare, C., Suzuki, T., ... & Oosterlo, P. (2020). Benchmarking of numerical models for wave overtopping at dikes with shallow mildly sloping foreshores: Accuracy versus speed. *Environmental Modelling & Software, 130*, 104740. https://doi.org/10.1016/j.envsoft.2020.104740

Pachos, K., Huskova, I., Matrosov, E., Erfani, T., & Harou, J.J. (2022). Trade-off informed adaptive and robust real options water resources planning. *Advances in Water Resources, 161,* 104117. https://doi.org/10.1016/j.advwatres.2021.104117

Rijksoverheid. (2020). *Rapport Werkgroep discontovoet 2020.* Ministry of Finance. https://open.overheid.nl/repository/ronl-d985cdc5-5da7-4644-be09-4c22bfa885be/1/pdf/rapport-werkgroep-discontovoet-2020.pdf

Rijkswaterstaat. (n.d.). Waterinfo: Waterhoogte Oppervlaktewater IJgeul stroommeetpaal. https://waterinfo.rws.nl/#!/kaart/waterhoogte/

Roenby, J., Bredmose, H., Jasak, H. (2016). A computational method for sharp interface advection. *Royal society open science, 3 (11)*, 160405. https://doi.org/10.1098/rsos.160405

Sigalas, N. (2019). *Investigation of crown wall stability on top of rubble mound structures with OpenFOAM* [Master's thesis, Delft University of Technology]. http://resolver.tudelft.nl/uuid:ab209a8a-079b-44b1-afb8-f2159361a906

TAW. (2002). *Technical report wave run-up and wave overtopping at dikes* (tech. rep.). Technical Advisory Committee for Flood Defence in the Netherlands (TAW).

Trommelen, J. (2022). *Applying the Dynamic Adaptation Policy Pathways (DAPP) approach to select future flood risk reduction strategies* [Master's thesis, Delft University of Technology]. http://resolver.tudelft.nl/uuid:901c6cec-f50c-40a1-8f6c-d2508310e24e

Van den Bos, J. P., & Verhagen, H. J. (2018). *Breakwater design lecture notes CIE5308*. Delft University of Technology.

Van der Meer, J.W. (1988). *Rock slopes and gravel beaches under wave attack*. Ph.D. thesis Delft University of Technology.

Van Gent, M.R.A. (1995a). *Wave interaction with permeable coastal structures.* Ph.D. thesis, Delft University of Technology, ISBN 90-407-1182-8, Delft University Press, Delft.

Van Gent, M.R.A. (1995b). Porous flow though rubble mound material. *Journal of Waterway, Port, Coastal and Ocean Engineering, 121 (3)*, 176-181. https://doi.org/10.1061/(ASCE)0733-950X(1995)121:3(176)

Van Gent, M.R.A. (1999). *Physical model investigations on coastal structures with shallow foreshores*. Delft Hydraulics (Deltares) Report H3608, January 1999, Delft.

Van Gent, M. R. A., Kuiper, C., & Smale, A. (2003). Stability of rock slope with shallow foreshores. In: Coastal structures 2003. https://doi.org/10.1061/40733(147)9

Van Gent, M.R.A. (2019). Climate Adaptation of Coastal Structures, Keynote in Proc. Applied Coastal Research (SCACR 2019), Bari, Italy.

Van Gent, M.R.A., Wolters, G., & Capel, A. (2022). Wave overtopping discharges at rubble mound breakwaters including effects of a crest wall and a berm. *Coastal Engineering, 176,* 104151. https://doi.org/10.1016/j.coastaleng.2022.104151

Van Hoven, A., De Groot, M.B., & Janssen, J.P.F.M. (2004). IJmuiden Breakwaters: A special case. *Coastal Engineering, 4,* 3666-3676. https://doi.org/10.1142/9789812701916_0296

Versteeg, S. (2023). *A design of the Delta21 sea defence using the adaptive pathway approach* [Master's thesis, Delft University of Technology]. http://resolver.tudelft.nl/uuid:70d3280e-d3e6-4a1e-aaac-7fe76f345628

Vos-Rovers, I., Reedijk, B., & Ekelmans, S. (2008). Crown-wall with extended base slab. *Coastal Engineering 2008, (in 5 volumes),* p. 3830-3841*.* https://doi.org/10.1142/9789814277426_0317

Walker, W.E., Haasnoot, M., & Kwakkel, J.H. (2013). Adapt or Perish: A Review of Planning Approaches for Adaptation under Deep Uncertainty. *Sustainability, 5:2013,* 955-979. https://doi.org/10.3390/su5030955

Woodward, M., Gouldby, B., Kapelan, Z., Khu, S.-T., & Townend, I. (2011). Real Options in flood risk management decision making. *Journal of Flood Risk Management, 4-4,* 339-349. https://doi.org/10.1111/j.1753-318X.2011.01119.x

XBeach User Manual. (2020). *XBeach Documentation*. https://xbeach.readthedocs.io/en/latest/user_manual.html

Appendix A: Tipping points of adaptation measures

The tipping points of all pathways of the case study (Chapter 4 and 5) are presented in Table A.1 through A.5, expressed in sea level rise (SLR) relative to 1995-2014 baseline. Also, an example is given on how the tipping points are determined.

Table A.1: Increased armour crest as first measure.

Pathway	Tipping point (m SLR)		
	1st	2nd	3rd
A-B-C	1.01	1.66	2.03
A-B-F			2.29
A-B-L			2.21
A-C-B		1.36	2.05
A-C-F			2.12
A-C-L			1.98
A-F-B		1.76	2.32
A-F-C			2.13
A-F-L			2.16
A-L-B		1.58	2.15
A-L-C			1.92
A-L-F			2.11

Table A.2: Added berm as first measure.

Pathway	Tipping point (m SLR)		
	1st	2nd	3rd
B-A-C	0.76	1.62	1.99
B-A-F			2.26
B-A-L			2.18
B-C-A		1.14	1.62
B-C-F			1.76
B-C-L			1.63
B-F-A		1.39	2.26
B-F-C			1.76
B-F-L			1.68
B-L-A		1.21	2.05
B-L-C			1.57
B-L-F			1.66

Table A.3: Added crest wall as first measure.

Pathway	Tipping point (m SLR)		
	1st	2nd	3rd
C-A-B	0.53	1.01	1.66
C-A-F			1.76
C-A-L			1.58
C-B-A		1.15	1.64
C-B-F			1.78
C-B-L			1.65
C-F-A		1.28	1.76
C-F-B			1.82
C-F-L			1.62
C-L-A		1.03	1.5
C-L-B			1.58
C-L-F			1.57

Table A.4: Raised foreshore as first measure.

Pathway	Tipping point (m SLR)		
	1st	2nd	3rd
F-A-B	0.92	1.76	2.32
F-A-C			2.12
F-A-L			2.16
F-B-A		1.42	2.29
F-B-C			1.8
F-B-L			1.72
F-C-A		1.28	1.76
F-C-B			1.82
F-C-L			1.62
F-L-A		1.21	2.03
F-L-B			1.67
F-L-C			1.57

Table A.5: Low-crested structure as first measure.

Pathway	Tipping point (m SLR)		
	1st	2nd	3rd
L-A-B	0.62	1.44	2.03
L-A-C			1.79
L-A-F			1.99
L-B-A		1.15	1.99
L-B-C			1.52
L-B-F			1.61
L-C-A		0.98	1.44
L-C-B			1.53
L-C-F			1.53
L-F-A		1.17	1.99
L-F-B			1.64
L-F-C			1.53

Using the limit state function in Equation 2.6 from Section 2.2.1 (Van Gent et al., 2022), the tipping points of adaptation measures can be determined. However, because depth-induced breaking is accounted for as described in Section 3.1, the significant wave height is also dependent on sea level rise. Furthermore, multiple other parameters in Equation 2.6 are dependent on the significant wave height or the freeboard. Equation 2.6 is therefore solved iteratively using a simple Python script. This iterative process is elaborated with an example below.

$$q = 0.016 \cdot \frac{\sqrt{g \cdot H_{m0}^3}}{s_{m-1,0}} \cdot \exp\left(-\frac{2.4 \cdot R_c}{\gamma_f \cdot \gamma_b \cdot \gamma_\beta \cdot \gamma_v \cdot \gamma_p \cdot H_{m0}}\right) < q_{max} \qquad (2.6)$$

With:

q	= Overtopping discharge	[m³/s/m]
g	= Gravitational acceleration	[m/s²]
H_{m0}	= Spectral significant wave height at toe of structure	[m]
$s_{m-1,0}$	= Wave steepness	[-]
R_c	= Freeboard relative to still water level	[m]
γ_f	= Influence factor roughness	[-]
γ_b	= Influence factor berm	[-]
γ_β	= Influence factor oblique waves	[-]
γ_v	= Influence factor crest wall	[-]
γ_p	= Influence factor recurved parapet	[-]

The example shows how to determine the tipping point for raising the foreshore bed level (F) using the values of the IJmuiden case study in Chapter 4. The value of this tipping point is 0.92 m, see Table A.4.

First, the significant wave height is determined based on the sea level rise value using Equation 3.1, 3.2 and 3.3 from Section 3.1. In this example, an initial assumption of 0.5 m of sea level rise is used. Filling in the known parameters from the case study of Chapter 4 gives Equation A.1 through A.5 below. For the adaptation measure of raising the foreshore, the bed level (BL) in Equation A.4 is increased with 2 m.

$$DWL(SLR) = DWL_0 + SLR \qquad (A.1)$$

$$DWL(0.5) = DWL_0 + SLR = 3.95 + 0.5 = 4.45 \, m \, NAP \qquad (A.2)$$

$$h_t = DWL(SLR) - BL \qquad (A.3)$$

$$h_t = DWL(0.5) - BL = 4.45 - (-8 + 2) = 10.45 \, m \qquad (A.4)$$

$$H_{m0,t} = \frac{h_t}{2} = \frac{10.45}{2} = 5.225 \, m \qquad (A.5)$$

With:

$H_{m0,t}$	= Significant wave height at the toe	[m]
h_t	= Water depth at the toe	[m]
$DWL(SLR)$	= Design water level as function of sea level rise	[m NAP]
BL	= Bed level at the toe	[m NAP]

$$DWL_0 \qquad = \text{Original design water level} \qquad \text{[m NAP]}$$
$$SLR \qquad = \text{Sea level rise} \qquad \text{[m]}$$

Now that the significant wave height is calculated for the assumed value of sea level rise, it can be used in Equation 2.6. The waves are assumed to arrive perpendicular to the structure and no berm or crest wall is added, thus the influence factors for oblique waves, berm, crest wall, and parapets are all equal to 1.

The influence factor of roughness and the wave steepness can be calculated using Equation 2.2 and 2.3 from Section 2.2.2 (Van Gent et al., 2022), repeated in Equation A.6 and A.7. The freeboard can simply be determined to be 5.55 m with the design water level of +4.45 m NAP and the crest height of +10 m NAP.

$$s_{m-1,0} = \frac{2\pi \cdot H_{m0}}{g \cdot T_{m-1,0}^2} = \frac{2\pi \cdot 5.225}{9.81 \cdot 10.59^2} = 0.0298 \qquad (A.6)$$

$$\gamma_f = 1 - 0.7 \cdot \left(\frac{D_{n50}}{H_{m0}}\right)^{0.1} = 1 - 0.7 \cdot \left(\frac{1.68}{5.225}\right)^{0.1} = 0.375 \qquad (A.7)$$

Now all parameters in Equation A.8 are known and the overtopping can be determined:

$$q = 0.016 \cdot \frac{\sqrt{9.81 \cdot 5.225^3}}{0.0298} \cdot \exp\left(-\frac{2.4 \cdot 5.55}{0.375 \cdot 1 \cdot 1 \cdot 1 \cdot 1 \cdot 5.225}\right) = 22.42 \text{ l/s/m } < q_{max} \qquad (A.8)$$

This calculated overtopping discharge is lower than the maximum allowable overtopping of 50 l/s/m, so the tipping point of the adaptation measure is not yet reached. The next value of sea level rise must be assumed higher than 0.5 m, using iterations until the tipping point of 0.92 m is found (see Table A.4). Below, the calculations are repeated briefly for the sea level rise of 0.92 m in Equation A.9 through A.14.

$$DWL(0.92) = DWL_0 + SLR = 3.95 + 0.92 = 4.87 \; m \; NAP \qquad (A.9)$$

$$h_t = DWL(0.92) - BL = 4.87 - (-8 + 2) = 10.87 \; m \qquad (A.10)$$

$$H_{m0,t} = \frac{h_t}{2} = \frac{10.87}{2} = 5.435 \; m \qquad (A.11)$$

$$s_{m-1,0} = \frac{2\pi \cdot H_{m0}}{g \cdot T_{m-1,0}^2} = \frac{2\pi \cdot 5.435}{9.81 \cdot 10.59^2} = 0.0310 \qquad (A.12)$$

$$\gamma_f = 1 - 0.7 \cdot \left(\frac{D_{n50}}{H_{m0}}\right)^{0.1} = 1 - 0.7 \cdot \left(\frac{1.68}{5.435}\right)^{0.1} = 0.378 \qquad (A.13)$$

$$q = 0.016 \cdot \frac{\sqrt{9.81 \cdot 5.435^3}}{0.0310} \cdot \exp\left(-\frac{2.4 \cdot 5.13}{0.378 \cdot 1 \cdot 1 \cdot 1 \cdot 1 \cdot 5.435}\right) = 50.70 \text{ l/s/m } > q_{max} \qquad (A.14)$$

When using steps of 0.01 m of sea level rise, the first point at which q_{max} is exceeded is the found sea level rise value of 0.92 m. This process can be done for any combination of measures.

Appendix B: Cost estimation of pathways

In Section 5.2 the cost estimation of a small selection of pathways is presented, and reference is made to this appendix, as here all cost estimations are presented. The results in Table B.1 to B.20 are sorted per starting measure and from lowest to highest cost for each scenario. At the end of the appendix, a brief example is given on how the cost of pathway F-C-A is estimated using present value.

Cost using present value

Table B.1: Cost of pathways starting with the adaptation measure: increased armour crest level.

SSP1-1.9		SSP2-4.5		SSP5-8.5		SSP5-8.5 LC	
Pathway	Cost (€/m)	Pathway	Cost (€/m)	Pathway	Cost (€/m)	Pathway	Cost (€/m)
A-C-F	5407	A-C-F	5599	A-F-C	5825	A-F-C	5955
A-F-C	5407	A-F-C	5599	A-C-F	5830	A-C-F	6058
A-F-L	5705	A-F-L	5897	A-F-L	6123	A-F-L	6310
A-L-F	6106	A-L-F	6298	A-L-F	6751	A-F-B	6973
A-L-C	6120	A-L-C	6312	A-C-L	6764	A-C-L	7028
A-B-F	6317	A-B-F	6509	A-L-C	6765	A-L-F	7059
A-B-C	6331	A-B-C	6523	A-F-B	6770	A-L-C	7076
A-C-L	6341	A-C-L	6533	A-C-B	6771	A-C-B	7252
A-C-B	6348	A-C-B	6540	A-B-F	7028	A-B-F	7359
A-F-B	6352	A-F-B	6544	A-B-C	7042	A-B-C	7375
A-L-B	7057	A-L-B	7249	A-L-B	7702	A-L-B	8159
A-B-L	7251	A-B-L	7443	A-B-L	7962	A-B-L	8404

Table B.2: Cost of pathways starting with the adaptation measure: adding a berm.

SSP1-1.9		SSP2-4.5		SSP5-8.5		SSP5-8.5 LC	
Pathway	Cost (€/m)	Pathway	Cost (€/m)	Pathway	Cost (€/m)	Pathway	Cost (€/m)
B-C-F	4932	B-F-C	5237	B-F-C	5506	B-F-C	5666
B-F-C	4932	B-C-F	5241	B-C-F	5605	B-C-F	5751
B-F-L	5158	B-F-L	5463	B-F-L	5732	B-F-L	5949
B-C-A	5205	B-C-A	5514	B-C-A	5925	B-C-A	6136
B-L-F	5551	B-C-L	5997	B-C-L	6493	B-L-F	6814
B-L-C	5565	B-L-F	6026	B-F-A	6539	B-C-L	6817
B-C-L	5688	B-L-C	6040	B-L-F	6610	B-L-C	6833
B-A-F	5965	B-F-A	6270	B-L-C	6626	B-F-A	6959
B-F-A	5965	B-A-F	6551	B-A-F	7256	B-A-F	7430
B-A-C	5979	B-A-C	6565	B-A-C	7270	B-A-C	7446
B-L-A	6598	B-L-A	7073	B-L-A	7765	B-L-A	8239
B-A-L	6885	B-A-L	7471	B-A-L	8176	B-A-L	8476

Table B.3: Cost of pathways starting with the adaptation measure: adding a crest wall.

SSP1-1.9		SSP2-4.5		SSP5-8.5		SSP5-8.5 LC	
Pathway	Cost (€/m)	Pathway	Cost (€/m)	Pathway	Cost (€/m)	Pathway	Cost (€/m)
C-F-L	2796	C-F-L	3128	C-F-L	3295	C-F-L	3513
C-F-A	2857	C-F-A	3189	C-F-A	3358	C-F-A	3592
C-A-F	2921	C-A-F	3398	C-A-F	3766	C-A-F	3891
C-L-F	3278	C-F-B	3853	C-F-B	4044	C-F-B	4467
C-F-B	3521	C-L-F	3909	C-L-F	4336	C-L-F	4473

C-L-A	3551	C-A-L	4111	C-L-A	4689	C-L-A	4881
C-A-L	3634	C-L-A	4182	C-A-L	4706	C-A-L	4971
C-B-F	3694	C-A-B	4322	C-B-F	4948	C-B-F	5118
C-A-B	3845	C-B-F	4504	C-A-B	4983	C-A-B	5289
C-B-A	3967	C-B-A	4777	C-B-A	5266	C-B-A	5500
C-L-B	4203	C-L-B	4834	C-L-B	5532	C-L-B	5854
C-B-L	4453	C-B-L	5263	C-B-L	5832	C-B-L	6183

Table B.4: Cost of pathways starting with the adaptation measure: raising the foreshore bed level.

SSP1-1.9		SSP2-4.5		SSP5-8.5		SSP5-8.5 LC	
Pathway	Cost (€/m)	Pathway	Cost (€/m)	Pathway	Cost (€/m)	Pathway	Cost (€/m)
F-L-C	2564	F-L-C	2635	F-L-C	2965	F-L-C	3210
F-C-L	2652	F-C-L	2722	F-C-L	2978	F-C-L	3272
F-C-A	2713	F-C-A	2783	F-C-A	3041	F-C-A	3351
F-B-C	3359	F-B-C	3442	F-C-B	3727	F-C-B	4226
F-C-B	3377	F-C-B	3447	F-L-B	3979	F-B-C	4423
F-L-B	3484	F-L-B	3555	F-B-C	4044	F-L-B	4461
F-A-C	3487	F-A-C	3572	F-L-A	4104	F-A-C	4546
F-B-L	3593	F-L-A	3668	F-A-C	4226	F-L-A	4616
F-L-A	3597	F-B-L	3676	F-B-L	4278	F-B-L	4712
F-A-L	3812	F-A-L	3897	F-A-L	4551	F-A-L	4896
F-B-A	4392	F-B-A	4475	F-B-A	5077	F-A-B	5564
F-A-B	4432	F-A-B	4517	F-A-B	5171	F-B-A	5699

Table B.5: Cost of pathways starting with the adaptation measure: placing a low-crested structure.

SSP1-1.9		SSP2-4.5		SSP5-8.5		SSP5-8.5 LC	
Pathway	Cost (€/m)	Pathway	Cost (€/m)	Pathway	Cost (€/m)	Pathway	Cost (€/m)
L-C-F	3728	L-F-C	4129	L-F-C	4397	L-F-C	4543
L-F-C	3728	L-C-F	4137	L-C-F	4511	L-C-F	4629
L-C-A	4001	L-C-A	4410	L-C-A	4880	L-C-A	5049
L-B-F	4618	L-F-B	5047	L-F-B	5446	L-F-B	5816
L-B-C	4632	L-C-B	5059	L-F-A	5578	L-F-A	5976
L-F-B	4646	L-F-A	5162	L-C-B	5758	L-C-B	6052
L-C-B	4650	L-B-F	5528	L-B-F	6077	L-B-F	6263
L-A-F	4761	L-B-C	5542	L-B-C	6094	L-B-C	6283
L-F-A	4761	L-A-F	5753	L-A-F	6263	L-A-F	6449
L-A-C	4775	L-A-C	5767	L-A-C	6277	L-A-C	6466
L-B-A	5665	L-B-A	6575	L-A-B	7208	L-A-B	7605
L-A-B	5706	L-A-B	6698	L-B-A	7296	L-B-A	7731

Cost using present value and levelised cost

Table B.6: Cost of pathways starting with the adaptation measure: increased armour crest level.

SSP1-1.9		SSP2-4.5		SSP5-8.5		SSP5-8.5 LC	
Pathway	Cost (€/m²)	Pathway	Cost (€/m²)	Pathway	Cost (€/m²)	Pathway	Cost (€/m²)
A-F-C	7289	A-F-C	7517	A-F-C	7809	A-F-C	8039
A-C-F	7360	A-C-F	7588	A-C-F	8137	A-C-F	8593
A-F-L	7929	A-F-L	8158	A-F-L	8450	A-F-L	8813
A-B-F	8216	A-B-F	8444	A-F-B	9024	A-F-B	9347

Pathway	Cost (€/m²)	Pathway	Cost (€/m²)	Pathway	Cost (€/m²)	Pathway	Cost (€/m²)
A-L-F	8304	A-L-F	8532	A-B-F	9219	A-B-F	9734
A-F-B	8503	A-F-B	8732	A-L-F	9289	A-L-F	9844
A-C-B	8791	A-C-B	9019	A-C-B	9567	A-C-L	10347
A-B-C	8813	A-B-C	9042	A-C-L	9792	A-B-C	10404
A-L-C	8874	A-L-C	9103	A-B-C	9817	A-C-B	10409
A-C-L	9015	A-C-L	9244	A-L-C	9860	A-L-C	10506
A-L-B	9906	A-L-B	10134	A-L-B	10891	A-L-B	11697
A-B-L	10030	A-B-L	10258	A-B-L	11033	A-B-L	11764

Table B.7: Cost of pathways starting with the adaptation measure: adding a berm.

SSP1-1.9		SSP2-4.5		SSP5-8.5		SSP5-8.5 LC	
Pathway	Cost (€/m²)	Pathway	Cost (€/m²)	Pathway	Cost (€/m²)	Pathway	Cost (€/m²)
B-C-F	8801	B-F-C	9328	B-F-C	9761	B-F-C	10161
B-F-C	8825	B-C-F	9455	B-F-A	10147	B-C-F	10539
B-F-A	9211	B-F-A	9714	B-C-F	10267	B-F-A	10642
B-A-F	9219	B-A-F	9991	B-A-F	10844	B-A-F	11069
B-C-A	9606	B-C-A	10260	B-F-L	10925	B-F-L	11619
B-A-C	9830	B-F-L	10492	B-C-A	11211	B-C-A	11674
B-F-L	9989	B-A-C	10602	B-A-C	11454	B-A-C	11763
B-L-F	10272	B-C-L	11213	B-C-L	12331	B-L-F	12961
B-C-L	10559	B-L-F	11238	B-L-F	12503	B-C-L	13017
B-L-C	10589	B-L-C	11555	B-A-L	12598	B-A-L	13064
B-A-L	10974	B-A-L	11746	B-L-C	12855	B-L-C	13393
B-L-A	11000	B-L-A	11966	B-L-A	13308	B-L-A	13952

Table B.8: Cost of pathways starting with the adaptation measure: adding a crest wall.

SSP1-1.9		SSP2-4.5		SSP5-8.5		SSP5-8.5 LC	
Pathway	Cost (€/m²)	Pathway	Cost (€/m²)	Pathway	Cost (€/m²)	Pathway	Cost (€/m²)
C-F-A	6504	C-F-A	7039	C-F-A	7315	C-F-A	7787
C-A-F	6725	C-F-L	7524	C-F-L	7816	C-F-L	8428
C-F-L	6989	C-A-F	7763	C-F-B	8400	C-A-F	8611
C-F-B	7554	C-F-B	8089	C-A-F	8426	C-F-B	9171
C-L-F	7620	C-L-F	8931	C-B-F	9770	C-L-F	10037
C-B-F	7649	C-B-F	9030	C-L-F	9780	C-B-F	10038
C-A-L	8187	C-A-L	9225	C-A-L	10353	C-A-L	10825
C-A-B	8249	C-A-B	9288	C-A-B	10434	C-A-B	10917
C-L-A	8339	C-L-A	9651	C-B-A	10684	C-L-A	11112
C-B-A	8434	C-B-A	9815	C-L-A	10711	C-B-A	11137
C-L-B	9284	C-L-B	10596	C-B-L	11779	C-B-L	12458
C-B-L	9375	C-B-L	10756	C-L-B	11933	C-L-B	12523

Table B.9: Cost of pathways starting with the adaptation measure: raising the foreshore bed level.

SSP1-1.9		SSP2-4.5		SSP5-8.5		SSP5-8.5 LC	
Pathway	Cost (€/m²)	Pathway	Cost (€/m²)	Pathway	Cost (€/m²)	Pathway	Cost (€/m²)
F-C-A	4944	F-C-A	5049	F-C-A	5716	F-C-A	6430
F-A-C	5173	F-A-C	5283	F-A-C	6065	F-A-C	6509
F-C-L	5429	F-C-L	5534	F-C-L	6217	F-C-L	7071
F-L-C	5488	F-L-C	5602	F-L-C	6658	F-A-L	7230
F-A-L	5843	F-A-L	5953	F-A-L	6734	F-L-C	7420

Pathway	Cost (€/m²)	Pathway	Cost (€/m²)	Pathway	Cost (€/m²)	Pathway	Cost (€/m²)
F-L-A	5944	F-L-A	6057	F-C-B	6802	F-A-B	7775
F-C-B	5994	F-C-B	6099	F-L-A	7160	F-C-B	7814
F-B-C	6096	F-B-C	6221	F-A-B	7241	F-L-A	8040
F-A-B	6349	F-A-B	6459	F-B-C	7410	F-B-C	8247
F-B-A	6518	F-B-A	6643	F-B-A	7832	F-B-A	8768
F-L-B	7176	F-L-B	7290	F-L-B	8518	F-B-L	9658
F-B-L	7238	F-B-L	7363	F-B-L	8552	F-L-B	9715

Table B.10: Cost of pathways starting with the adaptation measure: placing a low-crested structure.

SSP1-1.9		SSP2-4.5		SSP5-8.5		SSP5-8.5 LC	
Pathway	Cost (€/m²)	Pathway	Cost (€/m²)	Pathway	Cost (€/m²)	Pathway	Cost (€/m²)
L-C-F	8368	L-F-C	9145	L-F-C	9720	L-F-C	10105
L-F-C	8368	L-C-F	9439	L-F-A	10241	L-C-F	10524
L-A-F	8824	L-F-A	9601	L-C-F	10286	L-F-A	10735
L-F-A	8824	L-A-F	10152	L-A-F	10816	L-A-F	11105
L-C-A	9140	L-C-A	10211	L-C-A	11329	L-C-A	11712
L-A-C	9386	L-A-C	10714	L-A-C	11378	L-A-C	11792
L-B-F	9766	L-F-B	10763	L-F-B	11569	L-F-B	12348
L-F-B	9986	L-C-B	11115	L-A-B	12356	L-B-F	12980
L-C-B	10045	L-B-F	11523	L-C-B	12553	L-A-B	12988
L-B-C	10070	L-A-B	11692	L-B-F	12596	L-C-B	13111
L-A-B	10364	L-B-C	11826	L-B-C	12951	L-B-C	13406
L-B-A	10519	L-B-A	12276	L-B-A	13473	L-B-A	14035

Cost using present value, levelised cost and model uncertainty

Table B.11: Cost of pathways starting with the adaptation measure: increased armour crest level.

SSP1-1.9		SSP2-4.5		SSP5-8.5		SSP5-8.5 LC	
Pathway	Cost (€/m²)	Pathway	Cost (€/m²)	Pathway	Cost (€/m²)	Pathway	Cost (€/m²)
A-F-B	4310	A-F-B	5274	A-F-B	5499	A-F-C	5620
A-F-C	4310	A-F-C	5274	A-F-C	5499	A-F-B	5623
A-F-L	4310	A-F-L	5274	A-F-L	5499	A-F-L	5629
A-C-B	4311	A-C-B	5277	A-C-B	5526	A-C-L	5822
A-C-F	4311	A-C-F	5277	A-C-F	5526	A-C-F	5835
A-C-L	4311	A-C-L	5277	A-C-L	5526	A-C-B	5897
A-B-C	4311	A-B-C	5279	A-L-B	5546	A-L-F	5972
A-B-F	4311	A-B-F	5279	A-L-C	5546	A-L-C	5978
A-B-L	4311	A-B-L	5279	A-L-F	5546	A-B-F	5979
A-L-B	4312	A-L-B	5280	A-B-C	5548	A-B-C	5982
A-L-C	4312	A-L-C	5280	A-B-F	5548	A-L-B	5990
A-L-F	4312	A-L-F	5280	A-B-L	5548	A-B-L	5992

Table B.12: Cost of pathways starting with the adaptation measure: adding a berm.

SSP1-1.9		SSP2-4.5		SSP5-8.5		SSP5-8.5 LC	
Pathway	Cost (€/m²)	Pathway	Cost (€/m²)	Pathway	Cost (€/m²)	Pathway	Cost (€/m²)
B-F-A	5495	B-F-A	6761	B-F-A	7197	B-F-C	7442
B-F-C	5495	B-F-C	6761	B-F-C	7197	B-F-A	7456
B-F-L	5495	B-F-L	6761	B-F-L	7197	B-F-L	7487
B-C-A	5512	B-C-A	6810	B-C-F	7373	B-C-F	7827
B-C-F	5512	B-C-F	6810	B-C-A	7379	B-C-A	7936

Pathway	Cost (€/m²)	Pathway	Cost (€/m²)	Pathway	Cost (€/m²)	Pathway	Cost (€/m²)
B-C-L	5512	B-C-L	6812	B-C-L	7387	B-A-F	7983
B-A-C	5525	B-A-C	6850	B-A-C	7505	B-A-C	7991
B-A-F	5525	B-A-F	6850	B-A-F	7505	B-A-L	8000
B-A-L	5525	B-A-L	6850	B-A-L	7505	B-C-L	8062
B-L-A	5547	B-L-A	6914	B-L-F	7728	B-L-F	8503
B-L-C	5547	B-L-C	6914	B-L-C	7729	B-L-C	8535
B-L-F	5547	B-L-F	6914	B-L-A	7731	B-L-A	8573

Table B.13: Cost of pathways starting with the adaptation measure: adding a crest wall.

SSP1-1.9		SSP2-4.5		SSP5-8.5		SSP5-8.5 LC	
Pathway	Cost (€/m²)	Pathway	Cost (€/m²)	Pathway	Cost (€/m²)	Pathway	Cost (€/m²)
C-F-A	3517	C-F-A	4515	C-F-B	4986	C-F-A	5163
C-F-B	3517	C-F-B	4515	C-F-A	4986	C-F-L	5196
C-F-L	3517	C-F-L	4515	C-F-L	4987	C-F-B	5235
C-A-F	3753	C-A-F	5103	C-A-F	6028	C-A-F	6356
C-A-B	3755	C-A-B	5108	C-A-L	6075	C-A-L	6702
C-A-L	3756	C-A-L	5109	C-A-B	6077	C-A-B	6716
C-L-F	3882	C-L-F	5422	C-L-F	6588	C-L-F	7022
C-L-A	3882	C-L-A	5424	C-L-A	6607	C-B-F	7082
C-L-B	3884	C-L-B	5427	C-L-B	6632	C-L-A	7178
C-B-A	3913	C-B-A	5502	C-B-F	6711	C-B-A	7182
C-B-F	3913	C-B-F	5502	C-B-A	6717	C-B-L	7302
C-B-L	3913	C-B-L	5504	C-B-L	6723	C-L-B	7382

Table B.14: Cost of pathways starting with the adaptation measure: raising the foreshore bed level.

SSP1-1.9		SSP2-4.5		SSP5-8.5		SSP5-8.5 LC	
Pathway	Cost (€/m²)	Pathway	Cost (€/m²)	Pathway	Cost (€/m²)	Pathway	Cost (€/m²)
F-C-A	1572	F-C-A	1930	F-C-B	2104	F-C-A	2574
F-C-B	1572	F-C-B	1930	F-C-A	2104	F-C-L	2607
F-C-L	1572	F-C-L	1930	F-C-L	2105	F-A-C	2609
F-A-B	1574	F-A-B	1936	F-A-B	2136	F-A-L	2611
F-A-C	1574	F-A-C	1936	F-A-C	2136	F-A-B	2613
F-A-L	1574	F-A-L	1936	F-A-L	2136	F-C-B	2646
F-L-A	1574	F-L-A	1941	F-L-C	2163	F-L-C	2850
F-L-B	1574	F-L-B	1941	F-L-A	2165	F-L-A	2893
F-L-C	1574	F-L-C	1941	F-L-B	2169	F-B-C	2984
F-B-A	1578	F-B-A	1949	F-B-A	2216	F-B-A	2997
F-B-C	1578	F-B-C	1949	F-B-C	2216	F-L-B	3011
F-B-L	1578	F-B-L	1949	F-B-L	2216	F-B-L	3019

Table B.15: Cost of pathways starting with the adaptation measure: placing a low-crested structure.

SSP1-1.9		SSP2-4.5		SSP5-8.5		SSP5-8.5 LC	
Pathway	Cost (€/m²)	Pathway	Cost (€/m²)	Pathway	Cost (€/m²)	Pathway	Cost (€/m²)
L-F-A	5063	L-F-A	6372	L-F-C	6958	L-F-C	7252
L-F-B	5063	L-F-B	6372	L-F-A	6961	L-F-A	7305
L-F-C	5063	L-F-C	6372	L-F-B	6968	L-F-B	7441
L-C-F	5122	L-C-F	6548	L-C-F	7359	L-C-F	7783
L-C-A	5124	L-C-A	6551	L-C-A	7393	L-A-F	7963
L-C-B	5125	L-C-B	6557	L-C-B	7434	L-A-C	7978

Pathway	Cost	Pathway	Cost	Pathway	Cost	Pathway	Cost
L-A-B	5168	L-A-B	6690	L-A-B	7639	L-C-A	7989
L-A-C	5168	L-A-C	6690	L-A-C	7639	L-A-B	8005
L-A-F	5168	L-A-F	6690	L-A-F	7639	L-C-B	8230
L-B-A	5251	L-B-C	6940	L-B-F	8184	L-B-F	8741
L-B-C	5251	L-B-F	6940	L-B-C	8185	L-B-C	8780
L-B-F	5251	L-B-A	6941	L-B-A	8188	L-B-A	8838

Cost using present value, levelised cost, and model & scenario uncertainty

Table B.16: Cost of pathways starting with the adaptation measure: increased armour crest level.

Pathway	Cost (€/m)	Pathway	Levelised cost (€/m/m)	Pathway	Expected levelised cost (€/m/m)
A-F-C	5697	A-F-C	7664	A-F-C	5176
A-C-F	5724	A-C-F	7920	A-F-B	5176
A-F-L	6009	A-F-L	8338	A-F-L	5178
A-L-F	6554	A-F-B	8901	A-C-L	5234
A-L-C	6568	A-B-F	8903	A-C-F	5237
A-F-B	6660	A-L-F	8992	A-C-B	5253
A-C-L	6667	A-C-B	9447	A-L-F	5277
A-C-B	6728	A-B-C	9519	A-L-C	5279
A-B-F	6803	A-L-C	9586	A-B-F	5279
A-B-C	6818	A-C-L	9600	A-B-C	5280
A-L-B	7542	A-L-B	10657	A-L-B	5282
A-B-L	7765	A-B-L	10771	A-B-L	5283

Table B.17: Cost of pathways starting with the adaptation measure: adding a berm.

Pathway	Cost (€/m)	Pathway	Levelised cost (€/m/m)	Pathway	Expected levelised cost (€/m/m)
B-F-C	5335	B-F-C	9519	B-F-C	6724
B-C-F	5382	B-C-F	9766	B-F-A	6727
B-F-L	5576	B-F-A	9928	B-F-L	6735
B-C-A	5695	B-A-F	10281	B-C-F	6881
B-C-L	6249	B-C-A	10688	B-C-A	6909
B-L-F	6250	B-F-L	10756	B-C-L	6943
B-L-C	6266	B-A-C	10912	B-A-F	6966
B-F-A	6433	B-L-F	11743	B-A-C	6968
B-A-F	6801	B-C-L	11780	B-A-L	6970
B-A-C	6815	B-A-L	12096	B-L-F	7173
B-L-A	7419	B-L-C	12098	B-L-C	7181
B-A-L	7752	B-L-A	12557	B-L-A	7191

Table B.18: Cost of pathways starting with the adaptation measure: adding a crest wall.

Pathway	Cost (€/m)	Pathway	Levelised cost (€/m/m)	Pathway	Expected levelised cost (€/m/m)
C-F-L	3183	C-F-A	7161	C-F-A	4545
C-F-A	3249	C-F-L	7689	C-F-L	4554
C-A-F	3494	C-A-F	7881	C-F-B	4563
C-F-B	3971	C-F-B	8304	C-A-F	5310
C-L-F	3999	C-L-F	9092	C-A-L	5410

Pathway	Cost (€/m)	Pathway	Levelised cost (€/m/m)	Pathway	Expected levelised cost (€/m/m)
C-L-A	4326	C-B-F	9122	C-A-B	5414
C-A-L	4356	C-A-L	9648	C-L-F	5729
C-B-F	4566	C-A-B	9722	C-L-A	5773
C-A-B	4610	C-L-A	9953	C-B-F	5802
C-B-A	4878	C-B-A	10017	C-B-A	5828
C-L-B	5106	C-L-B	11084	C-L-B	5831
C-B-L	5433	C-B-L	11092	C-B-L	5860

Table B.19: Cost of pathways starting with the adaptation measure: raising the foreshore bed level.

Pathway	Cost (€/m)	Pathway	Levelised cost (€/m/m)	Pathway	Expected levelised cost (€/m/m)
F-L-C	2844	F-C-A	5535	F-C-A	2045
F-C-L	2906	F-A-C	5758	F-C-L	2054
F-C-A	2972	F-C-L	6063	F-C-B	2063
F-C-B	3694	F-L-C	6292	F-A-C	2064
F-B-C	3817	F-A-L	6440	F-A-L	2064
F-L-B	3870	F-C-B	6677	F-A-B	2064
F-A-C	3958	F-L-A	6800	F-L-C	2132
F-L-A	3996	F-A-B	6956	F-L-A	2143
F-B-L	4065	F-B-C	6993	F-L-B	2174
F-A-L	4289	F-B-A	7441	F-B-C	2182
F-B-A	4911	F-L-B	8175	F-B-A	2185
F-A-B	4921	F-B-L	8203	F-B-L	2191

Table B.20: Cost of pathways starting with the adaptation measure: placing a low-crested structure.

Pathway	Cost (€/m)	Pathway	Levelised cost (€/m/m)	Pathway	Expected levelised cost (€/m/m)
L-F-C	4199	L-F-C	9335	L-F-C	6411
L-C-F	4251	L-C-F	9654	L-F-A	6425
L-C-A	4585	L-F-A	9850	L-F-B	6461
L-F-B	5239	L-A-F	10224	L-C-F	6703
L-F-A	5369	L-C-A	10598	L-C-A	6764
L-C-B	5380	L-A-C	10817	L-C-B	6837
L-B-F	5622	L-F-B	11166	L-A-F	6865
L-B-C	5638	L-C-B	11706	L-A-C	6869
L-A-F	5807	L-B-F	11716	L-A-B	6876
L-A-C	5821	L-A-B	11850	L-B-F	7279
L-A-B	6804	L-B-C	12063	L-B-C	7289
L-B-A	6817	L-B-A	12576	L-B-A	7304

Example cost estimation using present value

Here, an example is given for the estimating the cost of pathways using present value. The example shows the cost calculation of pathway F-C-A for scenario SSP5-8.5, which is €3041 as shown in Table B.4 at the beginning of this appendix.

Table 4.4 from Section 4.6.1 is repeated below in Table B.21 and shows the material and construction costs (C_{MC}) necessary to calculate the cost of each measure without inflation or discount rate (C_0) for the year 2022. Equation B.1 through B.3 show how to calculate the cost of measures based on material and construction cost.

Table B.21: Assumed material and construction cost (Appelquist & Halsnæs, 2015; Hogeveen, 2021).

Cost category	Value	Unit
Armour rock	30	€/ton
Non-armour, mixed size rock	20	€/ton
Rock placement	10	€/ton
Sand nourishment	5	€/m³
Concrete	300	€/m³

$$Foreshore/Crest\ wall: \quad C_0 = A \cdot C_{MC} \qquad\qquad (B.1)$$

$$Armour: \quad C_0 = W \cdot C_{MC} \qquad\qquad (B.2)$$

$$W = A \cdot \rho_s \cdot (1 - n_v) \qquad\qquad (B.3)$$

With:

C_0	= Cost of measure per meter breakwater	[€/m]
C_{MC}	= Cost of material and construction	[€/m³ or €/ton]
W	= Weight of the rock per meter breakwater	[ton/m]
A	= Volume of material per meter breakwater	[m²]
ρ_s	= Density of rock	[ton/m³]
n_v	= Volumetric porosity of rock layer	[-]

Based on the dimensions of the adaptation measures as stated in Section 4.6.1, the volume of material per meter breakwater can be determined using simple geometric shapes. This calculation of geometric shapes is not elaborated here, but the result for measures F, C, and A is presented in Table B.22 below. An important note is that due to applying A after C, so raising the armour crest after placing the crest wall, only half of the rock volume is needed for measure A. This

Table B.22: Volume of material per meter breakwater for the relevant measures.

Measure	Material	A [m²]
F	Sand	350
C	Concrete	6
A	Non-armour rock	56

As stated in Section 4.4, the assumed density of rock is 2700 kg/m³ and porosity of 0.4 is used. Together with the information presented in Table B.21 and B.22, the cost of the measures can now be calculated for the year 2022.

$$Measure\ F: \quad C_0 = A \cdot C_{MC} = 350 \cdot 5 = 1750\ €/m \qquad\qquad (X)$$

$$Measure\ C: \quad C_0 = A \cdot C_{MC} = 6 \cdot 300 = 1800\ €/m \qquad\qquad (X)$$

$$\text{Measure A:} \quad W = A \cdot \rho_s \cdot (1 - n_v) = 56 \cdot \frac{2700}{1000} \cdot (1 - 0.4) = 90.72 \; ton/m \qquad (X)$$

$$C_0 = W \cdot C_{MC} = 90.72 \cdot (20 + 10) = 2721.6 \; €/m \qquad (X)$$

To determine the cost of the measures using present value, the time at which the measures are applied must be known. The measures are applied at the tipping point, so at a certain value of sea level rise. The timing is thus dependent on the sea level rise scenario. As stated in Section 3.3, the median values of the scenarios are used to determine when a certain value of sea level rise is reached. Table B.23 shows the relevant values of the median projection for scenario SSP5-8.5. The adaptation measures are applied at the tipping point of the previous measure (or the original breakwater in case of the first measure). By using the tipping points and median sea level rise values in Table B.23, the year in which the measures are applied can be determined using linear interpolation. The sea level rise values and corresponding years are displayed in Table B.24, with the latter being rounded to whole numbers.

Table B.23: The timing and sea level rise values for the median projection of SSP5-8.5.

Year	Median SLR [m]
2030	0.122
2040	0.187
2110	0.876
2120	0.99
2140	1.21
2150	1.314

Table B.24: Sea level rise values and corresponding years when the adaptation measures are applied.

Measure	Applied at SLR [m]	Applied in year
F	0.17	2037
C	0.92	2114
A	1.28	2147

To calculate the cost considering inflation and discount rate the formulae from Section 3.3 are used. These are repeated below in Equation B.4 and B.5.

$$C_{PV} = \frac{C_t}{(1 + r)^{t - t_c}} \qquad (B.4)$$

In which:

$$C_t = C_0 \cdot (1 + i)^{t - T} \qquad (B.5)$$

With:

C_{PV}	= Present value of the cost	[€]
C_t	= Cost in year t	[€]
C_0	= Cost based on data from year T	[€]
r	= Discount rate per year	[-]
i	= Inflation rate per year	[-]
t	= Year in which the cost is made	[-]
T	= Year in which the cost data is determined	[-]
t_c	= Current year	[-]

As stated in Section 4.6.2, the assumed discount rate is 3% and the inflation is 2%. With the assumption that the material and construction cost are valid for the year 2022 (T equals 2022) and the information gathered previously, the present value of the cost can be computed. This is done in Equation B.6 through B.12 below.

$Measure\ F:$ $\quad C_t = C_0 \cdot (1+i)^{t-T} = 1750 \cdot (1+0.02)^{2037-2022} \approx 2373\ €/m$ $\qquad$ (B.6)

$$C_{PV} = \frac{C_t}{(1+r)^{t-t_c}} = \frac{2373}{(1+0.03)^{2037-2022}} \approx 1506\ €/m \qquad (B.7)$$

$Measure\ C:$ $\quad C_t = C_0 \cdot (1+i)^{t-T} = 1800 \cdot (1+0.02)^{2114-2022} \approx 11{,}130\ €/m$ $\qquad$ (B.8)

$$C_{PV} = \frac{C_t}{(1+r)^{t-t_c}} = \frac{11{,}130}{(1+0.03)^{2114-2022}} \approx 735\ €/m \qquad (B.9)$$

$Measure\ A:$ $\quad C_t = C_0 \cdot (1+i)^{t-T} = 2721.6 \cdot (1+0.02)^{2147-2022} \approx 32{,}348\ €/m$ $\qquad$ (B.10)

$$C_{PV} = \frac{C_t}{(1+r)^{t-t_c}} = \frac{32{,}348}{(1+0.03)^{2147-2022}} \approx 800\ €/m \qquad (B.11)$$

$$Pathway\ cost = 1506 + 735 + 800 = 3041\ €/m \qquad (B.12)$$

Adding up the cost of each measure gives the pathway cost of F-C-A of 3041 €/m, which is the value found in Table B.4 for scenario SSP5-8.5.

Appendix C: Numerical test programme and results

In this appendix the numerical test programme and results of the OpenFOAM and XBeach models are given. Section 6.2.2 and 6.3.2 present only a brief overview of the numerical test programme, in Section 7.2.1 only relative overtopping figures are given, and Section 7.2.2 omitted low wave steepness results for the influence of the foreshore.

Here, a complete overview of both the tested model configurations and the results are given. Table C.1 and Table C.2 display the test programme and results of the XBeach and OpenFOAM model, respectively. The dimensionless overtopping discharges are presented in Figure C.1 through C.4. Lastly, the low wave steepness results are displayed in Figure C.5 through C.7.

The following parameters are given for each simulation (if applicable):

Input
- Peak period (T_p)
- Foreshore bed level raise (F)
- Sea level rise (SLR)
- Crest wall height (C), only for OpenFOAM

Output
- Offshore significant wave height ($H_{m0,o}$)
- Offshore spectral period ($T_{m-1,0,o}$)
- Significant wave height at the toe of the breakwater ($H_{m0,t}$)
- Spectral period at the toe of the breakwater ($T_{m-1,0,t}$)
- Overtopping discharge (q), only for OpenFOAM

Table C.1: XBeach test programme and results.

T_p [s]	F [m]	SLR [m]	$H_{m0,o}$ [m]	$T_{m-1,0,o}$ [s]	$H_{m0,t}$ [m]	$T_{m-1,0,t}$ [m]
11.65	0	0	7.26	11.84	6.05	11.92
		1	7.24	11.75	6.33	11.90
		2	7.33	11.62	6.62	11.82
	2	0	7.26	11.82	5.27	12.21
		1	7.23	11.74	5.77	12.02
		2	7.32	11.61	6.18	11.81
	4	0	7.25	11.84	4.61	12.66
		1	7.23	11.74	5.11	12.73
		2	7.32	11.61	5.56	12.71
15.5	0	0	7.28	16.59	5.98	16.72
		1	7.30	16.27	6.33	16.34
	2	0	7.28	16.67	5.38	17.72
		1	7.30	16.33	5.84	17.08
	4	0	7.28	16.68	4.83	19.19
		1	7.30	16.37	5.33	18.10

Table C.2: OpenFOAM test programme and results.

T_p [s]	F [m]	C [m]	SLR [m]	$H_{m0,o}$ [m]	$T_{m-1,0,o}$ [s]	$H_{m0,t}$ [m]	$T_{m-1,0,t}$ [m]	q [l/m/s]
11.65	0	0	0	7.24	10.93	5.14	14.49	33.3
			1	7.31	10.93	5.42	13.89	136.3
			2	7.28	10.91	5.79	13.04	469.1
	2		0	7.07	10.89	4.76	17.83	17.2
			1	7.09	10.92	5.13	14.35	82.6
			2	7.30	10.95	5.47	14.76	308.7
	4		0	7.02	10.90	4.29	20.23	8.7
			1	7.16	10.92	4.80	19.20	47.5
			2	7.16	10.97	5.20	18.13	198.5
	0	1	0	7.22	10.90	5.17	16.50	19.2
			1	7.31	10.91	5.48	14.71	96.7
			2	7.32	10.89	5.79	13.35	345.6
	2		0	7.20	10.86	4.74	17.23	9.8
			1	7.22	10.90	5.15	15.85	55.5
			2	7.29	10.89	5.51	15.16	227.7
	4		0	7.10	10.87	4.33	19.30	5.4
			1	7.12	10.91	4.73	16.77	29.6
			2	7.20	10.87	5.16	15.64	139.0
15.5	0	0	0	7.27	14.21	5.18	16.92	63.2
			1	7.33	14.22	5.54	16.35	261.3
	2		0	7.20	14.23	4.71	21.34	33.3
			1	7.24	14.20	5.30	16.28	145.2
	4		0	7.24	14.16	4.51	21.25	21.5
			1	7.24	14.20	5.00	20.42	88.9
	4	1	0	7.23	14.17	4.46	21.27	14.0
			1	7.22	14.20	4.95	20.45	61.0

Figure C.1 through C.4 show the dimensionless overtopping results of the OpenFOAM model. The overtopping and the freeboard are made dimensionless with the offshore significant wave height instead of the significant wave height at the toe which is typically used. This is done because raising the foreshore bed level reduces the incoming wave height at the toe. Therefore, if the wave height at the toe is used to make the overtopping dimensionless, raising the foreshore bed level does not decrease the dimensionless overtopping while it does decrease the actual measured overtopping discharge. Since using the wave height at the toe does not correctly represent the overtopping results, the offshore value is used instead. Figure C.4 shows an example of what the dimensionless overtopping looks like when using the wave height at the toe compared to Figure C.3 which shows the same results normalised with the offshore value.

The figures essentially show the same as in Section 7.2.1:

- Low wave steepness shows consistently larger overtopping discharge than the high steepness counterparts.
- Raising the foreshore bed level decreases the overtopping.

Notable in Figure C.3 is that for the same freeboard, the overtopping is higher with a crest wall than without. This agrees with the findings of Van Gent et al. (2022).
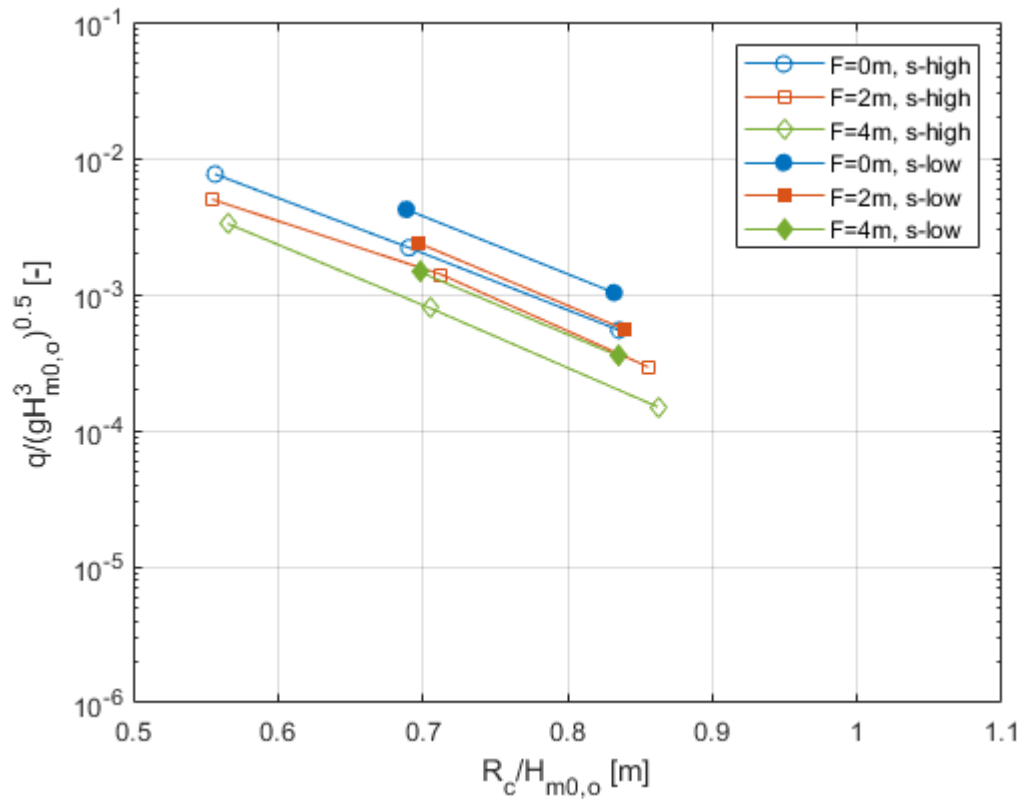
Figure C.1: Overtopping for high and low wave steepness, made dimensionless with offshore wave height.
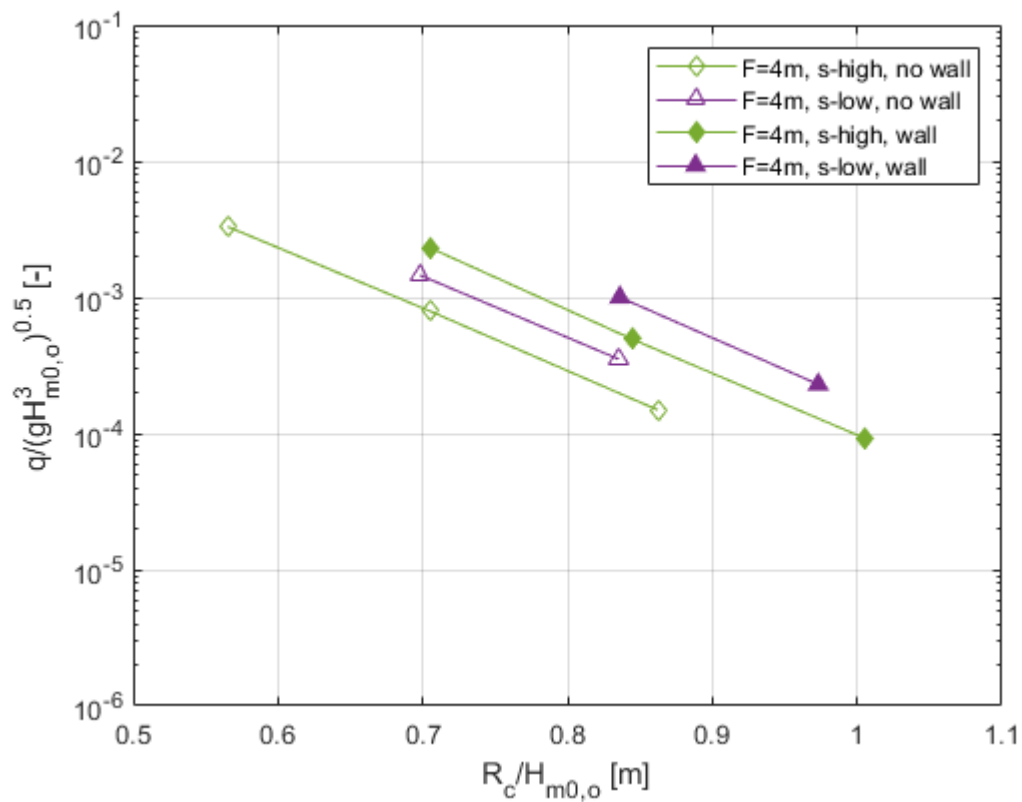

Figure C.2: Overtopping for high and low wave steepness, made dimensionless with offshore wave height.
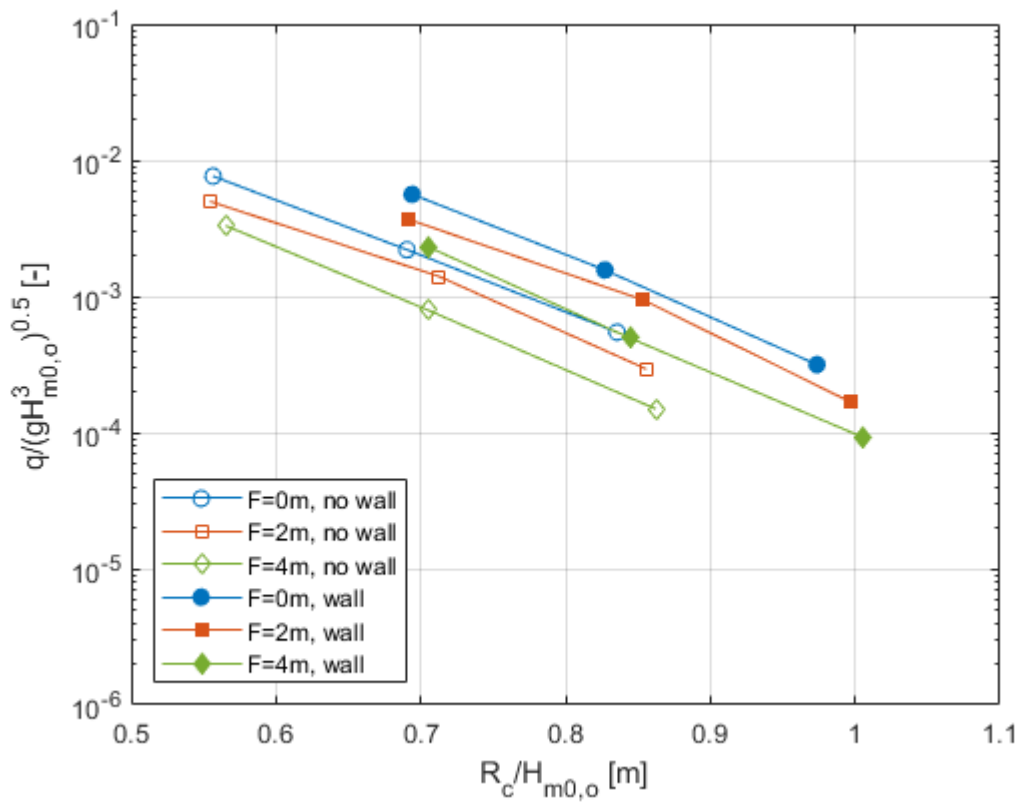
Figure C.3: Overtopping with and without crest wall for different foreshore bed levels, made dimensionless with offshore wave height.
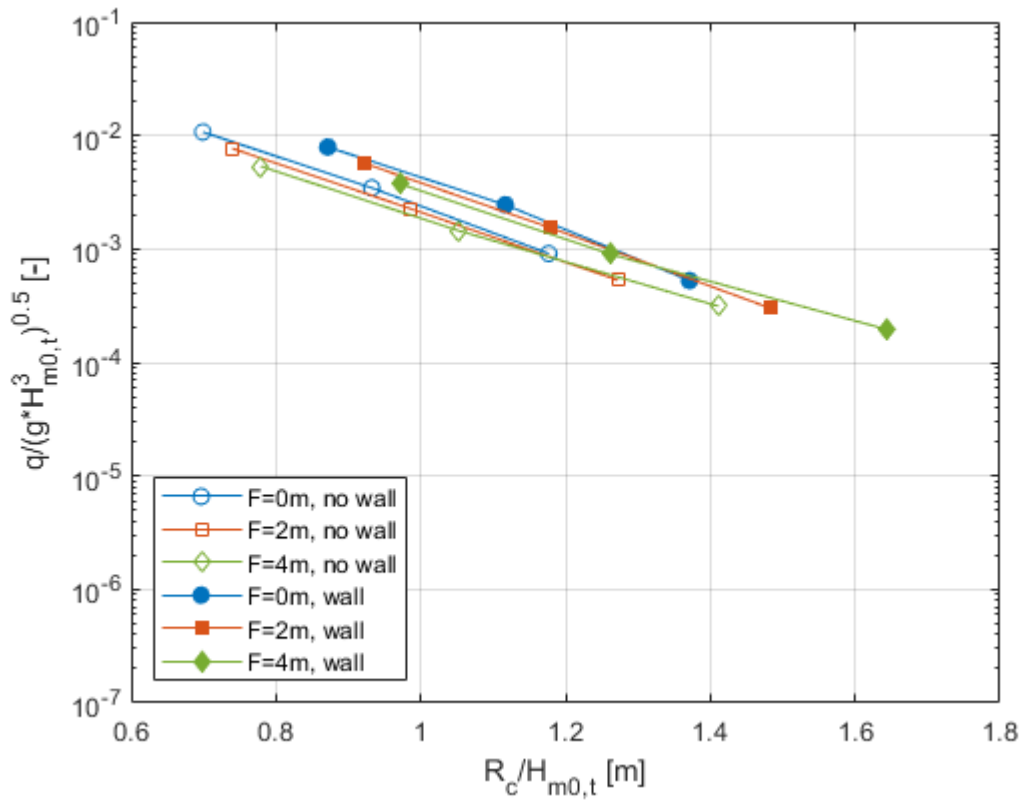

Figure C.4: Overtopping with and without crest wall for different foreshore bed levels, made dimensionless with the significant wave height at the toe.

Below, the low wave steepness results for the influence of the foreshore are presented. The same approach taken in Section 7.2.2 for the high wave steepness simulations is followed here. Figure C.5 to C.7 compare the numerical overtopping discharges to the overtopping expressions of Van Gent et al. (2022), where three different sources of wave parameter input (empirical estimates of Section 3.1, OpenFOAM and XBeach) were used. The main outcomes are:

- In Figure C.5, a very similar trend can be seen as for the corresponding high steepness results. The combination of empirical formulae again predicts higher reduction of overtopping. Similarly, the empirical F=2 m line crosses the numerical F=4 m line at 1 m sea level rise
- The combination of measured OpenFOAM wave parameters and overtopping expressions is shown in Figure C.6. The empirical lines start relatively close the numerical lines at 0 m sea level rise but show the same drastic decrease for 1 m sea level rise as the high steepness counterparts in Section 7.2.2. The empirical lines also cross each other at approximately 1 m sea level rise, indicating that F=4 m has higher overtopping than F=2 m for higher sea level rise.
- Using XBeach wave parameters in the overtopping expressions again gives the most similar reduction to the numerical lines, see Figure C.7. An important difference with high steepness is that the empirical and numerical lines cross each other at a much lower sea level rise. The accuracy might be worse at higher sea level rise.

The decreasing trend of the reduction for increasing sea level rise is not as apparent for the low steepness numerical results compared to the high steepness counterparts, but this could be due to having only two data points.
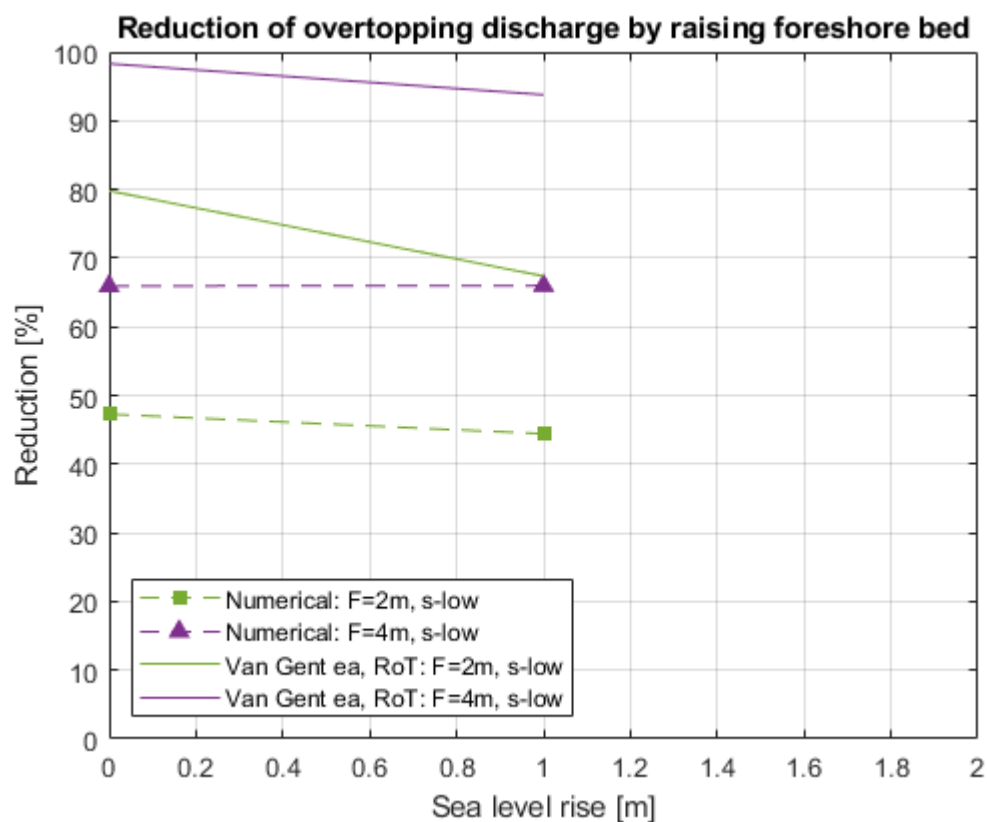

Figure C.5: OpenFOAM and empirical (rule of thumb with Van Gent et al. (2022)) relative overtopping reduction $(q_0-q)/q_0$ with q_0: F=0 m, no wall, low steepness
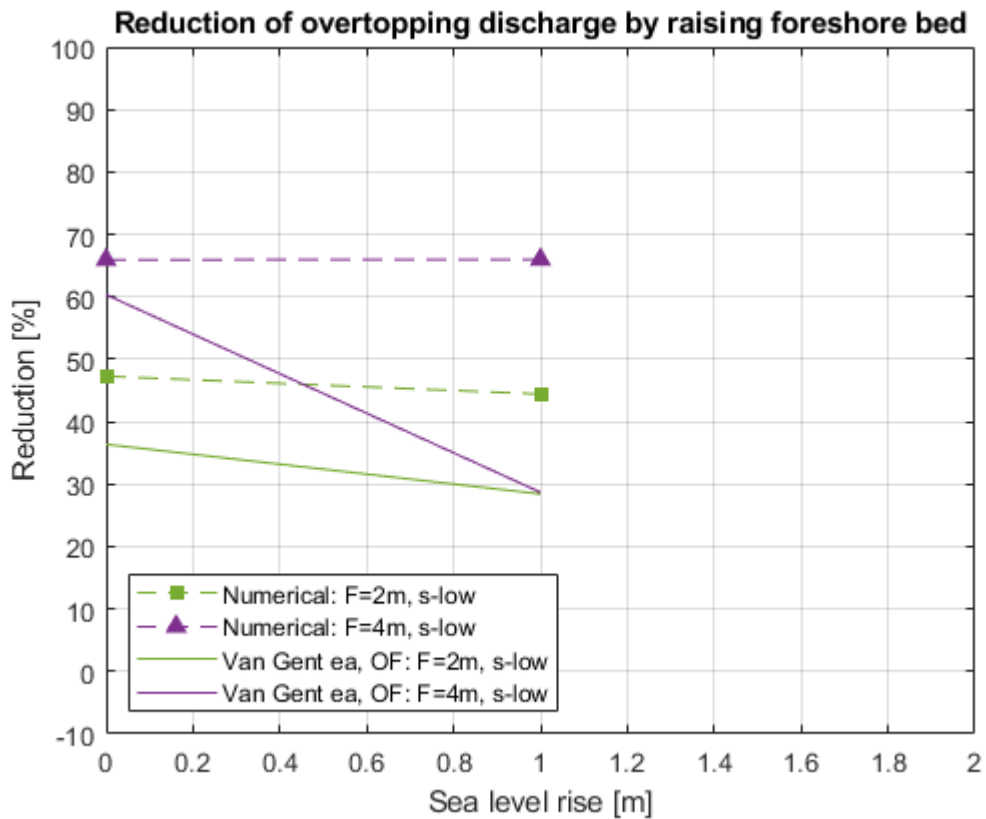
Figure C.6: OpenFOAM and empirical (OpenFOAM wave conditions with Van Gent et al. (2022)) relative overtopping reduction $(q_0-q)/q_0$ with q_0: F=0 m, no wall, low steepness
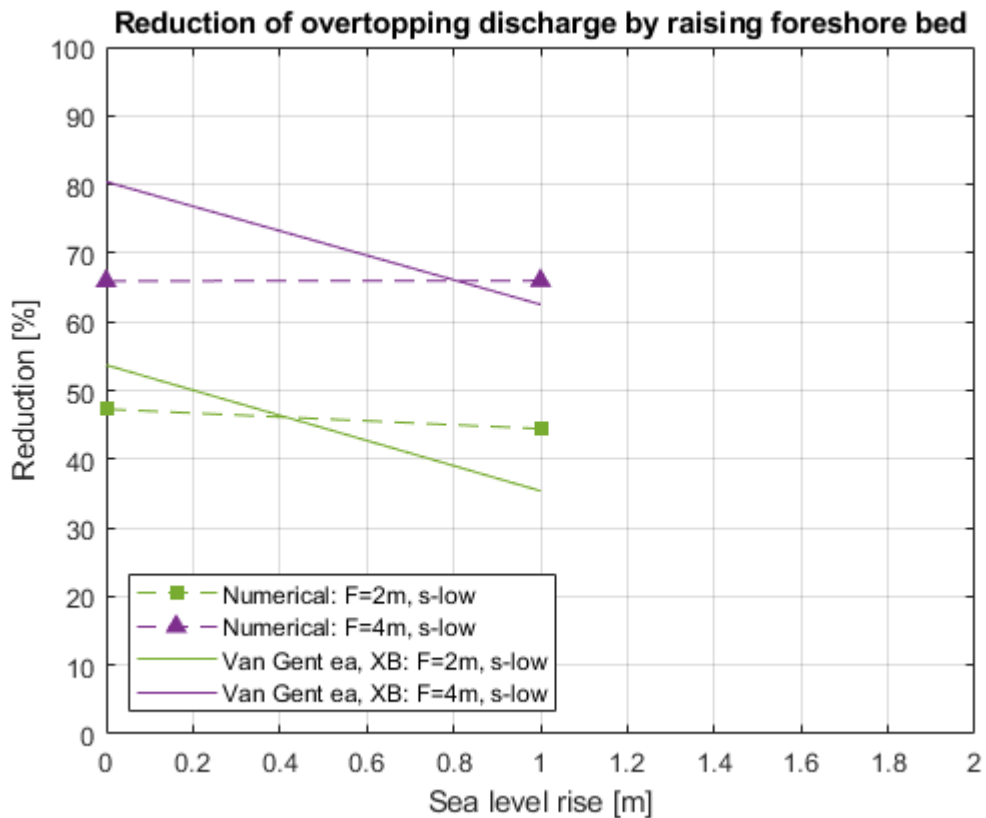

Figure C.7: OpenFOAM and empirical (XBeach wave conditions with Van Gent et al. (2022)) relative overtopping reduction $(q_0-q)/q_0$ with q_0: F=0 m, no wall, low steepness